ALDEN

Solving flow problems since 1894

HYDRAULIC MODEL STUDY OF WALLER CREEK TUNNEL PROJECT FOR THE CITY OF AUSTIN, TEXAS

By:

Dan Gessler Ph.D., P.E.

Andrew E. Johansson

Randy Lagumbay Ph.D.

Songheng Li, Ph.D., P.E.

Submitted to

CRESPO CONSULTING SERVICES, INC

KBR/ESPEY JOINT VENTURE

Austin, Texas

October, 2010

2010-177-H-CR1360

ALDEN Research Laboratory, Inc.
30 Shrewsbury Street, Holden, Massachusetts 01520-1843

508-829-6000/phone • 508-829-5939/fax
info@aldenlab.com • www.aldenlab.com

HYDRAULIC MODEL STUDY OF WALLER CREEK TUNNEL PROJECT FOR THE CITY OF AUSTIN, TEXAS

By:

Dan Gessler Ph.D., P.E.

Andrew E. Johansson

Randy Lagumbay Ph.D.

Songheng Li, Ph.D., P.E

Submitted to:

CRESPO CONSULTING SERVICES, INC

KBR/ESPEY JOINT VENTURE

Austin, Texas

October, 2010

ALDEN RESEARCH LABORATORY, INC.

30 Shrewsbury Street

Holden, MA 01520

The following information was developed in cooperation with Crespo Consulting Services, Inc. through a subcontract agreement with the KBR/Espey Joint Venture (JV) in support of the final design of the Waller Creek Tunnel Project. Given the unique nature of the project, special attention and analyses have been conducted to better evaluate the performance of the proposed system so that the design team can improve the design over and above a design that would otherwise be limited to information in readily available literature. During the development of these model studies conducted by Alden Laboratory, the detailed design has continued to develop and evolve based on many factors including the results from these models as they became available. The geometry used in the model studies may not necessarily reflect the geometry included in the final construction plans developed by the design team.

LIST OF TABLES

LIST OF FIGURES

ABSTRACT

Waller Creek is centrally located within the City of Austin, Texas, and has one of the most densely developed watersheds in the locality. The main stem is approximately seven miles in length and generally flows from north to south. The total drainage area for Waller Creek is 5.74 square miles (3700 acres) and the watershed lies entirely within the jurisdictional boundaries of the City of Austin and Travis County as shown in Figure 1 and Figure 2.

Flood impacts to development adjacent to the creek have been a concern since the area was developed in the 1950's. Central Texas (including the City of Austin) is prone to flooding, especially in creeks with highly impervious watersheds. The Waller Creek Tunnel Project (WCTP) will reduce the threat of flood damages to existing infrastructure and development, along the Lower Reach of Waller Creek. In addition to flood control, the proposed design will improve water quality, create ecological benefits, mitigate erosion problems, and provide safety to individuals and businesses located in the downtown Austin Waller Creek area.

At the request of Crespo Consulting Service Inc., Austin, Texas (Crespo), Alden Research Laboratory (Alden) conducted a hydraulic model study using Computational Fluid Dynamics (CFD) and physical model studies for the proposed WCTP for the City of Austin, Texas. The objective of the study included evaluation of the flow patterns approaching and in the various hydraulic structures. Additionally, the model study was used to:

- Establish a rating curve for the morning glory spillway,
- Evaluate the potential air entrainment in the tunnel and the need for any air bleed structures,
- Establish junction loss coefficients for the 4th Street and 8th Street lateral junctions,
- Determine the fluctuating pressures due to flow induced excitations at the tunnel portal to the recirculation pump intake when the valve is closed and,
- Obtain a rating curve for the outlet spillway/weir.

Inlet CFD Model

A CFD model of the inlet at Waterloo Park was used to design and evaluate the approach channel geometry, training wall and bar screens. The intake structure is comprised of a morning glory type inlet and includes six bar screen type trash racks which remove a portion of any debris before entering the vertical drop shaft and the underground tunnel. A training wall was designed to improve flow distribution approaching the structure. Model results show that 80% of the bar screen area has a velocity of less than 4 ft/s. The maximum velocity at any location on the screens is less than 5.5 ft/s.

To address concerns that debris may accumulate along the training wall, modifications were made to fill in the backside of the barbs (the barbs were developed as part of the design to improve flow distribution and conditions at the screens). With the modifications the model results show that two screens did not have 80% of the bar screen area velocities of less than 4 ft/s and one screen exceeded the 50 % flow variation from the target flow.

The final alternative was evaluated in the physical model.

Lateral Junction CFD Models

Lateral junctions at 4th Street and 8th Street were evaluated using CFD models. The models were used to simulate flow conditions where the lateral flow is relatively large and the main conduit flow is relatively small. This condition results in the largest impact of the lateral junctions on the main conduit flow. Model results showed that the lateral junctions are not predicted to cause significant flow separations in the main conduit and cavitation potential is small.

Outlet CFD Model

A CFD model of the outlet structure was used to design the riser shaft from the tunnel to the surface, and a flip bucket at the toe of the spillway. Based on the CFD model results, Outlet connection 2 as shown in Figure 17 was selected. The final structure design, based on CFD results, shows uniform flow distribution over the spillway. The flip bucket at the toe of the dam decreased the water velocity near the bed of the discharge channel as compared to a no flip

bucket condition. Water velocity near the end of the spillway with the 2.25 ft high flip bucket is not predicted to erode the spillway apron.

Inlet/Tunnel/Lateral Junctions/Outlet Physical Model

A 1:33 scale model of the Inlet, Tunnel, Lateral Junctions and Outlet of the Waller Creek Tunnel Project was constructed at Alden. The design flow for the model to simulate the friction losses and the expected Hydraulic Gradient Line (HGL) along the tunnel corresponded to the 100 year flood flow. The rating curves for the inlet spillway and outlet weir and the closed conduit flow loss coefficients for tunnel junctions were obtained from the model by testing a range of flows, as they were not affected by the tunnel HGL.

Upon initial model start up, air entrainment at the morning glory vertical shaft was observed. The measured average Volume Fraction of air (VF_a) in the model was about 5% for 25 year flow and 4% for the 100 year flow. Maximum Volume Fraction of air (VF_a) in the model for the 25 year and 100 year flows were 8% and 6%, respectively. The volume fractions obtained from the model data could be corrected for any scale effects on generation of air entrainment using correction factors available in the literature. Also, as the Volume Fraction of air, VF_a, can be a function of pressure and temperature, corrections need to be applied taking into account the expected pressure (from HGL calculations) and temperature in the field.

The morning glory rating curve (Figure 64) was established in the physical model using inlet flows for the 2, 5, 10, 25, 50, 100 and 500 peak tunnel/ peak intervening events. During the 500 year event the morning glory spillway was submerged and an air drawing free-surface vortex was observed however it should be noted that 1) the building operations deck, which could interfere with vortex formation, was not included in the model and 2) the emergency spillway was not modeled which would result in lower water levels for the 500 yr event. Data was also recorded for two additional flows to determine the point at which the inlet weir becomes drowned out (approximately at a flow of 9,950 cfs at EL 483.2 ft water level). For the 100 year peak inlet flow condition (8,247 cfs) the average HGL was increased in the inlet shaft to above the morning glory crest elevation (474.0 ft) to elevations 478.2 and 479.7 ft to determine any effect on the inlet rating curve. For these submerged conditions, no change in the head on the

morning glory spillway was observed. Therefore, the inlet rating curve is hydraulically disconnected from the inlet shaft tailwater up to at least 479.7 ft.

Testing was conducted to determine any fluctuating pressures due to flow induced excitations at the tunnel portal to the recirculation pump intake when the valve is closed using the 100 year peak tunnel/ peak intervening condition. A plot of the prototype pressure versus time fluctuation referenced to EL 427 ft is included in Figure 65. The predicted maximum, minimum and average pressures were 16.9, 15.5 and 13.4 psi, respectively. This range of fluctuating pressure was not of concern to the JV in terms of design criteria for the valve.

Tests were conducted using the model to determine the Minor Losses and corresponding junction Loss Coefficients at the 8th Street and 4th Street lateral junctions and the tunnel (tees combining main flow in the tunnel with flow from side inlet weir branch). Results indicating the Loss Coefficients determined from the model for the 100 year flood for both Peak Tunnel-Peak Intervening and Lagging Tunnel-Peak Intervening are shown below:

	100 yr Peak Tunnel-Peak Int.		100 yr Lagging Tunnel-Peak Int.	
Loss Coefficient	8th St.	4th St.	8th St.	4th St.
Tunnel: K_{2-3}	0.3	0.2	0.3	0.3
Branch: K_{1-3}	-0.6	-0.7	-0.4	-0.4

The branch loss coefficients (K_{1-3}) are negative due to transfer of energy from the through flow in the tunnel to the flow from the branch as the branch flow is only about 10% or so of the tunnel flow.

The outlet spillway rating curve was also established in the physical model using inlet flows for the 2, 5, 10, 25, 50, 100 and 500 year peak tunnel/ peak intervening events. The outlet spillway rating curve is shown in Figure 70.

HYDRAULIC MODEL STUDY OF WALLER CREEK TUNNEL PROJECT FOR THE CITY OF AUSTIN, TEXAS

1.0 INTRODUCTION

Waller Creek is centrally located within the City of Austin, Texas, and has one of the most densely developed watersheds in the locality. The main stem is approximately seven miles in length and generally flows from north to south. Waller Creek has one major tributary, Hemphill Branch, which confluences with the main stem at approximately river mile 2.4 (upstream from Lady Bird Lake). The headwaters of the main stem are located near Anderson Lane and Burnet Road in north Austin. The mouth is located in eastern downtown where Waller Creek confluences with Lady Bird Lake, an impounded segment of the Colorado River formerly known as Town Lake. The total drainage area for Waller Creek is 5.74 square miles (3700 acres) and the watershed lies entirely within the jurisdictional boundaries of the City of Austin and Travis County as shown in Figure 1 and Figure 2. This urban watershed includes much of the University of Texas campus and downtown Austin, and only 3% of the watershed remains undeveloped.

Flood impacts to development adjacent to the creek have been a concern since the area was developed in the 1950's. Central Texas (including the City of Austin) is prone to flooding, especially in creeks with highly impervious watersheds. Flooding of Waller Creek has been an enduring problem for the City of Austin because of lives lost, damage to property, and safety concerns. Over the years, improvements have been made to the channel banks and surrounding properties of lower Waller Creek in an attempt to mitigate vulnerability to flooding; however, the success of such endeavors has been very limited. Trash, debris, bank erosion, and wastewater overflows have been ongoing secondary problems in addition to the significant flooding issues. This history of challenges has brought serious attention to the need for flood control along the Lower Reach of Waller Creek.

The Waller Creek Tunnel Project (WCTP) will reduce the threat of flood damages to existing infrastructure and development, along the Lower Reach of Waller Creek. In addition to flood control, the proposed design will improve water quality, create ecological benefits, mitigate

erosion problems, and provide safety to individuals and businesses located in the downtown Austin Waller Creek area.

The proposed Waller Creek Tunnel Project includes four major components:

1. The Tunnel Inlet: a 42 ft diameter (at crest) circular spillway ('morning glory') drop structure within a channelized segment of Waller Creek upstream of 12th Street.

2. The Tunnel: an arch-pipe approximately one mile in length with a diameter varying from 20-26 feet, located at a depth of between 60-80 feet below grade.

3. Two Side Inlet Weirs: on the east side of the creek just upstream of 8th Street and 4th Street, a lateral weir upstream of each street will intercept additional flow and divert it to the Tunnel.

4. The Tunnel Outlet: a 40-foot diameter vertical shaft connected to a horseshoe-shaped stilling basin that conveys tunnel flow across a 150-foot weir into Lady Bird Lake.

The flood control tunnel is being designed to divert flood flows such that, downstream of 12th Street, events up to the 1% annual chance (100 year) flood do not exceed the main channel banks. All of the creek flow from the upstream watershed is captured just upstream of 12th Street at the Tunnel Inlet located within a segment of channelized reach, which forms the Tunnel Inlet Pool, shown in Figure 3 and Figure 4. The tunnel inlet and associated diversion structures are sized to divert 100% of the 1% annual chance hydrograph at 12th Street. In the model it was assumed that floods up to the 0.2% annual chance (500 year) event will be intercepted by the tunnel without overtopping the diversion structure however in actuality there is an emergency spillway which will overtop in the prototype. Figure 4 through 22 provide an overview of the Tunnel components.

Associated with the Tunnel Inlet Pool is a diversion structure, which will create sufficient backwater to allow the Tunnel Inlet to accept the peak flood flow for up to the 0.2% annual chance event. The Inlet connects to a 20-foot diameter vertical shaft with a gradual bend to

provide a relatively efficient transition to the near horizontal Tunnel Pipe, which is approximately 80 feet below grade at this location.

The tunnel generally follows the alignment of Waller Creek and Sabine Street. The Tunnel Pipe is 20 feet in diameter from the upstream segment down to 8th Street. The pipe length between 8th Street downstream to 4th Street is 22 feet in diameter, and downstream of 4th Street the Tunnel Pipe is 26 feet in diameter (see section 4.1.3 for additional tunnel diameter information).

There are two additional diversions into the Tunnel Pipe, which divert flow from Waller Creek through a 200-foot long Side Inlet Weir, a lateral weir located on the east (left) bank of the channel. The two Side Inlet Weirs are located just upstream of 8th and 4th Streets. An Inline Weir is located just downstream of each of the two Side Inlet Weirs in order to improve the efficiency of flow diversion to the Side Inlet Weirs.

The Tunnel Outlet is located on the north (left) bank of Lady Bird Lake (the Colorado River), west of the mouth of Waller Creek. The Outlet facility includes a 40-foot diameter vertical shaft, which conveys flood flows from the 26-foot diameter Tunnel Pipe to a horseshoe-shaped discharge basin. There is a gradual transition from the 26-foot diameter tunnel to the 40-foot diameter vertical shaft. Flow exits the transition area across a 150-foot long weir with a 60-foot concrete apron into Lady Bird Lake.

At the request of Crespo Consulting Service Inc., Austin, Texas (Crespo), Alden Research Laboratory (Alden) conducted a hydraulic model study using Computational Fluid Dynamics (CFD) and physical model studies for the proposed WCTP for the City of Austin, Texas. The objective of the study included evaluation of the flow patterns approaching and in the various hydraulic structures. The model study was also used to:

- Establish a rating curve for the morning glory spillway,
- Evaluate the potential air entrainment in the tunnel and the need for any air bleed structures,
- Establish junction loss coefficients for the 4th Street and 8th Street lateral junctions,
- Determine the fluctuating pressures due to flow induced excitations at the tunnel portal to the recirculation pump intake when the valve is closed and,

- Obtain a rating curve for the outlet spillway/weir.

The model study results were used to suggest and evaluate any modifications to the designs to improve flow conditions.

2.0 OVERVIEW OF HYDRAULIC MODEL STUDY APPROACH

To address the study objectives, Alden applied both Computational Fluid Dynamics (CFD) Modeling and Physical Modeling techniques. Generally speaking, CFD is well suited to predict the (single-phase) flow patterns and the impact of any proposed modifications in the various structures of the Waller Creek Tunnel Project. Compared to a physical model, it is easier, quicker and less expensive to obtain detailed velocity data along any desired flow sections and identify high velocity regions, flow separation and resulting eddies and any swirling flows. However, a physical model study of the project components including the intake structure, tunnel and discharge structure system was still required. CFD models cannot predict air entrainment in the tunnel and have some difficulty in predicting unsteady flow conditions such as water surface disturbances induced by the flow approaching the morning glory spillway and flow exiting the discharge structure which may influence the rating curves. The study was conducted in two phases with the CFD model studies being conducted first so that any modifications derived from the CFD studies could be incorporated and tested in the physical model.

2.1 CFD Modeling:

Four CFD models were developed to compute the flow patterns at the following locations:

- Inlet structure (morning glory spillway),
- 4th Street lateral junction,
- 8th Street lateral junction and,
- Outlet discharge structure into Lady Bird Lake.

The models were also used to develop modifications to improve the flow conditions as necessary.

2.2 Physical Modeling:

Upon completion of the CFD modeling Alden conducted a 1:33 reduced scale physical hydraulic model study of the intake structure, tunnel, lateral junctions and the outlet structure. Modifications developed from the CFD models were incorporated into the physical model and the model was tested for various flow events to establish a rating curve for the morning glory spillway, evaluate the potential air entrainment in the tunnel and the need for any air bleed structures, and establish junction loss coefficients for the 4th Street and 8th Street lateral junctions. In addition, the physical model was used to determine fluctuating pressures due to flow induced excitations at the tunnel portal to the recirculation pump intake with closed valve. The final rating curve for the outlet spillway/weir was determined from the physical model.

3.0 CFD MODELING

Computational Fluid Dynamics (CFD) was used to evaluate the hydraulic performance of three components of the project: 1) The inlet at Waterloo Park, 2) Lateral junctions with the tunnel at 4th and 8th Street, and 3) The discharge structure into Lady Bird Lake. It is not practical or cost effective to construct one model of the entire system; therefore, each component is analyzed separately. In the following sections, the models for each feature are presented.

3.1 Waterloo Park Inlet Model

The inlet at Waterloo Park is proposed to be a morning glory type inlet. Morning glory inlets are compact and provide an efficient means for transitioning flow from a reservoir into a round vertical conduit. The morning glory has a fixed crest elevation at EL 474 ft and is 41 ft in diameter at the crest. The shape of the morning glory principally follows the guidelines set forth in Design of Small Dams (USBR, 1987). The diameter of the vertical shaft is 20 ft. The purpose of the inlet is to divert water from Waller Creek to the tunnel when the water level at the intake exceeds the crest elevation of the spillway.

3.1.1 Introduction

The intake structure is comprised of a morning glory type inlet and includes six bar screen type trash racks which prevent debris from entering the vertical drop shaft and the underground tunnel. Satisfactory performance of the bar screens depends on a relatively equal distribution of flow between the six screens. Non equal flow distribution increases the likelihood of excessive debris build up on some screens and probability that material will be lodged in screen or forced through the screen. A computational fluid dynamics (CFD) simulation was used to evaluate the following hydraulic characteristics at the screen:

- Evaluate the flow patterns and flow distribution between the six trash racks.
- Develop modifications to the approach channel to meet the following flow split requirements between screens:
    - Eighty percent of screen area is below 4 ft/sec.
    - Maximum allowable velocity in the screen area is 5.5 ft/s.
    - Maximum allowable variation from the target flow is 50 %.
- Development of the final design for testing in the physical model.

A three-dimensional Computational Fluid Dynamics (CFD) program was used to predict the system hydraulics including flow patterns, water velocities, flow separation, flow split between trash racks, and velocity distribution through the trash racks. There are several commercially available CFD models which are applicable to this problem, Alden maintains licenses for two: Fluent by ANSYS and ***FLOW-3D***® by Flow Science. ***FLOW-3D***® is better suited to simulating this type of free surface flow problem and was selected for this simulation. The program solves the fully three dimensional Navier-Stokes equations in conjunction with an appropriate turbulence model for the creation, transport and dissipation of turbulent kinetic energy.

FLOW-3D® uses the Fractional Area/Volume Obstacle Representation (FAVOR) method (Hirt and Sicilian, 1985) for the modeling of solid obstacles, such as topology. The FAVOR method allows complex shapes to be simulated without resorting to 'stair stepping' the boundaries. It approaches the accuracy of more computationally intensive deformed boundary fitted grids.

The location of the free surface in ***FLOW-3D***® is computed using the Volume of Fluid (VOF) method (Hirt and Nichols, 1980). This formulation consists of three parts, a scheme to describe the shape and location of the free surface, a method to track the evolution of the shape and location of the free surface through time and space and a means for applying boundary conditions to the free surface. The simulations do not include the movement of the air above the water; it is assumed that the air has no significant effect on the water surface or the flow of the water.

A number of guide vane configurations were investigated with the most promising design fully documented in terms of flow distributions. A final design evaluation was conducted and the best design was selected for final evaluation in the physical model. The physical model did not include instrumentation to quantify the flow distribution between the bar screens or collect extensive velocity measurements for model validation. The physical model was able to confirm that general flow patterns observed were consistent with the numeric model. No further design modifications were made based on the physical model testing.

3.1.2 Assumptions and Limitations

The numeric model of the intake required that several assumptions be made about the flow field. The following key assumptions were made for the inlet CFD model:

- Motion of the air above the water does not affect the flow of the water. This simplification yields a considerable reduction in required computational resources and is reasonable for this application.
- Water surface tension was assumed not to impact the results. This assumption is reasonable for large scale flow problems with high Webber numbers.
- Flow over and in the morning glory spillway was modeled until it passed through critical depth, i.e. the model included only a very short section of the riser shaft. This simplification reduces computer time and does not affect flows approaching the morning glory.
- All of the fixed model boundaries such as the tunnel, riser shaft, spillway, apron etc. are made of concrete and that these surfaces are approximately hydraulically smooth.

- The trash racks were modeled as a porous media with an imposed flow resistance based on the bar diameter and spacing. The model did not resolve every bar and opening in the bar screens.

3.1.3 Model Geometry and Computational Mesh

The model geometry was created using AutoCAD and Gambit based on drawings provided by Crespo and modifications developed by Alden. Creating the model geometry for the Waller Creek Inlet involved defining the morning glory spillway, approach channel, flow guidance vanes and training structures, piers, and bridges. Figure 4 shows the geometry of the Waller Creek Inlet with the final design of turning vane. The model extends about 800 ft upstream of the inlet to an area about 100 feet upstream of the 14th Street bridge. The intake structure design went through many revisions, and the design shown in Figure 4 is significantly different from first design. Over 50 simulations were evaluated, only the final design testing is presented in this report.

Grid generation in ***FLOW-3D***® involves the creation of a structured mesh block over the model domain. Cell spacing can vary along the three coordinate directions (x,y,z) however, variations in the grid spacing must be carried through the entire model domain. The ability of the model to accurately reproduce the flow field is dependent on the grid resolution in the area of interest. A smaller computational cell (higher resolution model) can capture smaller flow features than a coarser grid. The finer grid however requires more computational time to solve as 1) the number of calculations increases because there are more elements and 2) the allowable time step decreases. The mesh size varied throughout the model domain. In regions where high gradients of flow variables were present, the mesh was refined enough to capture the detailed behavior of fluid flow. The mesh size in the horizontal direction is about 1.4 ft and in the vertical direction it is about 1.2 ft. Approximately 2 million cells with multiple mesh blocks were used for the model.

3.1.4 Boundary Conditions

Model boundary conditions were specified at all internal and external model boundaries. Walls were specified as smooth, no slip boundaries. Flow turning vanes and training structures, piers, and bridges were modeled as solid walls. The screens were modeled as porous media with a specified flow resistance. A mass sink was used in the bottom of the morning glory spillway to remove water from the system. A flow and water surface elevation are specified upstream of the 14th Street bridge at the upstream model boundary. The water surface was modeled as a free surface where the water-air interface can be tracked.

3.1.5 Post-Processing

The results of the simulations were post-processed and analyzed using the Field View software. Post processing involved evaluating flow patterns and distribution through the trash racks and in the approach channel. For each trash rack, the average velocity was determined. In addition, the percentage of the area at or below 4 ft/s was computed and shown graphically. A figure was made which shows vertical planes colored by velocity normal to the direction of flow in the river. In addition, a figure was made which shows the water velocity in a horizontal plane at elevation 476 and the water surface.

The simulations for the intake model are time dependent; therefore the velocity and flow patterns vary with time. For each bar screen, a plot was made which shows the percentage of flow as a function of time. The percentage of flow shown on the vertical axis is the percentage of the nominal flow if all screens were passing the same amount of flow. A value of -20%, for example, indicates that the screen is passing 20 percent less flow than average. For each screen it is desired to have an average velocity of less than 4 ft/s at all times. Therefore, a plot was made for each screen which shows the average velocity on the vertical axis and time on the horizontal axis. The horizontal axis shows results for about 3.5 minutes.

3.1.6 Flow Scenarios

The design of the morning glory intake evolved significantly during the design process. During the process, the design was evaluated at a range of flows. The final design was only evaluated

for the 100 year flow of 8,250 cfs. Model results are only included for the final design and the 100 year flow.

3.1.7 CFD simulation results

Several designs including various inlet pool geometries and flood control vane configurations were investigated with the most promising design selected for final evaluation in the physical model. Due to the extensive number of model revisions, all of the results are not presented. Figure of model results are included in Appendix A.

Figures A-1 through A-5 show the results of the first inlet pool geometry modeled. Due to the non-uniform flow distribution through the screen the inlet pool grading and screen configuration was modified by the JV.

Figures A-6 through A-9 show the results of the modified inlet pool geometry without any training walls and Figures A-10 through A-13 show the results of the modified inlet pool geometry with a single turning vane (without barbs).

Figure 23 shows the geometry of the training wall developed with the modeling effort. The flow field meets the following three acceptance criteria:

1. Eighty percent of bar screen area must have velocity below 4 ft/sec.
2. Peak velocity in the bar screen area must not exceed 5.5 ft/s.
3. Flow variations from the target flow must not exceed 50 %.

Figures showing the model results are included in Appendix A. Figure A-14 shows the velocity distribution and the average velocity through each bar screen at the conclusion of the simulation. It is important to note that the simulations are time dependent and the flow patterns do change with time. Figure A-14 shows that the average velocity through the bar screens are less than 4 ft/s for all screens.

Figure A-15 shows the percentage of the screen which is at or below 4 ft/s. The stated objective was to have at least 80 percent of the screen with a velocity of less than 4 ft/s. Figure A-15 shows that the objective is met.

Figure A-16 shows vertical planes upstream of the intake colored by water velocity. The figures show both the lateral and vertical variation in the water velocity. The flow field is very complex.

Figure A-17 shows a horizontal plane at elevation 476 colored by water velocity. The figure also shows velocity vectors which show the flow direction. Elevation 476 is above the spillway crest elevation of EL 474 ft. The flow field is complex and has flow separations which vary with time.

Figure A-18 shows the water surface colored by water velocity. Comparing the Figures A-17 and A-18 shows the strong vertical structure in the flow field.

Figure A-19 shows the water surface colored by water velocity. The color range has been shifted from Figure A-18 to better show areas of low velocity.

Figures A-20 through A-25 show the percent flow variation as a function of time for bar screens 1 through 6 respectively. The flow through each screen varies because of the unsteady (time dependent) nature of flow separations in the system.

Figure A-26 shows the percent flow variation for all six screens on a single plot. Variations are up to plus or minus 50 percent of the nominal average flow.

Figures A-27 through A-32 show the average velocity through bar screens 1 through 6 respectively as a function of time. During the period considered in the model, the average velocity for each screen is less than 4 ft/s.

Figure A-33 shows the average velocity for all six screens on the same plot. The figure shows the temporal variability of the average velocity.

To address concerns that debris may accumulate along the training wall, modifications were made to fill in the backside of the barbs as shown in Figure 24. With the modified training wall, two of the six screens had less than eighty percent of the bar screen velocities below 4 ft/ sec and one screen exceeded the 50 % flow variation from the target flow. The filled training wall was selected by the JV as the final design to be included in the physical model.

Figure A-34 shows the velocity distribution and the average velocity through each bar screen at the conclusion of the simulation for the filled training wall. It is important to note that the simulations are time dependent and the flow patterns do change with time. Figure A-34 shows that the average velocity through the bar screens are less than 4 ft/s for all screens except for screen 3.

Figure A-35 shows the percentage of the screen which is at or below 4 ft/s for the filled training wall. The stated objective was to have at least 80 percent of the screen with a velocity of less than 4 ft/s. Figure A-35 shows that the objective is not met for screen 1 and 3.

Figure A-36 shows the percent flow variation for all six screens on a single plot for the filled training wall. Variations are up to plus or minus 60 percent of the nominal average flow.

Figure A-37 shows the average velocity for all six screens on the same plot for the filled training wall. The figure shows the temporal variability of the average velocity.

3.2 Lateral Junctions at 4th Street and 8th Street

3.2.1 CFD

The proposed tunnel system includes two lateral junctions where water joins the main tunnel through two vertical drop shafts. The drop shafts connect the side inlet weirs to the main tunnel. A CFD model was developed to evaluate the hydraulic conditions at the 8th Street and 4th Street lateral junctions. The model geometry was not modified during testing.

The following hydraulic characteristics of the lateral junctions were investigated using the CFD model:

- Flow patterns at the junction
- Velocity distribution
- Flow separations
- Cavitation potential

Flow in a pipe junction is complex and highly three dimensional. For this reason a fully three dimensional computational fluid dynamics (CFD) model or a physical model is required. The CFD model is significantly less expensive to construct and modify during testing and provides a cost effective means for developing the design to be used in the physical model. There are several commercially available CFD models which are applicable to this model. Alden maintains licenses for two: Fluent by ANSYS and ***FLOW-3D***® by Flow Science. Fluent is best suited to this type of problem, where the area of interest does not include a free surface. The program solves the fully three dimensional Navier-Stokes equations in conjunction with an appropriate turbulence model for the creation, transport and dissipation of turbulent kinetic energy.

3.2.2 Assumptions and Limitations

Most physical and numeric modeling efforts require that some assumptions be made about the flow field. The following key assumptions were made for the lateral junction CFD models:

- Steady-state flow conditions were modeled. Dynamic changes in flow were not considered.
- Effects from the free surface in the riser were assumed to be negligible
- It was assumed that the junction was water solid.
- All of the fixed model boundaries such as the pipe walls were assumed to be made of concrete and hydraulically smooth.

3.2.3 Geometry and Computational Mesh

The model geometry was created using AutoCAD 2008 and Gambit (version 2.4.6) using information provided directly or indirectly by Crespo. Figure 25 and Figure 26 show the model geometry for 4th and 8th Street tunnel and lateral junctions, respectively.

The computational domain was discretized into finite volumes using the mesh generating software Gambit. The variable size mesh is boundary fitted and follows exactly the model boundaries. In areas of high velocity or pressure gradient, the mesh was refined to capture the detailed behavior of the flow. Approximately one half million computational cells were used for the model; the mesh is a combination of tetrahedral and hexahedral cells. Figure 27 and Figure 28 show the computational mesh for 4th and 8th Street tunnel and lateral junctions, respectively. The governing equations were then solved on each finite volume using the FLUENT solver (version 6.3.26).

3.2.4 Boundary Conditions

Model boundary conditions were specified at all internal and external model boundaries. Walls were specified as smooth, no slip boundaries. Wall functions were used in the simulations for calculating the velocity gradient near the walls. At the upstream end of the tunnel, a velocity was specified based on the volumetric flow rate and the cross section area of the pipe. The velocity distribution was assumed to be uniform. At the upstream end of the connector tunnel a uniform velocity profile was also defined. At the downstream end of the model, an outflow boundary with zero normal diffusive flux for all flow variables is used.

3.2.5 Fluent Solver Settings

The solver settings selected in FLUENT are based on the physics involved in the simulation. The pressure-based numerical algorithm developed for incompressible flows is used for solving the governing equations for the conservation of mass and momentum. Each equation is solved with 2nd order accuracy. The standard ***k-e*** turbulence model is used to simulate the creation, transport and dissipation of turbulent kinetic energy. The turbulence model is consistent with the physics of turbulent flows and satisfies the mathematical constraints on the Reynolds stresses.

3.2.6 Post-Processing

The results of the simulations were post-processed and analyzed using the FieldView version 12.1 software. For each simulation two plots were made showing water velocity and pressure on a horizontal plane through the centerline of the tunnel. Each junction was evaluated at two flows, resulting in a total of 8 plots. The plots are included in Appendix B.

3.2.7 Simulations

The watershed from which storm flow is being diverted to the tunnel is large. Therefore, the peak flow from the 4th Street and 8th Street connectors may not be temporally displaced from the peak flow in the tunnel. The peak intervening flow can occur before during or after the peak tunnel flow. The largest flow separations and lowest pressures will occur when the main tunnel flow is low and the intervening flow is large. Therefore, the flows considered in the junction models were of a lagging tunnel flow and a peak intervening flow. Table 1 summarizes the conditions considered for the simulations, only the 1 year and 100 year flows were modeled. All units of flow are cubic feet per second.

3.2.8 CFD simulation results

Simulations were performed for the proposed lag tunnel/peak intervening flow for 4^{th} and 8^{th} Street lateral junctions to evaluate the flow patterns and cavitation potential. The 1 year and 100 year return period were modeled in the study. Figures showing velocity and total pressure contours for the 1 year and 100 year return periods for 4^{th} Street lateral junction are shown in Figures B-1 and B-2, respectively in Appendix B. Similarly, figures of velocity and total pressure contours for the 1 year and 100 year return period for 8^{th} Street lateral junctions are shown in Figures B-3 and B-4, respectively in Appendix B.

Model results for the 4th Street junction show no flow separations and minimal potential for cavitation.

The geometry of the 8th Street junction results in a higher potential for flow separations and cavitation, however, the potential remains minimal and no changes to the junction are

recommended based on the flows modeled. It should be noted that the potential for flow separations and cavitation is a function of the percentage of the total flow in the main tunnel and the connector. A higher percentage of flow in the connector will increase the potential for cavitation and flow separations.

3.3 Outlet Model

3.3.1 Introduction

The outlet CFD model was developed to investigate the hydraulics related to the discharge structure. The model includes a short section of the horizontal tunnel, the vertical riser shaft (bringing water back to the surface), and the discharge structure which conveys the water from the vertical riser to Lady Bird Lake. In addition to the base condition, three geometric (structural) changes were made to the model. The three changes evaluated the effects of various flip buckets on the downstream end of the ogee spillway and two transition alternatives from the horizontal tunnel to the vertical riser shaft. The changes were based on model results from previous runs and were not the result of a predefined test matrix.

The following issues related to the outlet structure were investigated using the CFD model:

- Flow patterns between the tunnel shaft and the spillway with a particular interest in the non-uniform flow across the ogee spillway.
- Effect of stacked rock on flow patterns near the ends of the spillway crest
- Velocity profiles along the ogee spillway section
- Hydraulic jump at the toe of the spillway
- Potential for scour in the exit channel, concrete apron and riprap section
- Water surface elevations at spillway crest and upstream
- Pressure force on the riser pipe and water intake screen downstream of the ogee spillway.

A fully three dimensional computational fluid dynamics (CFD) model was required for this model due to the highly three dimensional nature of the flow field. A two dimensional model is unable to simulate the flow field of interest. Of particular interest in this simulation is predicting

the location of the severely deformed free surface. There are several commercially available CFD models which are applicable to this problem, Alden maintains licenses for two: Fluent by ANSYS and ***FLOW-3D***® by Flow Science. ***FLOW-3D***® is best suited to simulating this type of free surface flow problem and was selected for this simulation.

FLOW-3D® is a commercially available CFD software package particularly well suited for steady and unsteady free surface simulations. The model solves the fully three dimensional Navier-Stokes equations on a structured hexagonal grid. Several models are included in the solver for computing the creation, transport and dissipation of turbulent kinetic energy (Flow Science, 2005). For this application, the Renormalized Group (RNG) k-ε model was used.

FLOW-3D® uses the Fractional Area/Volume Obstacle Representation (FAVOR) method (Hirt and Sicilian, 1985) for the modeling of solid obstacles, such as topology. The FAVOR method allows complex shapes to be simulated without resorting to 'stair stepping' the boundaries. It approaches the accuracy of more computationally intensive deformed boundary fitted grids.

The location of the free surface in ***FLOW-3D***® is computed using the Volume of Fluid (VOF) method (Hirt and Nichols, 1980). This formulation consists of three parts, a scheme to describe the shape and location the free surface, a method to track the evolution of the shape and location of the free surface through time and space and a means for applying boundary conditions to the free surface. The simulations do not include the movement of the air above the water; it is assumed that the air has no significant effect on the water movement.

3.3.2 Assumptions and Limitations

Most physical and numeric modeling efforts require that some assumptions be made about the flow field. The following key assumptions were made for the outlet CFD model:

- Motion of the air above the water does not affect the flow of the water. Therefore, air movement was not included in any of the simulations. This simplification yields a considerable reduction in required computational resources and is reasonable for this application.

- Effects of the water surface tension were assumed not to impact the results. This assumption is reasonable for large scale flow problems with high Webber numbers.
- It was assumed that air which may be entrained at the inlet is negligible. Therefore, at the upstream end of the outlet model the tunnel is assumed to be 'water solid'. Including entrapped air in the model would significantly complicate the model and increase computational time.
- The velocity profile in the tunnel is assumed to be uniform at the upstream end of the model. The assumption is reasonable given the length of pipe upstream of this location.
- Lady Bird Lake is a run of the river lake. As such, there is a velocity profile and water surface gradient in the lake. For the purpose of this model, it assumed that the velocity distribution is uniform (i.e. no lateral profile) at the upstream model boundary. It is also assumed that within the model domain, it can be assumed that the water surface elevation is approximately constant.
- All of the fixed model boundaries such as the tunnel, riser shaft, spillway, apron etc. are made of concrete and that these surfaces are approximately hydraulically smooth.

3.3.3 Geometry and Computational Mesh

All the geometry information used in the model was provided directly or indirectly by Crespo in an electronic format or CAD file. Based on this information, a solid model was created of the ground and concrete surfaces. The solid model is used by ***FLOW-3D***® in the form of a '.stl' file.

Grid generation in ***FLOW-3D***® involves the creation of a structured mesh block over the model domain. Cell spacing can vary along the three coordinate directions (x,y,z) however, variations in the grid spacing must be carried through the entire model domain. The ability of the model to accurately reproduce the flow field is dependent on the grid resolution in the area of interest. A smaller computational cell (higher resolution model) can capture smaller flow features than a coarser grid. The finer grid however requires more computational time to solve; both the number of calculations increases because there are more elements and the allowable time step decreases. ***FLOW-3D***® allows the use of multi block meshing to reduce the overall size of the model domain. Flow passes from one mesh block to another at the mesh block interface. At the block interface, the computational mesh of the two blocks is not required to match. ***FLOW-3D***® will

interpolate the flow field from one mesh block boundary onto another. This model used multiple mesh blocks.

Figure 29 shows a general three-dimensional view of CFD model. The main components including the tunnel, shaft, spillway, intake, riprap, are identified. Figure 30 is a plan view colored by ground elevation and shows the extents of the model.

3.3.4 Boundary Conditions

Boundary conditions must be specified at each location where water can enter or exit the model. Typically, where water exits a free surface model the water surface elevation is specified and where water enters the model the flow is specified. In ***FLOW-3D***® there are boundary definitions which may be used: The selected boundary types can affect model convergence and the accuracy of the solution. Boundaries for the outlet model are shown in Figure 31 and are defined as follows:

A constant velocity is specified at the tunnel inlet cross section. The tunnel is assumed to be water solid. The averaged velocity is obtained by dividing the tunnel flow by the sectional area. The flow direction is assumed to be normal to the model boundary.

At the upstream of the Lady Bird Lake a velocity boundary and water level are specified. The water velocity and elevation were provided by Crespo. For the 100 year flood in the tunnel, a 3.5 ft/s lake velocity is used and for the 2-year flood in the tunnel, a 1.25 ft/s velocity is specified. The lake level for all of the simulations is assumed to be EL 428 ft.

A constant water surface elevation is specified at the downstream end of the Lady Bird Lake. In ***FLOW-3D***®, a water surface elevation is defined as a pressure boundary with a hydrostatic pressure distribution and a fixed water surface elevation. The water level at the downstream model boundary is EL 428 ft.

3.3.5 Post Processing

Post processing of the results was primarily conducted in Tecplot 360 by Tecplot Inc. For each flow condition plots were created which show the water surface colored by the surface water velocity. In addition a series of plots was created which show various sections through the flow field. The sections are colored by velocity and in some cases include velocity vectors which show the flow direction. For each run, the same series of plots was made, making it possible to compare one design or flow condition with another. The plots are included in Appendix C. The numbering convention for the outlet model figures is Figure C-y-z, where *y* designates which of the seven outlet model runs and *z* is the figure number for the series. What follows is a description of the plots by figure number:

Appendix C Figure 1: This figure shows a general three-dimensional view of the water surface colored by velocity magnitude. The entire model domain is shown.

Appendix C Figures 2 through 5: These four figures show horizontal planes colored by water velocity at the following elevations:

- EL 406 ft, about mid height of the riser shaft
- EL 415 ft, 1 foot above the outlet cover slab
- EL 422 ft, about mid height between the outlet cover slab and spillway crest
- EL 430 ft, height of the spillway crest

Appendix C Figures 6 through 8: These figures show vertical planes parallel with the tunnel axis colored by water velocity and include velocity vectors at the following x coordinates:

- X=200 ft, centerline of outlet shaft
- X=150 ft, 50 ft left (looking downstream) of shaft center
- X=250 ft, 50 ft right of shaft center

Appendix C Figures 9 and 10: Vertical planes which are perpendicular to the tunnel axis and parallel with the spillway axis are shown in these figures. The planes are colored by velocity and include velocity vectors at the following locations:

- Y=400 ft, centerline of outlet shaft
- Y = 481.6 ft, spillway crest

Appendix C Figures 11 and 12: These figures show detailed views of the water surface colored by water velocity in the vicinity of the stacked rock at the ends of the spillway. Both figures are looking upstream at the spillway face, Figure 11 shows the left side of the spillway and figure 12 shows the right side of the spillway.

Appendix C Figures 13 through 15: This series of figures shows vertical planes through the spillway at three locations. The planes are colored by water velocity and include velocity vectors showing flow direction. Planes are cut at the following locations:

- X=200 ft, centerline of outlet shaft
- X=150 ft, 50 ft left (looking downstream) of shaft center
- X=250 ft, 50 ft right of shaft center

Appendix C Figures 16 and 17: These two figures show a vertical plane parallel to the spillway axis at the toe of the spillway. The planes are colored by velocity and the local Froude number respectively. The local Froude number is computed from the local velocity and uses the distance from the local velocity to the river bed for the length scale. By this definition, for a water column with constant velocity, the local Froude number will decrease with increasing height in the water column because the length scale increases. Therefore, the local Froude number should compared in a relative sense to the other local Froude number plots. The planes are located at Y=500 ft.

Appendix C Figures 18 and 19: These figures show a horizontal plane downstream of the spillway colored by water velocity and shown with velocity vectors. Planes are shown at elevation 415 and 422.

Appendix C Figures 20 and 21: Figures 20 and 21 show detailed views of the planes shown in Figures 18 and 19. The planes are at elevation 415 and 422 and show the velocity magnitude and direction between the spillway and the end of the retaining wall.

Appendix C Figures 22 through 26: This series of figures shows vertical planes on the spillway apron which are perpendicular to the spillway axis. The planes are colored by water velocity and include vectors to show the flow direction. Planes are shown at the following locations:

- X=200 ft, centerline of outlet shaft
- X=150 ft, 50 ft left (looking downstream) of shaft center
- X=250 ft, 50 ft right of shaft center
- X=126 ft, 1 ft from the left retaining wall
- X=274 ft, 1 ft from the right retaining wall

Appendix C Figure 27: Figure 27 shows how the water surface elevation varies across the width of the spillway crest. Ideally, the water surface elevation is constant along the length of the spillway. In evaluating the results shown in the plot, it is important to consider the depth over the spillway crest in addition to the variation in depth from one end to the other.

3.3.6 Simulations

Seven simulations were run to evaluate various flow conditions and four physical geometries of the outlet structure. Changes to the outlet structure included the addition of a flip bucket of various heights. In addition, two transitions from the horizontal tunnel to the vertical riser shaft were evaluated. The flip bucket height is critical for the energy dissipation characteristics downstream of the spillway. The transition from the horizontal to vertical shaft affects the flow patterns in the riser, which affects the flow distribution over the spillway. Table 2 lists the most important characteristics and differences of the seven runs. In Table 2, the transition design type is identified as outlet connection 1 or 2 (see Figure 17).

3.3.6.1 Results

Results of each outlet model simulation were used to improve the design and help direct the next simulation. In discussing the results, the discussion for each run builds on the previous run.

3.3.6.1.1 Run 1

Figures showing model results from Run 1 are shown in Appendix C-1. Figure C-1-1 shows a general view of velocity magnitude contours at the water surface throughout the computational domain. Figures C-1-2 through C-1-10 comprehensively show the flow patterns from the tunnel shaft to the spillway. Flow is unevenly distributed inside the shaft with a higher velocity towards the right side of the riser (looking downstream) and a lower velocity towards the left side. In addition, Figure C-1-2 shows a counter clockwise rotational flow. The skewed and rotational flow in the riser propagates downstream and persists in Figure C-1-3 and results in higher velocity and flow towards the right end of the spillway (Figures C-1-4 and C-1-5).

The longitudinal section through the centerline of the tunnel and riser shaft (Figure C-1-6), shows a complex flow field with high velocities at the upstream and downstream end of the riser and entrainment of flow in the middle of the shaft. The resulting flow pattern is undesirable because flow approaching the spillway is uneven and not normal to the spillway face. The flow patterns approaching the spillway were identified as a flow characteristic which should be targeted for improvement in subsequent designs.

Figures C-1-11 and C-1-12 show the water surface colored by velocity at the left and right side stacked rock. There may be some flow between the stacked rock and retaining walls; however, the impact of the stacked rock on flow patterns at the ends of the spillway is local. No changes were identified for this design feature.

Velocity profiles along the ogee spillway section are shown in Figures C-1-13, C-1-14, and C-1-15. Velocity contours and vectors are shown in these sections. Flow over the spillway is similar at all of the sections despite variations in the upstream approaching pattern. Velocity increases as flow progresses down the spillway with a maximum velocity of 25 to 30 ft/s at the hydraulic jump.

Figures C-1-16 and C-1-17 show velocity contours and local Froude number (defined as $Fr = \frac{V}{\sqrt{gh}}$, V is velocity, h is water depth, and g is gravity acceleration) in the cross section at the spillway toe (Y=500 ft). Maximum velocities are about 12 to 16 ft/s and are noted towards the bottom of the water column, below elevation 418 ft. The local Froude number varies significantly throughout the cross section. The maximum Froude number is about 1.8 to 2 and is noted near the concrete bottom. The high velocity along the spillway apron may impact the performance of the structure. The energy of the high velocity flow should be dissipated to some extent before it advances downstream to the T-Screen intake and riprap area. This was identified as a flow phenomenon which should be modified through the addition of a flip bucket at the toe of the spillway.

Figures C-1-18 through C-1-26 provides information for analysis of scour potential in the exit channel, concrete apron and riprap section area. One measure for the erosion potential of flow in this area is velocity. Velocity is as high as about 11 ft/s immediately upstream of the T-Screen and about 8 ft/s in the riprap area. There is a large eddy along the right side retaining wall (Figure C-1-21). At the end of the retaining wall the velocity is about 4 ft/s. At the downstream end of the left retaining wall the highest velocity is about 6 to 7 ft/s. The water velocity is about 5 ft/s in the riprap area. The high velocity along the retaining wall and in the riprap area may result in scour in this area.

The water surface elevation along the spillway crest and upstream of the crest is shown in Figure C-1-27. The water level is higher on the right end of the spillway, and approximately flat on the left half of the spillway.

3.3.6.1.2 Run 2

Figures showing results of Run 2 are collected in Appendix C-2. Run 2 differs from Run 1 in that it includes a 3.5 ft/s current in Lady Bird Lake; Run 1 assumed a static lake. The principal object of Run 2 was to determine if the lake current affects results in areas of interest and if it should be included in subsequent simulations based on a comparison with Run 1.

The lake current has no impact on flow patterns upstream of the spillway. In addition, no significant impacts on flow patterns are seen in the area between the spillway and riprap section. The impact on the eddy at the end of the right retaining wall is insignificant. Lake cross flow does have an impact on the flow downstream the riprap area. Flow turns more towards the left (downstream direction) when it merges the lake cross flow (Figures C-2-18 and C-2-19). Model results suggest that the impact extent may be more significant when the flow from spillway is decreased (i.e. a 2-year flood event) or when the flow over spillway is deflected by an energy dissipation structure. Therefore, it was recommended that the lake cross flow be included in the remaining runs.

3.3.6.1.3 Run 3

The tunnel connection in Run 1 created unfavorable hydraulic flow patterns inside the vertical riser and between the riser and the spillway. In Run 3, an alternative design, Connection #2, was tested. In addition, a 3 ft high spillway flip bucket was evaluated at the toe of the spillway (see Figure 32). The purpose of the flip bucket is to provide additional energy dissipation and reduce velocities in the bottom of the water column. Flow conditions in Run 3 were the same as those used in Run 2. Figures showing model results are included in Appendix C-3.

The hydraulic conditions in the riser and between the riser and the spillway are greatly improved. The improvements can be seen by comparing the flow patterns as shown in Figure C-3-1 through C-3-10 with the corresponding results of Run 2. The higher velocity region downstream of the riser is shifted from the right side of basin towards the center and flow approaching the spillway crest (Figure C-3-5) is more uniform.

The flip bucket at the toe of the spillway redirects flow following the apron towards the water surface (Figures C-3-13, C-3-14, and C-3-15). This modification significantly reduces the velocity magnitude along the floor and increases the velocity in the top of the water column. Figures C-3-18 through C-3-26 can be compared for Runs 2 and 3 to understand the impact of the flip bucket. Velocity is reduced to about 1 ft/s at the front of the T-Screen intake and to about 3 ft/s in the riprap area. A velocity of 6 to 8 ft/s is noted at the left retaining wall and a

velocity of about 6 ft/s is noted near the right retaining wall. These velocities give the potential for erosion along the retaining walls.

Figure C-3-27 shows a more symmetrical distribution of the water surface elevation along the spillway crest. Maximum water surface elevations are noted in the middle of the spillway.

3.3.6.1.4 Run 4

The results of Run 3 showed that Connection #2 with the 3 ft high flip bucket is a favorable design which significantly improves the hydraulic flow conditions relative to Run 2. In Run 4, the design is evaluated during a 500-year flood event.

In Run 4, the tunnel flow is increased from a 100-year flow (7,957 cfs) to a 500-year flow (11,270 cfs). The geometry remains the same as in Run 3. Model results are shown in Appendix C-4.

The water velocity increases significantly inside the riser shaft and at the mouth of the riser. The increase in velocity is particularly pronounced along the top of the downstream end of the riser, and can be seen in Figure C-4-6. Peak velocities at this location are approximately 25 ft/s.

The spillway flip bucket located at the toe of the spillway appears to perform well, and velocities on the spillway apron and riprap remain acceptable. However, high velocities are noted along the left and right side retaining walls (Figures C-4-18, through C-4-21). At this location, velocities are greater than was observed during Run 3.

3.3.6.1.5 Run 5

In Run 5, the design tested with the 100 year flow in Run 3 and the 500 year flow in Run 4 is tested with a 2-year flood (2,320 cfs) and a lower lake cross flow of 1.25 ft/s. The model geometry remains the same as in Runs 3 and 4. Model results are shown in Appendix C-5.

Model results show that Connection #2 performs well under low inflow condition. Flow patterns upstream of the spillway are more uniform than was observed for the 100-year and 500-year

flows (Figures C-5-4 and C-5-5). Flow approaches the spillway more uniformly and the water level upstream the spillway is more uniform (Figure C-5-27). The water depth and velocity over the spillway are significantly reduced relative to the higher flows. During the 2 year flow, the velocity at the T-Screen intake and the riprap area is about 1 ft/s. The highest velocity is about 3 ft/s along the retaining walls.

3.3.6.1.6 Run 6

The high velocities which are noted along the retaining walls in Runs 3 and 4 are the result of the 3 ft high spillway flip bucket. In Run 6, the height of the flip bucket was reduced in an effort to reduce the maximum velocity along the retaining walls. The flip bucket height was decreased to 1.5 feet (Figure 32) and the design was tested with the 100 year flow, the same flow used in Run 3. The post processed result figures are included in Appendix C-6.

Changing the configuration of the spillway flip bucket does not change the flow patterns upstream of the spillway. Therefore, discussion of Run 6 is limited to the flow patterns downstream of spillway. Figures C-6-13 through C-6-15 show the lower flip bucket results in a submerged jet which is approximately parallel with the spillway apron. The highest velocities are about 1.5 to 3 feet above the apron. Figures C-6-18 through C-6-26 show that velocities at the T-Screen intake are about 7 ft/s. Along the right retaining wall, velocities are reduced to about 2 ft/s. Along the left retaining wall velocities are similar but slightly lower than to those of Run 3.

3.3.6.1.7 Run 7

The results of Run 6 showed that the 1.5 ft high flip bucket is less effective at reducing the velocity along the apron floor and the left retaining wall than desired. In Run 7, a flip bucket height between the 1.5 ft and 3 ft flip buckets is investigated. Therefore, a height of 2.25 ft of the flip bucket (Figure 32) is incorporated into Run 7, all other aspects of Run 7 are the same as Run 3. The post processed result figures are presented in Appendix C-7.

Figures C-7-13 through C-7-15 show the 2.25 ft high flip bucket creates a reverse flow in the bottom of the water column along the apron. Near bed velocities for Run 7 are significantly

lower than those of Run 6. Figures C-7-18 through C-7-21 show the high velocity zone along the left and right retaining walls is separated from the walls and the near wall velocities are relatively low. The water velocity at the T-screen intake is about 1 to 2 ft/s. A maximum velocity of about 4 to 5 ft/s is noted in the riprap section area.

3.3.6.2 Pressure Force

For runs 2 through 7, the total pressure force on the pipe riser and water intake screen is listed in Table 3. In the table, a negative force means the direction of the force is towards the negative direction of the axis. For all the cases, the net Z direction force is negative which means that the intake structure experiences a vertical down force. For Run 7 the net horizontal force is about 1500 lbs and the net vertical force is about 1200 lbs.

4.0 PHYSICAL MODELING

4.1 Inlet, Tunnel and Outlet Model

4.1.1 Objectives

The objectives if the Inlet, Tunnel and Outlet Model were to 1) establish a rating curve for the inlet morning glory spillway 2) evaluate the potential air entrainment in the tunnel and the need for any air bleed structures 3) establish junction loss coefficients for the 4th Street and 8th Street lateral junctions 4) determine and fluctuating pressures due to flow induced excitations at the tunnel portal to the recirculation pump intake with closed valve and 5) obtain a rating curve for the outlet spillway/weir.

4.1.2 Similitude and Scaling Considerations

To properly simulate the kinematics and dynamics of the flow phenomena to be investigated, an undistorted geometric model is required. The flow in the approach channel to the morning-glory spillway inlet, flow over the morning-glory spillway and into the vertical shaft and the outflow from the outlet structure and weir are all free surface (or open-channel) flows and hence, inertial and gravitational forces are dominant. A necessary condition of similitude is for the model Froude number to be equal to the prototype value. In addition, the flow within the tunnel and the

4th and 8th Street junctions could be closed conduit flow and consideration must also be given to the model Reynolds number, such that viscous forces will not significantly affect the model similitude.

The Froude number represents the ratio of fluid inertia to gravitational forces, and is given by

$$F = \frac{V}{(gy)^{0.5}} \quad (1)$$

where

V = characteristic velocity, ft/sec

y = characteristic flow depth, ft

g = gravitational constant, ft/sec^2

In a Froude model,

$$F_m = F_p \quad (2)$$

or

$$F_r = 1 \quad (3)$$

where

m = model parameter

p = prototype parameter

r = ratio of model to prototype

Substituting Equation (1) to Equation (2), and defining the length ratio as in Equation (4), results in the velocity scale ratio given in Equation (5). The depth (y), velocity (V) and flow (Q) will be scaled in the model as follows:

$$y_p / y_m = L_r \tag{4}$$

where L_r is the length scale ratio,

$$V_r = (L_r)^{0.5} \tag{5}$$

The flow ratio, Q_r, may be written as

$$Q_r = A_r V_r \tag{6}$$

where

Q = flow, ft^3/s

A = area, ft^2

Substituting Equation (5) into Equation (6), and noting that A can be dimensionally expressed as L^2, yields

$$Q_r = L_r^{5/2} \tag{7}$$

4.1.2.1 Viscous Scale Effects in the Model

In addition to the dominant inertial and gravitational forces, viscous forces can affect the flow in the approach channel to the morning-glory spillway, being an open channel flow. The viscous forces are not completely scaled in a Froude model, resulting in "scale effects," which must be evaluated relative to their possible effect on model results. In the prototype, viscous forces are

small compared to inertial forces, i.e., the prototype has high Reynolds numbers. Scale effects due to viscous forces are minimized by selecting a model scale that produces Reynolds numbers well into the turbulent range and high enough to assume no significant effects on flow patterns involving flow separations. The Reynolds number (the ratio of inertial forces to viscous forces) for open channel flow is defined as

$$\mathrm{Re} = \frac{VD}{\nu} \tag{8}$$

where

Re = Reynolds number

ν = kinematic viscosity, ft^2/sec

V = average pipe velocity, ft/sec

D = 4x Hydraulic Radius (R_H), ft

For free surface channel flow, the hydraulic radius, R_H, is given by,

$$R_H = A/P \tag{9}$$

and

A = flow area, ft^2

P = wetted perimeter, ft

Turbulent flow occurs when the Reynolds number is above approximately 2,000. The model scale should be chosen so that the model Re for the inflow and outflow channels (with open channel flow) is well above 2,000.

To simulate the closed conduit flow patterns in the long tunnel correctly, the form losses due to bends, expansions, contractions and junctions should be scaled correctly. This requires the corresponding loss coefficients are more or less independent of the Reynolds number (Re) in the tunnel. For Re above 1 x 10^5, the loss coefficients are considered independent of Re [1]. The model Re should be above this value at the Froude scaled design flow in the model.

4.1.2.2 Simulation of Tunnel Hydraulic Gradient Line (HGL)

To have the upstream water levels correct, the Hydraulic Gradient Line (HGL) that is governed by total losses in the tunnel including friction losses and minor losses (form losses) also need to be properly simulated. A design flow (100 year flood flow) was selected for HGL simulation as the tunnel friction loss (governed by the friction factor for the tunnel) can be exactly simulated for only one selected flow in the model, the losses being a function of Reynolds number. The tunnel friction losses for other tested flows would only be approximate. However, the rating curves for both upstream morning glory spillway and the downstream ogee spillway would be independent of the water levels in the inlet and outlet shafts and hence the HGL. Also, the loss coefficients of the 4th and 8th Street junctions as well as the bends and expansions are not significantly influenced by friction losses as they are dominated by form losses.

To allow a correct simulation of the velocity profiles in the tunnel, the friction factor, f, should be as close as possible to that in the field at the flow corresponding to design flow (100 year flood flow). In the model, as both the flow and Re would be much lower than that in the field, the model needs to use a smooth walled pipe such as Plexiglas pipes. Even with the use of smooth pipes in the model, the friction factor in the model may be higher than that in the prototype (due to lower Re values in the model than prototype). In order to get the total losses scaled correctly, some reductions to the straight lengths of the tunnel between the junctions were needed. Such reductions are acceptable as long as the sufficient straight lengths are provided upstream and downstream of junctions so that fully developed flow velocity profiles are reasonably simulated. Simulation of friction losses usually require a trial and error procedure and if the reduced lengths result in somewhat lower total losses than that is required, it would be necessary to add few inserts along the modeled tunnel length (orifices), as needed. However, the

inserts should not cause large constrictions that could result in any significant air bubble accumulation upstream.

4.1.2.3 Selection of Geometric Scale

Based on the above considerations and other practical considerations such as availability of commercial pipes, space requirements and cost, a geometric model scale of 1:33 was chosen for the physical model. With this scale, the length (or water depth), velocity, flow, and time scales would be:

$$L_r = L_m / L_p \quad : \quad 1{:}33 \qquad (10)$$

$$V_r = V_m / V_p \quad : \quad 1{:}5.74 \qquad (11)$$

$$Q_r = Q_m / Q_p \quad : \quad 1{:}6255.8 \qquad (12)$$

$$T_r = T_m / T_p \quad : \quad 1{:}5.74 \qquad (13)$$

4.1.2.4 Similitude of Air Entrainment in the Vertical Downward Flow Shaft

The 1:33 geometric scale hydraulic model study is based on Froude Similitude. The air concentration , C, in self aerated flow generated by the morning-glory spillway just at the nappe (jet) impact location in the vertical shaft, expressed as Qa/Qw (where Qa is the volume flow rate of air and Qw is the volume flow rate of water) is a function of Froude number, as documented in literature [2,3]. Hence, C is theoretically the same in the model as in the prototype at the impact location in the shaft. (see Reference [2] for C versus F relationships in Morning Glory Spillways). However, based on Reference [4] (the paper titled “Aeration in jets and High Velocity Flows” by Henry Falvey and Alan Ervine), even though the air entrainment generated by a plunging jet, given by the air concentration Qa/Qw, is mainly a function of Froude Number, in a reduced scale hydraulic model the air entrainment in the model may be affected by the much lower magnitude of the impact velocity in the model and a scale effect term (to obtain a correction factor) may have to be considered to address the ratio of air entrainment in the model

to that in the prototype. Air entrainment (concentration of air) for high velocity jet impingement is given by,

$$Qa/Qw = E^* f(F) \quad (14)$$

where E* , the scale effect term, is calculated from the following equation:

$$E^* = 1-(Um/Uj) \quad (15)$$

where Um is the minimum velocity to entrain air (assumed to be 1 m/s based on Ref.4) and Uj is the jet velocity at the point of impact in the model; f(F) is a function of Froude Number. Using Eq. (15) the value of E* in the model (Em*) and that in the prototype (Ep*) can be calculated separately. In a model operated based on Froude similitude, f(F) in Eq. (14) would be same in the model as in the prototype. Hence, the ratio of air entrainment in the prototype to that in the model (operated based on Froude similitude) will be given by Ep*/Em*.

4.1.2.5 Similitude of Air Entrainment in the Tunnel

As discussed in the previous section, the air entrainment in the model shaft due to the jet impingement on the water surface can be used to predict the corresponding air entrainment in the prototype only after incorporating correction factors to account for scale effects. The bubble sizes in the air entrained flow from the vertical shaft will not be scaled as both the model and prototype can have similar bubble sizes (i.e. the bubble size in the model is not reduced as the length scale would require). As the bubble rise velocities generally are much lower than the downward flow velocity in the shaft in model and prototype, the volume rate at which the bubbles rise to the surface in the shaft would be negligible compared to the volume rate of bubbles carried by the flow into the tunnel. The actual pressures in the model tunnel would be significantly lower, noting that pressure affects bubble sizes. The two-phase flow regime in the tunnel will not be the same in the model as in the prototype, as the flow regime (whether slug flow or elongated bubbly flow or stratified flow) depends on the magnitudes of water and air velocities in addition to air concentrations.

4.1.2.6 Bar Racks

The model bar racks were fabricated to simulate approximately the same percent open area and bar thickness to depth ratio as in the prototype, thus giving the same guidance to the flow. The actual bar thickness was not scaled geometrically, but bars of suitable thickness were used to provide a model bar Reynolds number above 100 so that any Reynolds number effects in the model are negligible, see Reference [5]. Bar racks with 0.125" thick and 0.833" deep bars at 0.417" spacing were used in the model to represent 0.375" thick and 2.5" deep bars at 1.25" spacing in the prototype. A comparison of the model and prototype bar racks/screens is given below.

	Parameter	Prototype Bar Rack	Model Bar Rack
1.	Bar Thickness, b	0.375"	0.125"
2.	Bar Depth, d	2.5"	0.833"
3.	Clear Spacing of Bars, w	1.25"	0.417"
4.	d/b	6.66	6.66
5.	Percent Open Area	77%	77%
6.	Bar Reynolds Number+ @ 100 yr average screen flow	8,411	488

+ Reynolds number based on approach velocity and bar thickness [5].

Based on the above, the model racks/screens should provide similar guidance to the flows and scaled losses as in the prototype. It should also be noted that the velocity profiles upstream of the bar screens would be simulated correctly in a Froude scaled model and any influence of velocity profiles on losses will be accounted for in the model.

4.1.2.7 Assumptions and Limitations of Hydraulic Model

Based on the similitude and scaling considerations the following are the assumptions and consequent limitations of the hydraulic model:

a. Froude similitude is required, gravity being the predominating force governing the flows in both inlet and outlet structures including the flow approaching and entering the morning-glory spillway. In order to minimize any viscous scale effects in the approach channel and tunnel and to simulate correctly the tunnel losses that govern the upstream water level in the vertical shaft for a controlled downstream water level in the outlet structure and thereby establish the expected HGL, the model had to be designed for one selected design flow, which is determined to be the 100 year flood flow. Hence, for other flows such as 10 year, 25 year or 50 year flow, the model will not exactly simulate the tunnel losses, the HGL along the tunnel and the water level in the vertical shaft downstream of the morning-glory spillway. However, the flow over the spillway and the upstream water surface elevations in the channel as well as the controlled water level in the outlet structure will not be affected and hence, the model can be used to develop rating curves.
b. The tunnel friction factor, f, in the field within the ranges of tunnel flows of interest and corresponding Reynolds numbers (Re) does not vary much as the tunnel wall is significantly rough. In a reduced scale hydraulic model operated based on Froude similitude, the Reynolds number would be lower than that in the prototype and even with smooth walled pipes; it is difficult to simulate the friction losses for a range of flows. Hence, the tunnel friction losses are simulated in the model only for the selected design flow (with inserts to add headloss, if needed) as the full tunnel length is not simulated and the friction factor, f, in the model piping (smooth Plexiglas) varies with Reynolds number.
c. The junction loss coefficients in the tunnel can be determined from the model under closed conduit flow conditions. The loss coefficient is obtained for the design flow simulated in the model. The same value can be used for lower flows in the prototype as long as the flow ratios are the same and the values of Re in the prototype are above 1×10^5.

d. The bubble sizes are not scaled and hence the bubble rise velocities are not scaled. Also, the two-phase flow regime in the tunnel will not be the same in the model as in the prototype, as the flow regime (whether slug flow or elongated bubbly flow or stratified flow) depends on the magnitudes of water and air velocities.

e. Even though the air entrainment generated by jet impact inside the morning-glory shaft is mainly a function of Froude number, any measured air concentrations or volume fractions of air in the model tunnel would not exactly duplicate those in the prototype due to possible air entrainment scale effects in the reduced scale model resulting from significantly lower impingement velocities in the model shaft. Further, the bubbles sizes, pressures that affect their sizes, the bubble rise velocities and the two–phase flow regime are not exactly simulated in the model. Nevertheless, the data obtained from measurements of air concentrations (volume fractions) in the model would provide useful information towards determining the likely air entrainment in the tunnel in conjunction with further calculations based on literature.

f. The volume fraction of air in the tunnel were measured well upstream of the flow restriction orifices in the model. Also, these orifices had beta ratios (area of orifice divided by pipe area) above 80% and visual observations indicated no significant continuing air accrual upstream of the orifices.

g. Effect of air entrainment in the tunnel on HGL cannot be quantitatively evaluated from the physical model study in view of items d) and e) above. The discussions under items d) and e) are also applicable to the 4th Street and 8th Street shafts that could entrain air into the tunnel.

4.1.3 Model Description

A physical hydraulic model of the inlet structure, a portion of the tunnel, 8th and 4th Street lateral junctions and the outlet structure for the Waller Creek Tunnel Project was constructed to a scale of 1:33. The model boundary and photographs of the model can be seen in Figure 33 through 43. Model dimensions can be seen in Figure 44through 54.

The inlet portion of the model was constructed on an elevated steel platform and extended approximately 13 ft (model) upstream of the Morning Glory Spillway (MGS). The model

included the MGS intake structure and the graded area approaching the spillway. The inlet portion of the model also included any pertinent geometry which may influence the flow patterns such as the bar racks and piers at the MGS as well as the turning vane as derived by the CFD model.

Portions of the tunnel including the inlet drop shaft, 8th and 4th Street lateral junctions (including tunnel transitions) and outlet transition were modeled. The tunnel has a circular crown and side walls and 10 foot flat portion in the bottom. The flat bottom of the tunnel sections was modeled by adding flat insert of the appropriate scale width in the bottom of the model tunnel sections. No flow was able to pass under the flat insert in the model as would be with the prototype tunnel. A summary of the prototype and model tunnel parameters can be seen below:

Location	Prototype Diameter (ft)	Prototype Equivalent Diameter (ft)	1:33 Scale Model Diameter (in)
12th St Drop Shaft	20	20	7.25
Tunnel Between Inlet and 8th St Lateral	20.42	20	7.5
8th St Lateral Drop Shaft	16	16	6
8th St Lateral Junction	16.65	16	6
Tunnel Between 8th St and 4th St Laterals	22.35	22	8.125
4th St Lateral Drop Shaft	27	27	9.75
4th St Lateral Junction	20.42	20	7.5
Tunnel Between 4th St Lateral and Outlet	26.25	26	9.5
Vertical Shaft at Outlet Structure	40	40	14.56

The entire length and the slight bends of the tunnel were not simulated. Segments of the tunnel between the inlet, lateral junctions and outlet were shortened. The length of tunnel between the Inlet drop shaft and the 8th Street junction, the 8th and 4th Street junctions and the 4th Street junction and the outlet shaft were 31.7 ft, 33.7 ft. and 31.5 ft, (model) respectively. Provisions were made to adjust friction losses for the shortened portions, if required, by adding more losses artificially (using large beta ratio orifice plates) so that the expected friction losses in the prototype could be simulated as closely as possible. The portal that supplies flow to the recirculation pump intake was also modeled up to the knife gate valve with a dead end (to simulate a closed valve).

The outlet portion of the model was also constructed on an elevated steel platform and included the outlet alternative 2 from the tunnel (as selected from the outlet CFD model), outlet basin and containment, outlet spillway (with flip bucket as derived by the outlet CFD model), discharge apron and a portion of Lady Bird Lake. The T-screen located on the discharge apron was also modeled as an obstruction to the flow.

A flow loop, as shown in Figure 55, was formed with pumps drawing the appropriate flow from a depressed laboratory sump, discharging to the model inlet, lateral junctions and upstream boundary of Lady Bird Lake flowing via gravity to the discharge structure and out through Lady Bird Lake. The water level in Lady Bird Lake was set using an adjustable tip gate at the downstream model boundary. With this loop, flows were set and sufficient recirculation time was allowed for the model water levels and conditions to stabilize and become steady before any measurements were recorded.

4.1.4 Instrumentation and Measuring Techniques

4.1.4.1 Flow

All inflows including the inflow to the model simulating flow from Waller Creek, the lateral junctions and Lady Bird Lake were measured with a standard ASME orifice meters installed in the corresponding inflow lines. The differential head from the orifice meters were measured using differential pressure transducers recorded with a computerized data acquisition system. The accuracy of the flow meters is estimated at ±2%.

4.1.4.2 Water Levels

Water surface elevations were measured using piezometric taps connected to a calibrated differential pressure cell, the output of which was recorded and displayed by computer. The accuracy of the system was approximately ±0.2 ft prototype. The locations of the piezometers are shown in Figure 56 through 59.

4.1.4.3 Velocity

Velocities in the model were measured using a miniature propeller velocity meter. The meter was calibrated to an accuracy of approximately ±2 percent by means of calibrated tow tests, and had a low end stall threshold of approximately 0.2 ft/sec model, (about 1.2 ft/sec prototype).

4.1.4.4 Pressure

Pressure fluctuations at the tunnel portal to the recirculation pump intake with closed valve were measured using a single sided pressure transducer with a range of 0-2.5 PSIG and response time of less than 1 millisecond (0.001sec). The accuracy of the transducer was approximately ± 0.5 percent.

4.1.4.5 Free Surface Vortices

In order to systematically evaluate the strength of vortices at submerged intakes, Alden uses a vortex strength scale of Type 1 to Type 6, as shown in Figure 60, where Type 1 is a surface swirl and Type 6 is an open air-core vortex to the inlet. Vortex types were identified in the model by visual observations.

4.1.5 Test Plan

The scope of testing included the following:

- Evaluate the potential air entrainment in the tunnel and the need for any air bleed structures,
- Establish a rating curve for the morning glory spillway,
- Determine any fluctuating pressures due to flow induced excitations at the tunnel portal to the recirculation pump intake when the valve is closed,
- Establish junction loss coefficients for the 4th Street and 8th Street lateral junctions and,
- Obtain a rating curve for the outlet spillway/weir.

The rating curves were established using the 2, 5, 10, 25, 50, 100 and 500 year peak tunnel/peak intervening flow conditions. Fluctuating pressures at the tunnel portal to the recirculation pump intake when the valve is closed were measured for the 100 year peak tunnel/peak intervening flow condition only and junction loss coefficients for the 8th and 4th Street lateral junctions were determined for both the 100 year peak tunnel/peak intervening and lagging tunnel/peak intervening. Test flow conditions can be seen in Table 4.

4.1.6 Results

4.1.6.1 Air Entrainment

Upon model start up with the simulated 100 year flood flow (and at subsequently tested lower flows) air entrainment at the morning glory shaft was observed. The downward velocities in the shaft were high enough to draw air bubbles down into the tunnel resulting in air entrainment in the tunnel. Tests were conducted to estimate the air concentrations in the tunnel resulting from air entrainment at the morning glory spillway. These estimations could then be used to confirm additional hydraulic evaluation or calculations conducted by the Joint Venture (JV) to help determine the need for any air bleed structures in the tunnel.

For tunnel flows corresponding to the 100 year and 25 year floods as shown in the test matrix in Table 4, tests were conducted to estimate the air concentrations in the tunnel resulting from air entrainment at the morning glory spillway. The air bubbles entrained at the morning glory spillway resulted in a two-phase flow regime, which was more or less stratified or very elongated bubbles. However, the flow was not totally stratified since small bubbles were present in the liquid flow region, more so for the 100 year flood case where the flow velocities are higher in the tunnel. Once the flow was steady and no air accumulation or removal was evident, the Volume Fraction of air was determined from the fraction of the cross-sectional area occupied by the air at a selected location in the model (approximately 19 pipe diameters downstream of the 90 degree elbow at the tunnel entrance). The measurements were taken upstream of the most upstream orifice plate (used to simulate friction and HGL). Testing was conducted once the air-water interface along the top of the model tunnel had reached more or less an equilibrium point. Significant continuing air accrual upstream of the orifice was not observed during testing. Any

trapping of the air caused by orifice plate would yield conservative results as this would increase the cross-sectional area occupied by the air. Even though the flow was steady, the water–air interface was unstable. Using photographs, measurements of the depth to the interface from the pipe wall was measured several times and averaged to obtain an average cross-sectional area occupied by air, A_a and the average cross-sectional area occupied by water, A_w. Dividing A_a by the total flow area ($A_a + A_w$) gives the average volume fraction of air, VF_a. Since, the volume of the small air bubbles in the water region was very small compared to the volume of the stratified air, based on visual observations, the contribution of the small bubbles was ignored in determining VF_a.

As the Volume Fraction of air, VF_a, can be a function of pressure and temperature, the actual pressure and temperature at the measurement location were measured and recorded. Knowing the expected pressure (from HGL calculations) and temperature, one can calculate the estimated volume fractions in the field using ideal gas equation. It is expected that the pressure in the field will be greater than the pressures in the model hence, the volume fraction of air in the field should be less than that measured in the model.

Table 5 shows a summary of the test data and results. The average values of A_a and A_w shown in the Table are average values obtained from at least 16 measurements from photographs of the water-air interface. The maximum values of A_a and A_w are the maximum values obtained from the test photographs. Typical photos are shown in Figure 61 and 62.

Results show that the average Volume Fraction of air (VF_a) in the model is about 5% for 25 year flow and 4% for the 100 year flow. Maximum Volume Fraction of air (VF_a) in the model for the 25 year and 100 year flows are 8% and 6%, respectively.

Possible reasons why the Volume Fraction for 25 year flow is slightly higher (even though the flow is lower) may be that the water surface elevation in the shaft is lower for 25 year flood, which could increase the nappe (jet) drop height for the morning glory spillway resulting in higher impingement velocity on shaft water surface.

Taking into account measurement accuracies and scale effects, for hydraulic evaluation purposes, it is suggested that 5 % should be added to the model indicated VF_a value, irrespective of whether the average or maximum is used. Alternatively, using available literature (such as the Reference [4] (Model-Prototype Correlation of Hydraulic Structures "Aeration in Jets and High Velocity Flows"; Falvey and Ervine) the model values can be corrected to account for scale effects in the model and predict prototype values using correction factors. Further corrections may be needed to account for pressure differences between model and prototype. Calculations indicate that for the 25 year event (which has a significant fall height), the prototype VF_a would be about 1.75 times the VF_a measured in the model.

4.1.6.2 Inlet Rating Curve

Tests were conducted using the model to establish a rating curve for the morning glory spillway. Prior to testing, the HGL elevation in the inlet drop shaft in the model (corresponding to the 100 year peak tunnel/ peak intervening HGL) was confirmed to match closely the corresponding preliminary estimated elevation provided by the JV in January 2010. The peak tunnel/peak intervening flow condition was selected because initially junctions loss measurement were going to be conducted at the same time and this scenario would provide high enough flows for these measurements. Initially it was thought (based on friction calculations) that some additional losses may be required in the model to match the water level in the 12th Street inlet shaft. Addition loss would have been added by installing two or three large beta ratio orifice plates however, subsequent testing indicated that these plates were not required. The calculated HGL at the 12th Street inlet shaft for the 100 year peak tunnel/ peak intervening condition was EL 472.5 feet. Without any friction orifice plates installed the average HGL elevation at the 12th Street Inlet Shaft in the model for the 100 year peak tunnel/ peak intervening condition was EL 473.5 ft indicating good agreement between the calculated and model 12th Street inlet shaft water levels. Velocity measurements were also recorded at the leading edge of the flow distribution vane and adjustments were made to the flow distributor at the upstream model boundary to match approximately the flow distribution as predicted by the inlet CFD model. A comparison between the CFD and physical flow distribution at the flow distribution vane can be seen in Figure 63. Once the HGL and velocity distribution had been confirmed the morning glory rating curve was established.

The morning glory rating curve was established by setting the inlet flows for the 2, 5, 10, 25, 50, 100 and 500 year peak tunnel/ peak intervening events. The water levels were allowed to stabilize and then recorded. For the purpose of developing the rating curve, 5 second average water levels from three piezometric taps located upstream and downstream of the bar racks as shown on Figure 56 were used. Clean bar racks were used for all of the testing. During the 500 year event the morning glory spillway was submerged and an air drawing Type 6 vortex was observed. Data was also recorded for two additional flows to determine the point at which the weir becomes drowned out (approximately 9,950 cfs at EL 483.2 ft) and the transition from weir control to orifice control occurs. The morning glory rating curve is shown in Figure 64. Additional water levels in the inlet were also recorded at the position shown in Figure 56. A summary of these water levels can be seen in Table 6.

To determine any effects that the HGL in the inlet drop shaft may have on the morning glory rating curve, two additional tests were conducted. For the 100 year peak inlet flow condition (8,247 cfs), the average HGL was increased in the inlet shaft to above the morning glory spillway crest EL (474.0 ft) to EL 478.2 ft and 479.7 ft to test the effect on the inlet rating curve. For the case with the HGL of EL 478.2 ft the measured water levels upstream and downstream of the bar racks were EL 481.7 ft and EL 481.4 ft, respectively. For the case with the HGL of EL 479.7 ft the measured water levels upstream and downstream of the bar racks were EL 481.8 ft and EL 481.5 ft, respectively. These tests indicate that for these submerged conditions, no change in the head on the morning glory spillway was observed. Any differences in head were within the measurement accuracies of the model. Therefore, the inlet rating curve is hydraulically disconnected from the inlet shaft HGL for up to at least 479.2 ft

4.1.6.3 Pressure Fluctuations at the Portal

Testing was conducted to determine any fluctuating pressures due to flow induced excitations at the tunnel portal to the recirculation pump intake when the valve is closed using the 100 year peak tunnel/ peak intervening condition as shown in Table 4. The portal is expected to be subjected to significant pressure fluctuations being located very close to the 90 degree elbow. The pressure fluctuations were measured for a period of one minute in the model with a single sided pressure transducer which was mounted at the centerline of the tunnel portal valve

centerline (EL 427 ft.). A plot of the prototype pressure versus time fluctuation referenced to EL 427 ft can be seen in Figure 65. The maximum, minimum and average pressures were 16.9, 15.5 and 13.4 psi, respectively.

4.1.6.4 Lateral Junction Losses

Tests were conducted using the model to determine the minor losses and corresponding loss coefficients at the 8th Street and 4th Street lateral junctions and the tunnel (tees combining main flow in the tunnel with flow from side inlet weir branch). To allow accurate head loss measurements, air entrainment in the tunnel was not desired. Hence, for these measurements, the discharge of the model was modified to provide a higher water level such that the morning glory inlet was submerged and no air was entrained into the tunnel. Hence, loss coefficients were determined with the tunnel flowing full.

The loss coefficients for the main tunnel for determining the losses from upstream to downstream of the junction at both 8th Street and 4th Street included the losses in the tunnel transition piece immediately upstream of the junction. Similarly, the loss coefficient for the 8th Street and 4th Street shafts to determine the losses from the drop shaft to downstream of the junction included the losses in the upstream elbow (or drop shaft to lateral connection at 4th Street) and the entrance to the tunnel.

For convenience, the location in the shaft connector pipe upstream of the elbow, the location in the tunnel upstream of the tunnel transition and the location in the tunnel downstream of the junction are identified as 1, 2 and 3 respectively. The definition of the loss coefficients is as follows:

Main Tunnel loss coefficient ($K_{2\text{-}3}$) to calculate losses from upstream of the tunnel transition to downstream of the junction (including losses in the transition):

$$K_{2\text{-}3} = [(h_2 + V_2^2/2g) - (h_3 + V_3^2/2g)]/ (V_3^2/2g) \quad (16)$$

Eq. (16) can be written as,

$$K_{2\text{-}3} = [(V_2^2/2g) - (V_3^2/2g) + (h_2\text{-}h_3)]/ (V_3^2/2g) \quad (17)$$

Shaft loss coefficient ($K_{1\text{-}3}$) to calculate losses from upstream of junction in the drop shaft to downstream of junction in the tunnel (including elbow or drop shaft to lateral connection losses in the shaft piping):

Similar to Eq (17),

$$K_{1\text{-}3} = [(V_1^2/2g) - (V_3^2/2g) + (h_1\text{-}h_3)]/ (V_3^2/2g) \quad (18)$$

where h_1, h_2 and h_3 are the piezometric heads at locations 1, 2 and 3 respectively and V_1, V_2 and V_3 are the velocities at locations 1, 2 and 3 respectively.

Hydraulic Gradient Lines (HGL) were established upstream and downstream of each of the junctions to determine (h_2-h_3) for use in Equation 17. For the drop shaft, the piezometric heads at locations 1 and 3 were used to define (h_1-h_3) for use in Equation 18 as not enough straight piping along the shaft was available to establish an HGL in the drop shaft. The HGL data in the tunnel was collected with a differential pressure transducer and scanning valve system to scan through four piezometer taps located along the modeled tunnel upstream of each junction (upstream of tunnel transition) and four taps downstream of each junction with a sampling time of 1 minute in the model for each port to average any pressure fluctuations. For the drop shaft to tunnel losses, measurements were made using an air over water manometer to determine the differential between the downstream tunnel and drop shaft grades. The HGL data was imported into a spreadsheet and both the HGL and Energy Gradient Lines (EGL) were determined for the tunnel upstream and downstream of each junction. Points on the energy gradient line are defined as $E= h + (V^2/2g)$. A straight line fit was made to the energy data points at each junction. The energy lines upstream of the junction were extrapolated to the beginning of the tunnel transition and the energy lines downstream of the junction were extrapolated to the junction centerline intersection, at which the difference in the elevation of these lines indicate the energy loss. The HGL, EGL plot and determination of $h_{2\text{-}3}$ and $h_{1\text{-}3}$ for the 8th and 4th Street lateral junctions are shown in Figure 66 through 69. All measurements were conducted at the 100 year condition, which was the base design flow for the model, as at lower flows some scale effects are possible

in the model. Both Peak Tunnel/Peak Intervening and Lagging Tunnel/Peak Intervening cases as shown in Table 4 were tested. The loss coefficients obtained from the 100 year flood case in the model can be used for lower flows in the prototype (with corresponding velocity heads downstream of the junctions) as long as the tunnel Reynolds numbers are above 1 x 10^5 and the flow splits are similar.

Results indicating the Loss Coefficients determined from the model for the 100 year flood for both Peak Tunnel/Peak Intervening and Lagging Tunnel/Peak Intervening are shown below:

	100 yr Peak Tunnel/Peak Int.		100 yr Lagging Tunnel/Peak Int.	
Loss Coefficient	8^{th} St.	4^{th} St.	8^{th} St.	4^{th} St.
K_{2-3}	0.3	0.2	0.3	0.3
K_{1-3}	-0.6	-0.7	-0.4	-0.4

The branch loss coefficients (K_{1-3}) are negative due to transfer of energy from the through flow in the tunnel to the flow from the branch as the branch flow is only about 10% or so of the tunnel flow. This phenomenon is documented in the literature [1] (see "Internal Flow: A guide to Losses in Pipe and Duct Systems" by Donald S. Miller, BHRA Report)

Even though, the junction designs do not exactly conform to the sharp edged 45 degree combining tees, the above loss coefficients obtained from the model data showed a reasonable agreement with those obtained from literature, allowing a margin to account for the geometry deviation from standard 45 degree tees. For example, the loss coefficient curves relating branch to main flow ratios, area ratios and loss coefficients for 45 degree combining flow tees (as per Figure 5.2.1 and 5.2.2 of Ref. 1) predicted a K_{1-3} value of about -0.6 for 100 year peak tunnel/peak intervening flows for both 8^{th} and 4^{th} street junctions, and a value of about -0.4 for 100 year lagging tunnel/peak intervening flow for both 8^{th} street and 4^{th} street junctions respectively. The corresponding predicted K_{2-3} values (based on Ref. 1) are about 0.15 for peak tunnel/peak intervening flows and 0.18 for lagging tunnel/peak int. for both 8^{th} and 4^{th} street

junctions. The model predicted values are higher as one would expect considering that the main tunnel diameters downstream of the junction is larger than the upstream resulting in an expansion loss in addition to the tee loss.

4.1.6.5 Outlet Rating Curve

The outlet structure spillway was established by setting the inlet flows for the 2, 5, 10, 25, 50, 100 and 500 year peak tunnel/ peak intervening events. The water levels were allowed to stabilize and recorded. For the purpose of developing the rating curve, average water levels from four piezometric taps located approximately 10 ft (prototype) upstream of the spillway as shown on Figure 59 were used. The outlet structure spillway rating curve is shown in Figure 70.

5.0 CONCLUSIONS

Based on the results of the hydraulic model studies including both CFD models and a physical model study using a 1:33 geometric scale model to evaluate the Waller Creek Tunnel Project structure hydraulics, the following conclusions are drawn:

5.1 CFD Models

- Initial inlet model results indicated a training wall was required to improve flow distribution approaching the morning glory spillway and bar racks
- A training structure was designed for the inlet. Model results show that with the training structure installed 80% of the bar screen area has a velocity of less than 4 ft/s. The maximum velocity at any location on the screens is less than 5.5 ft/s. The final design was evaluated in the physical model.
- To address concerns that debris may accumulate along the backside of the training wall barbs, modifications were made to fill in the backside of the inlet training wall barbs. With the modifications the model results show that two screens did not have 80% of the bar screen area velocities of less than 4 ft/s and one screen exceeded the 50 % flow variation from the target flow. This design was selected by the JV as the final design to be included in the physical model.

- The 8th Street and 4th Street lateral junction model results showed that the lateral junctions are not predicted to cause significant flow separations in the main conduit and cavitation potential is small.
- Based on the Outlet CFD model results, Outlet connection 2 was selected (Figure 17).
- The final structure design, based on CFD results, shows uniform flow distribution over the spillway.
- The 2.25 ft high flip bucket at the toe of the dam decreased the water velocity near the bed of the discharge channel as compared to a no flip bucket condition.
- Water velocity near the end of the spillway with the 2.25 ft high flip bucket is not predicted to erode the spillway apron.

5.2 Physical Model

- Air entrainment at the morning glory inlet was observed.
- Estimates from the model indicate the average Volume Fraction of air (VF_a) in the model is about 5% for 25 year flow and 4% for the 100 year flow. Maximum Volume Fraction of air (VF_a) in the model for the 25 year and 100 year flows are 8% and 6%, respectively.
- For hydraulic evaluation purposes, whichever value of VF_a is used, 5 % should be added to this value to account for any scale effects and measurement accuracies. Alternatively, corrections factors suggested in Reference [4] (Model-Prototype Correlation of Hydraulic Structures “Aeration in Jets and High Velocity Flows”; Falvey and Ervine) may be used correct air entrainment for scale effects. Calculations indicate that for the 25 year event (which has a significant fall height) the prototype VF_a would need be approximately 1.75 times the corresponding VF as measured in the model.
- As the Volume Fraction of air, VF_a, can be a function of pressure and temperature, knowing the expected pressure (from HGL calculations) and temperature, one can calculate the estimated volume fractions in the field using the ideal gas equation. It is expected that the pressure in the field will be greater than the pressures in the model hence, the volume fraction of air in the field should be less than that measured in the model.

- A rating curve for the morning glory spillway was developed which is shown in Figure 64.
- The flow at which the weir becomes drowned out and the transition from weir control to orifice control occurs is approximately 9,950 cfs at a water level of EL 483.2 ft.
- For the 100 year peak inlet flow condition the average HGL was increased to EL 479.7 ft at the 12th Street Inlet and no change in the head on the morning glory spillway was observed.
- A plot of the prototype pressure versus time fluctuation at the tunnel portal to the recirculation pump intake when the valve is closed using the 100 year peak tunnel/ peak intervening condition (referenced to EL 427 ft) be seen in Figure 65. The maximum, minimum and average pressures were 16.9, 15.5 and 13.4 psi, respectively.
- Results indicating the Loss Coefficients determined from the model for the 100 year flood for both Peak Tunnel/Peak Intervening and Lagging Tunnel/Peak Intervening are shown below:

	100 yr Peak Tunnel/Peak Int.		100 yr Lagging Tunnel/Peak Int.	
Loss Coefficient	8th St.	4th St.	8th St.	4th St.
K_{2-3}	0.3	0.2	0.3	0.3
K_{1-3}	-0.6	-0.7	-0.4	-0.4

- The branch loss coefficients (K_{1-3}) are negative due to transfer of energy from the through flow in the tunnel to the flow from the branch as the branch flow is only about 10% or so of the tunnel flow.
- A rating curve for the outlet structure spillway was developed which is shown in Figure 70.

6.0 DISCUSSION ON AIR VENTING

Air entrainment calculations by the JV have concluded that based on the estimated air entrainment for 100 yr and 25 yr events, the predicted flow regime in the tunnel is bubbly flow. Other flow pattern maps such as that by Hoogendoorn [7] (see Figure 10.12, "The Flow of Complex Mixtures in Pipes", Govier, G.W. and Aziz, K., Van Nostrand Reinhold 1972) show the same conclusion. Further, Hoogendoorn maps indicate that for flow velocities in the tunnel corresponding to 100 yr Lagging Tunnel and Peak Tunnel flows, bubbly flow regime prevails in the tunnel for air concentrations (volume fractions) of up to about 30%. Similarly for the flow velocities corresponding to the 25 yr Lagging Tunnel and Peak Tunnel flows bubbly flow regime exists for air concentrations (volume fractions) of up to about 20%. Hence, sufficient margin of safety to the calculated air concentrations using model data may be available for at least 25 yr and 100 yr Lagging Tunnel and Peak Tunnel flows to assure a dispersed bubbly two-phase flow regime in the tunnel. The bubbly flow in the horizontal (or near horizontal) tunnel, will have most of the bubbles dispersed over the upper half of the tunnel which may enable the bubbles to escape more easily through the outlet and the 4th and 8th Street shafts with proposed modification to tunnel geometry such as aligning the tunnel crests at junctions and avoiding any sudden elevation changes (at transitions) along the top of the tunnel. For lower flows such as 5 yr and 2 yr flood flows, the flow regime could be elongated bubble or slug flow. Air venting under this condition needs to be addressed by JV to confirm that any backing up of slugs of air towards the inlet would be avoided.

A flood event is described by the hydrograph, with the flow through the morning glory spillway as a function of time. Hence, the tunnel flow velocity and the air concentrations in the tunnel including air generated in the shaft and drawn into the tunnel, are all functions of time. An evaluation of all the above hydraulic parameters during the falling limb of the hydrograph may be required to evaluate proper venting of air in the tunnel at any time. At lower flows (rising and falling limbs of the hydrograph) air bubbles will be elongated bubbles at the top of the tunnel and many such elongated bubbles are likely to escape through the 4th and 8th Street shafts, even though the volume of air escaping through the 4th and 8th street shafts may be difficult to predict. The design modifications planned by JV since completion of the hydraulic model study (such as matching the crowns at 4th and 8th Street junctions with main tunnel, increasing lateral slopes to

2.5%, increasing lateral diameters and placing the transitions with the sloping side on the top and closer to the junctions) should provide a more favorable geometry for air venting through the laterals especially at the lower flows.

7.0 REFERENCES

1. Miller, D.S., “Internal Flow Systems”, Vol.5, BHRA Fluid Engineering Series, BHRA, Bedford, England, 1978.

2. Rao, N.S.L, and Kobus, H.E, “Characteristics of Self-Aerated Flows”, Water and Wastewater Current Research and Practice, Volume 10, Erich Schmidt Verlag, Germany.

3. Falvey, H.T., Air-Water Flow in Hydraulic Structures, USBR Engineering Monograph No. 41, Dec.1980.

4. Falvey, H.T., and Ervine, D.A., “Aeration in Jets and High Velocity Flows”, Proceedings of the International Symposium on Model-Prototype Correlation in Hydraulic Structures, ASCE, Aug.1988.

5. French, R.H., "Open Channel Hydraulics," McGraw Hill, 1985.

6. ASCE Manual 97 ”Hydraulic Modeling”, ASCE, 2000

7. Govier, G.W. and Aziz,K. The Flow of Complex Mixtures in Pipes, Van Nostrand Reinhold1972.

TABLES

Table 1: Proposed Lag Tunnel/Peak Intervening Flow for 8th and 4th Street Lateral Junctions Used for Lateral Junctions CFD Models

	Return Period	1 yr	2 yr	5 yr	10 yr	100 yr	500 yr
Proposed-Lag Tunnel/Peak Intervening Flow (8th Street Lateral Junction)	Tunnel Flow (12th St. Inlet)	632	979	1972	2743	4693	6208
	8th St. Connector Tunnel Flow	260	335	547	700	1258	1701
	% Flow of 8th St. Connector Tunnel	41.1%	34.2%	27.7%	25.5%	26.8%	27.4%
Proposed-Lag Tunnel/Peak Intervening Flow (4th Street Lateral Junction)	Tunnel Flow (12th St. Inlet + 8th St. Inlet)	892	1314	2519	3443	5951	7909
	4th St. Connector Tunnel Flow	194	239	361	447	763	1015
	% Flow of 4th St. Connector Tunnel	21.7%	18.2%	14.3%	13.0%	12.8%	12.8%

Table 2: Simulation Matrix of Outlet Model

Run	Description			
	Outlet Connection	Flow Rate	Lady Bird Lake Cross Flow	Spillway Flip Bucket
1	#1	100-yr flood, 7957 cfs	no cross flow	n/a
2	#1	100-yr flood, 7957 cfs	3.5 ft/s cross flow, EL 428 ft	n/a
3	#2	100-yr flood, 7957 cfs	3.5 ft/s cross flow, EL 428 ft	3 ft high
4	#2	500-yr flood, 11270 cfs	3.5 ft/s cross flow, EL 428 ft	3 ft high
5	#2	2-yr flood, 2320 cfs	1.25 ft/s cross flow, EL 428 ft	3 ft high
6	#2	100-yr flood, 7957 cfs	3.5 ft/s cross flow, EL 428 ft	1.5 ft high
7	#2	100-yr flood, 7957 cfs	3.5 ft/s cross flow, EL 428 ft	2.25 ft high

Table 3: Pressure Force on the Pipe Riser and Water Intake Screen

Run	Description							
	Outlet Connection	Flow Rate	Spillway Flip Bucket	X-Force (lbf)	Y-Force (lbf)	Z-Force (lbf)	Horizontal Resultant (lbf)	Total
2	#1	100-yr flood, 3.5 ft/s cfs	None	757	1191	-644	1410	1561
3	#2	100-yr flood, 3.5 ft/s cfs	3 ft high	1446	-107	-1213	1450	1901
4	#2	500-yr flood, 3.5 ft/s cfs	3 ft high	1040	547	-1056	1170	1580
5	#2	2-yr flood, 1.25 ft/s cfs	3 ft high	1774	-622	-622	1880	1895
6	#2	100-yr flood, 3.5 ft/s cfs	1.5 ft high	1651	1208	-776	2050	2204
7	#2	100-yr flood, 3.5 ft/s cfs	2.5 ft high	1470	-163	-1218	1480	1919

Table 4: Waller Creek Tunnel Project Physical Model Study; Test Matrix

Peak Tunnel/Peak Intervening						
Event	12th St Inlet (cfs)	8th St Lateral (cfs)	4th St Lateral (cfs)	Total Outlet (cfs)	LBL Cross Velocity (ft/sec)	LBL WL (ft)
500 yr	11,111	1,278	1,313	13,702	3.5	428
100 yr	8,247	960	1,001	10,208	3.5	428
50 yr	7,140	832	877	8,849	3.5	428
25 yr	6,151	712	763	7,626	3.5	428
10 yr	4,784	562	619	5,965	3.5	428
5 yr	3,873	452	515	4,840	3.5	428
2 yr	2,543	302	369	3,214	3.5	428
Lagging Tunnel/Peak Intervening						
Event	12th St Inlet (cfs)	8th St Lateral (cfs)	4th St Lateral (cfs)	Total Outlet (cfs)	LBL Cross Velocity (ft/sec)	LBL WL (ft)
100 yr	5,642	960	1,001	7,603	3.5	428

Table 5: Waller Creek Tunnel Project Model Study; Air Entrainment Estimate Summary

	25yr	100yr
Q_w (cfs)	0.98	1.32
P(inches)	18.17	18.63
P(psi)	0.66	0.67
P(psia)	15.36	15.37
Air Density (slugs/ft3)	0.002479	0.002482
Avg. A_w (in^2)	40.89	41.35
Avg. A_a (in^2)	2.14	1.69
Avg. $VF_{a\ model} = A_a/A_{a+}A_w$	0.05	0.04
Avg. $VF_{a\ model}$ (%)	5.0	3.9
Max. A_w (in^2)	39.53	40.45
Max. A_a (in^2)	3.50	2.59
Max. $VF_{a\ model} = A_a/A_{a+}A_w$	0.08	0.06
Max. $VF_{a\ model}$ (%)	8.1	6.0

Where:

Air Temp (^oF)	60
Water Temp (^OF)	60
Atm P (psia)	14.7
Water Density ($slugs/ft^3$)	1.938
Air Density ($slugs/ft^3$)	0.002373

Table 6: Waller Creek Tunnel Project Model Study: Summary of Additional Water Levels in Inlet Channel

Event	Tap 1 WSEL (ft)	Tap 2 WSEL (ft)	Tap 3 WSEL (ft)
2 yr	477.3	476.6	477.2
5 yr	478.7	477.5	478.0
10 yr	479.8	478.1	478.6
25 yr	481.3	478.6	479.2
50 yr	482.2	479.1	479.7
100 yr	483.0	479.3	480.3
500 yr	493.1	492.9	493.0

FIGURES

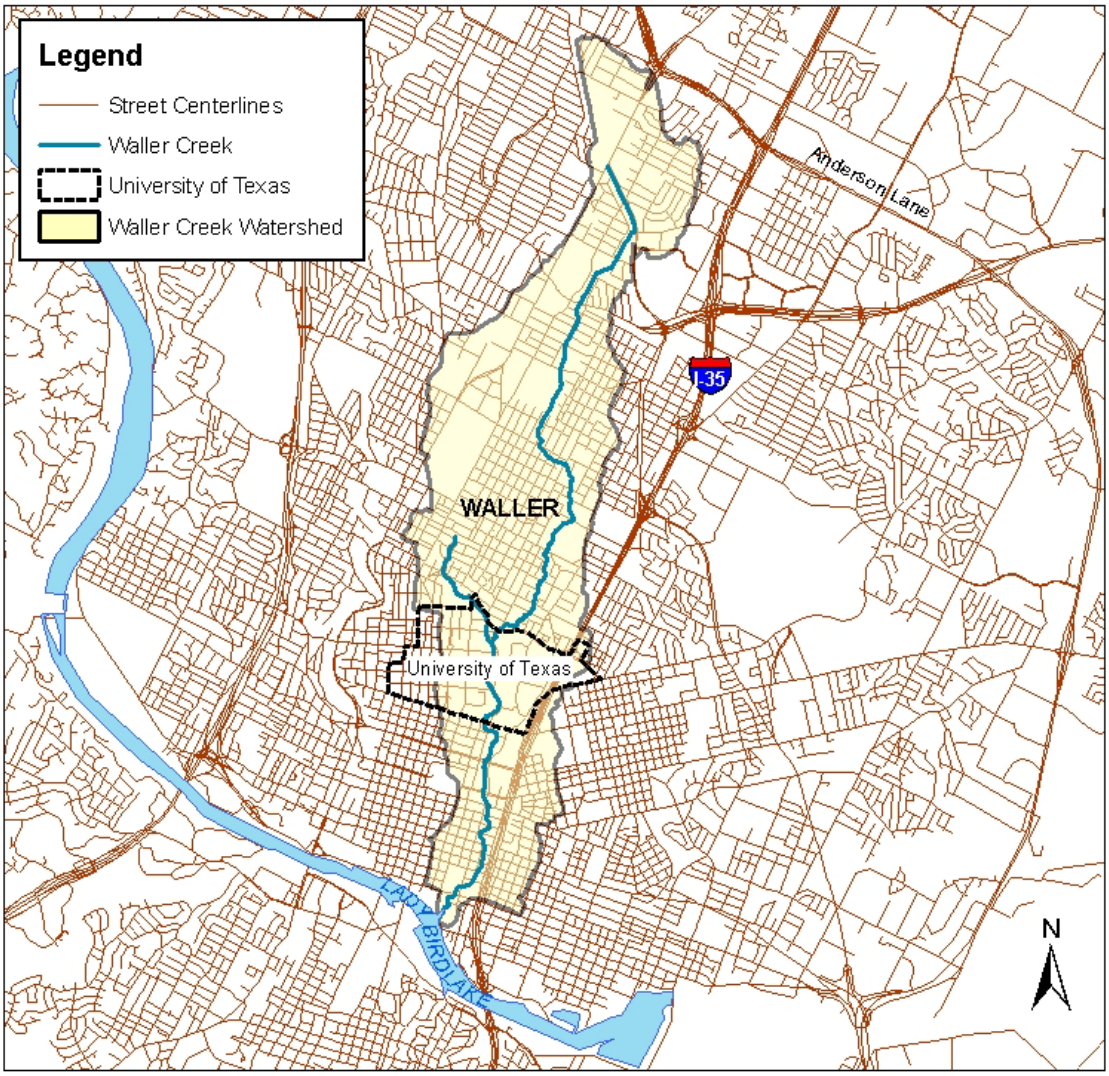

Figure 1: Waller Creek Watershed

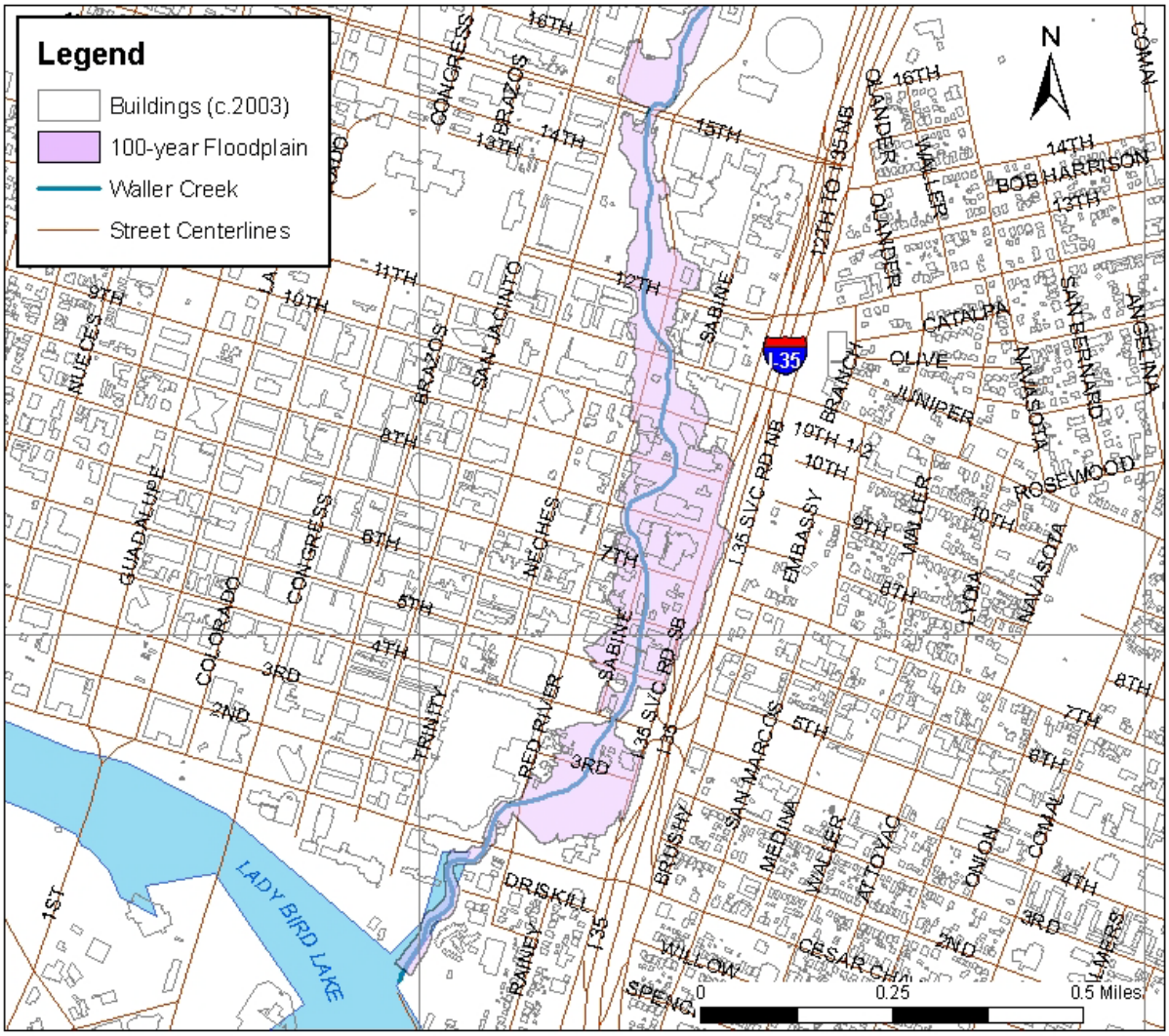

Figure 2: Lower Reach of Waller Creek; Downstream of 15th Street to Lady Bird Lake

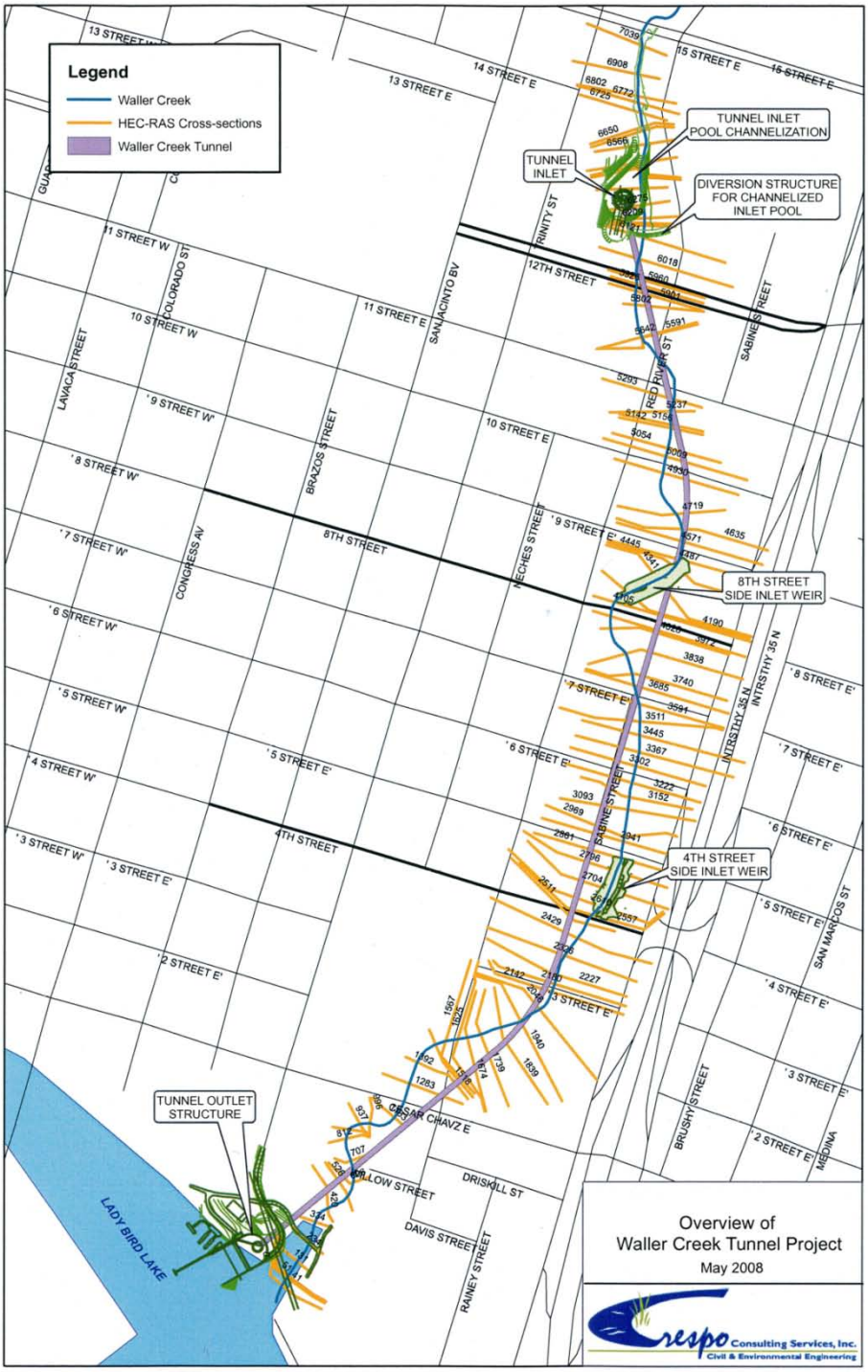

Figure 3: Overview of Waller Creek Tunnel Project

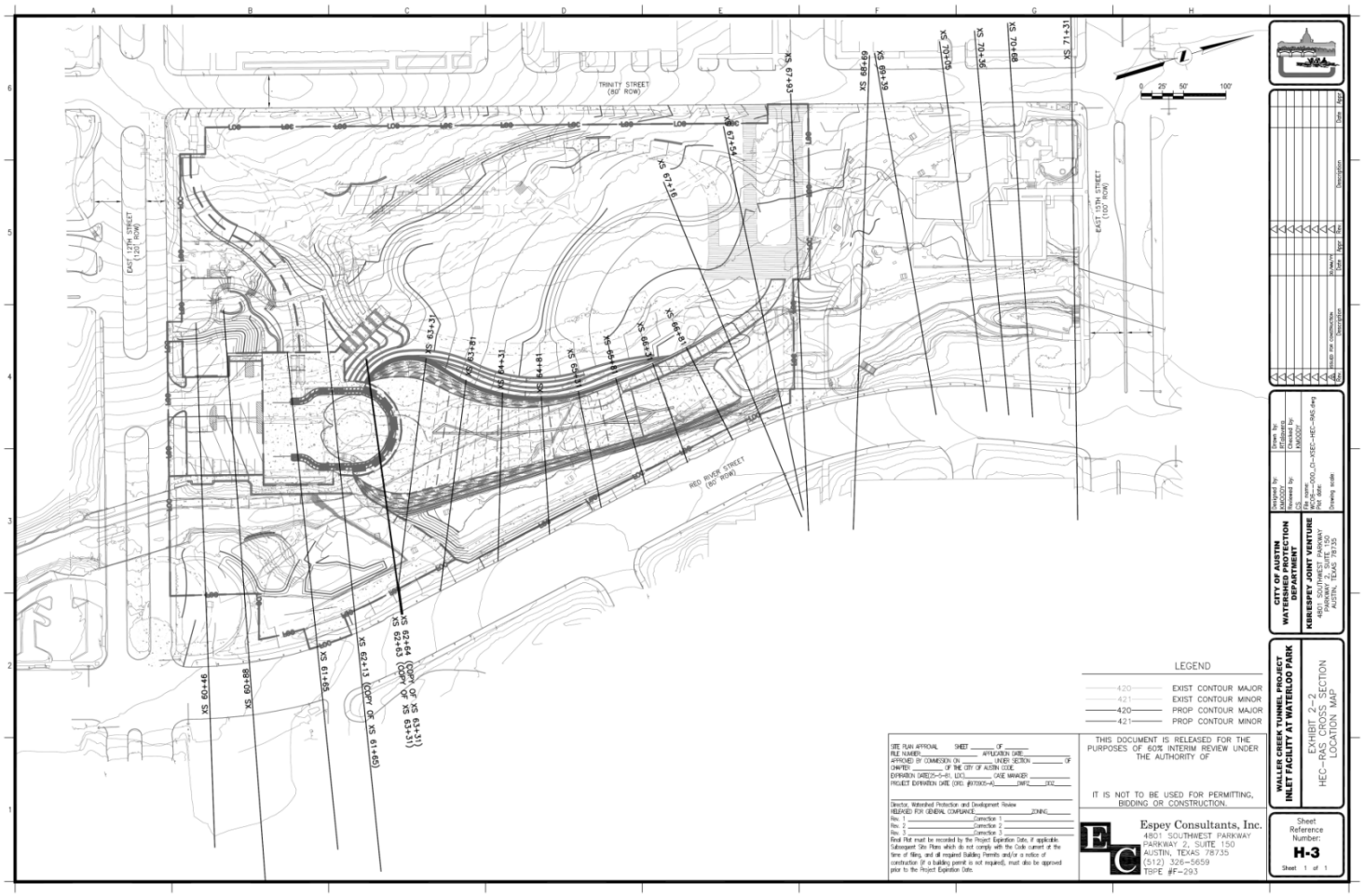

Figure 4: Waller Creek Tunnel Project; Inlet Pool Channelization – Plan View

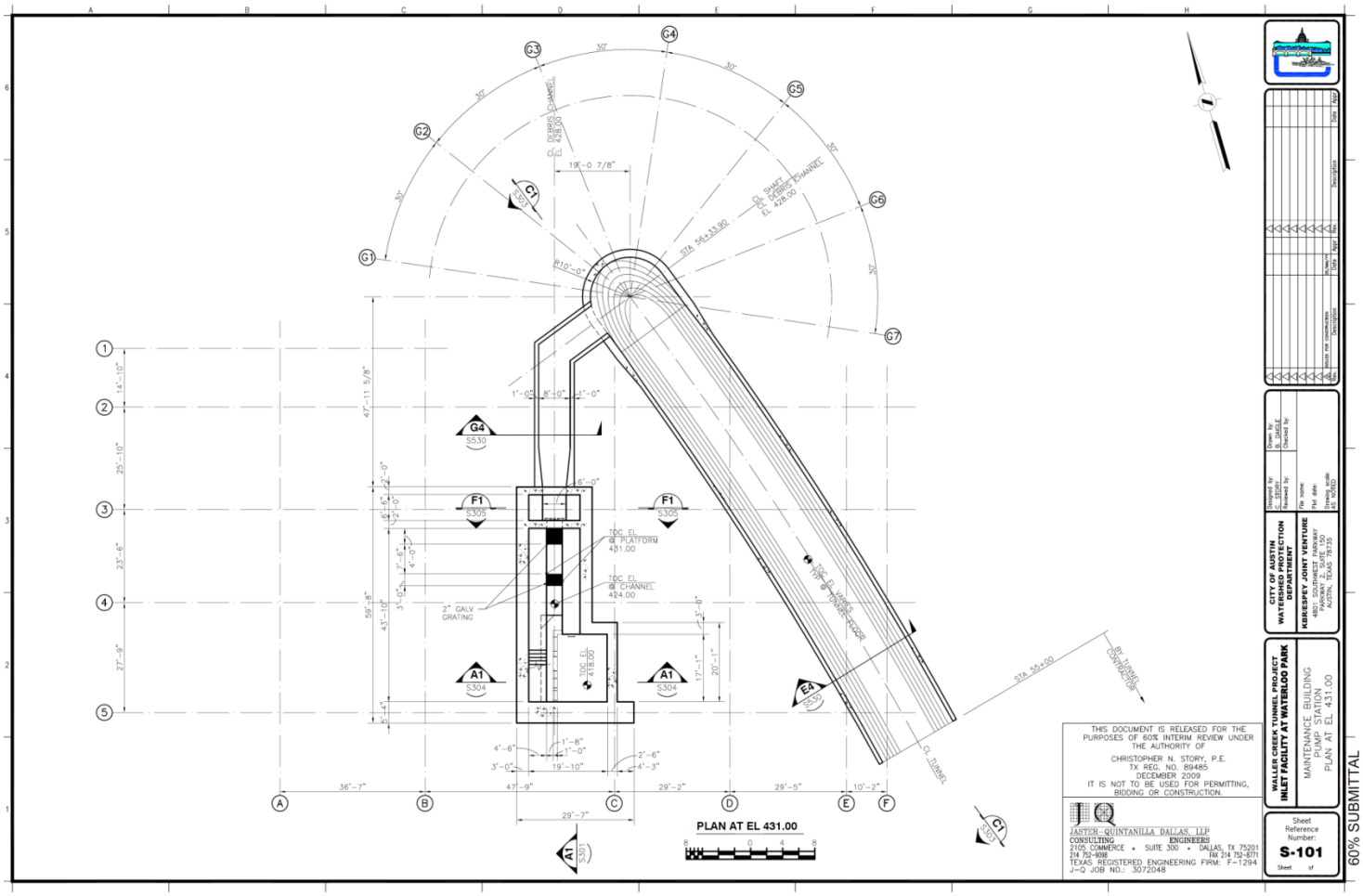

Figure 5: Waller Creek Tunnel Project; Morning Glory Spillway – Plan at EL 431

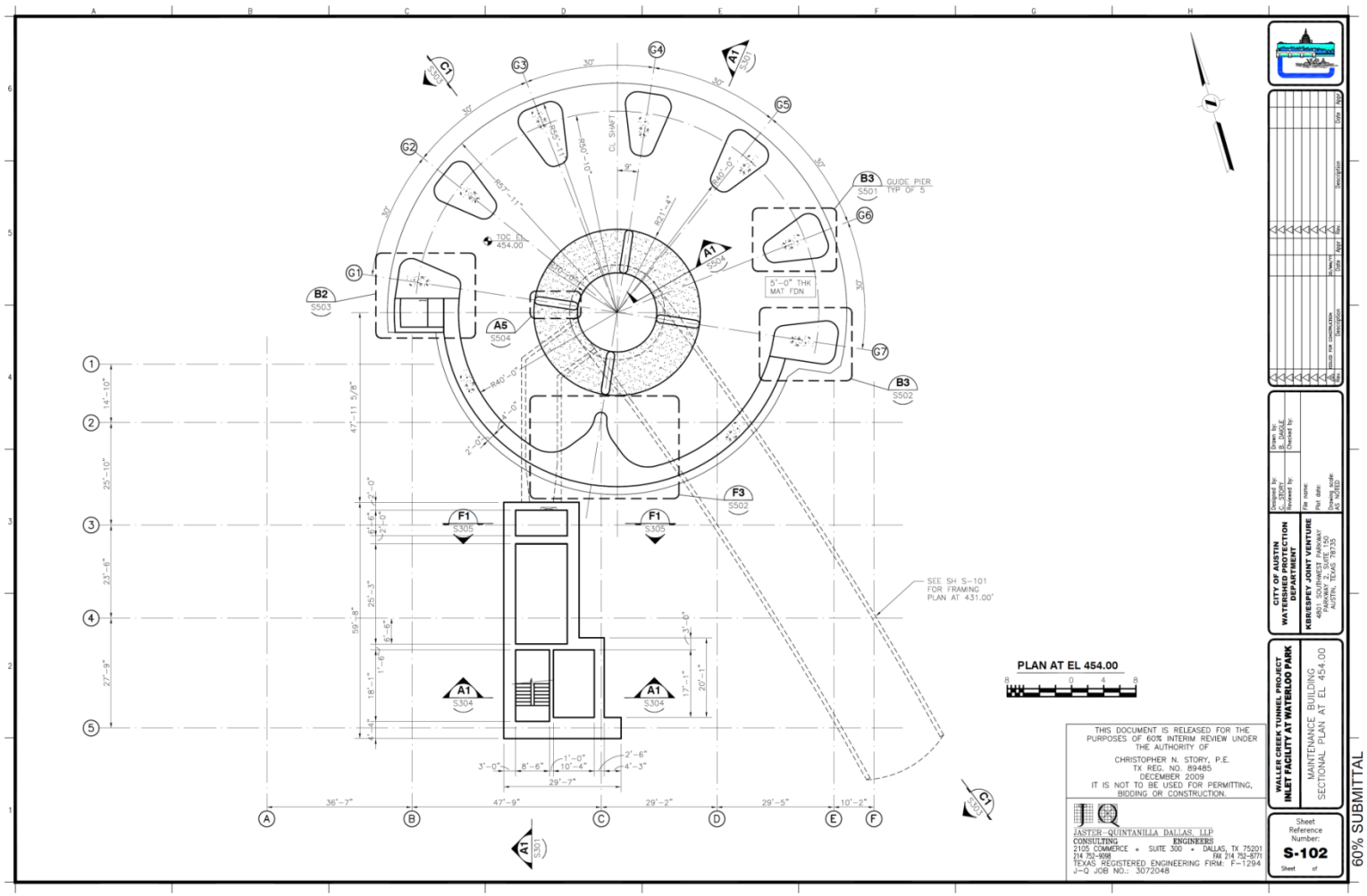

Figure 6: Waller Creek Tunnel Project; Morning Glory Spillway – Plan at EL 454

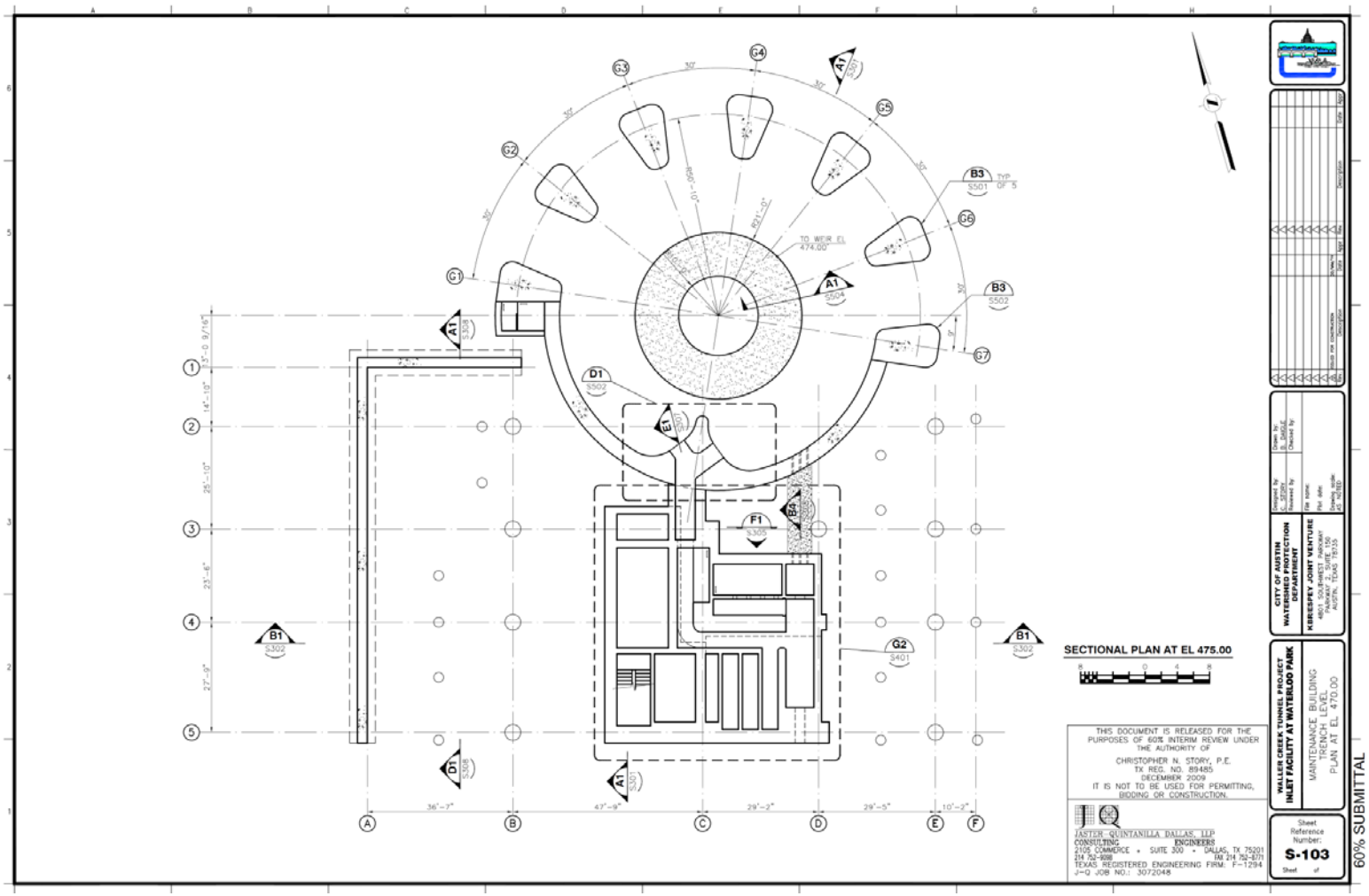

Figure 7: Waller Creek Tunnel Project; Morning Glory Spillway – Plan at EL 475

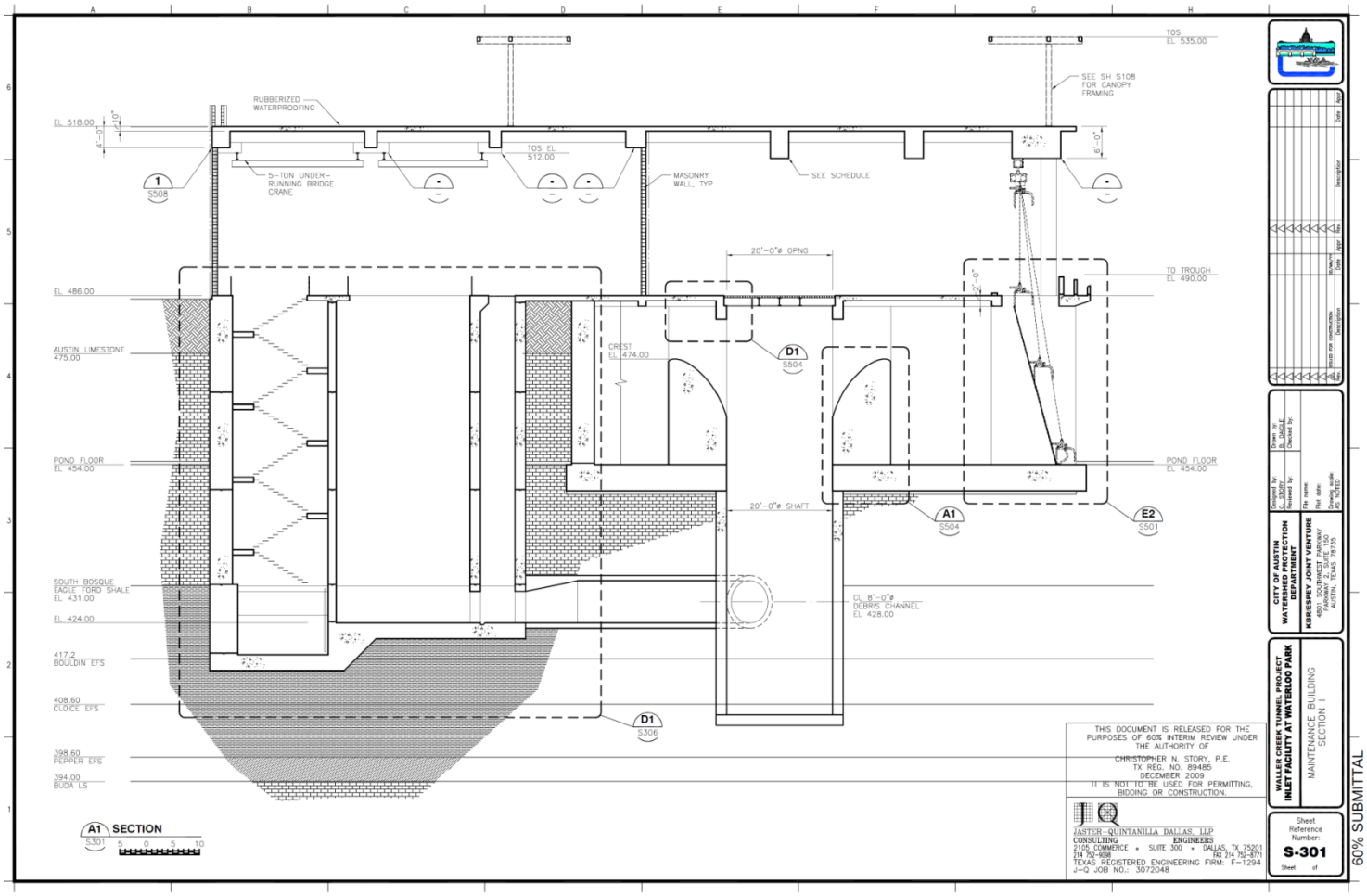

Figure 8: Waller Creek Tunnel Project; Morning Glory Spillway – Section

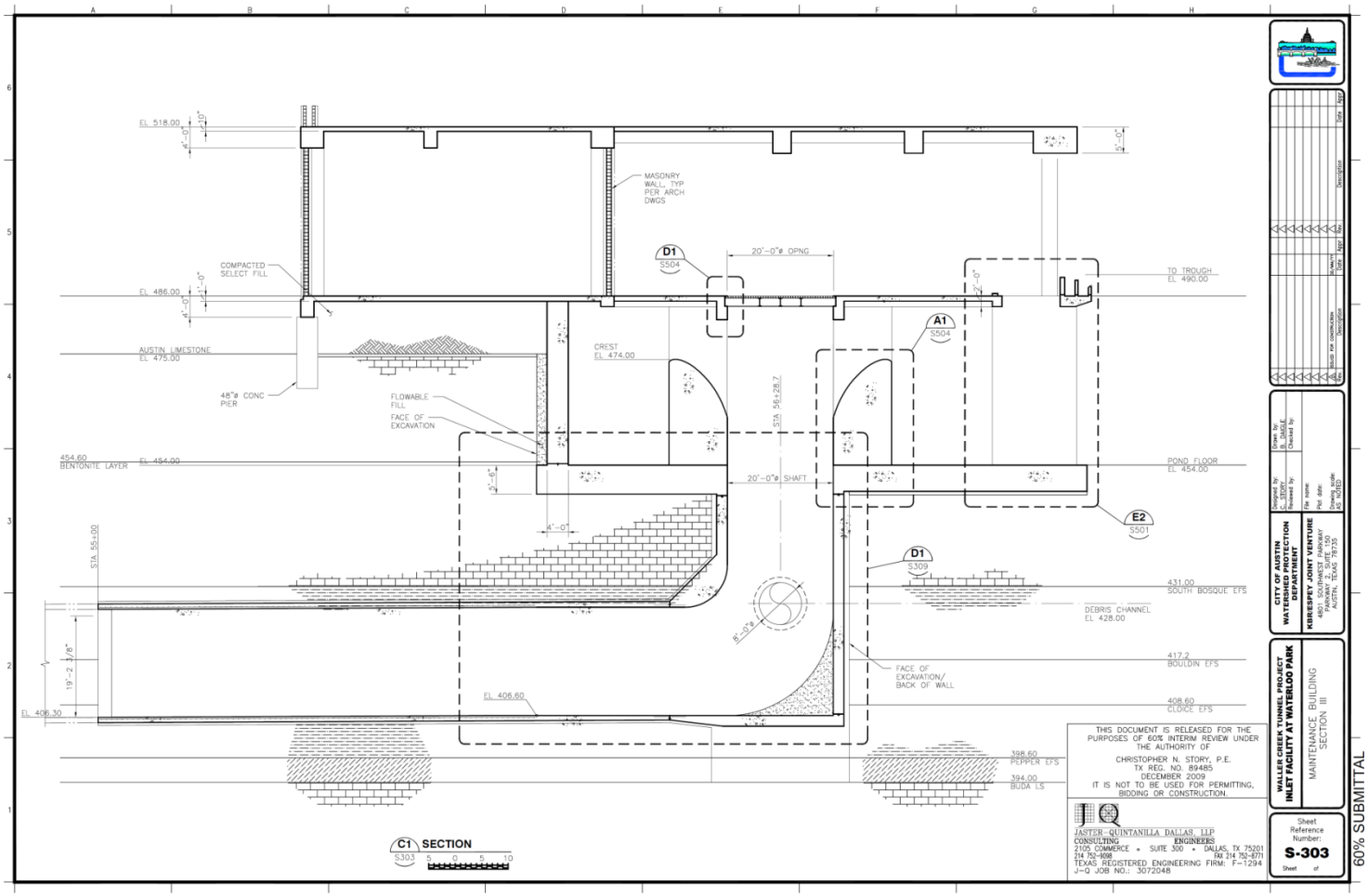

Figure 9: Waller Creek Tunnel Project; Morning Glory Spillway – Section

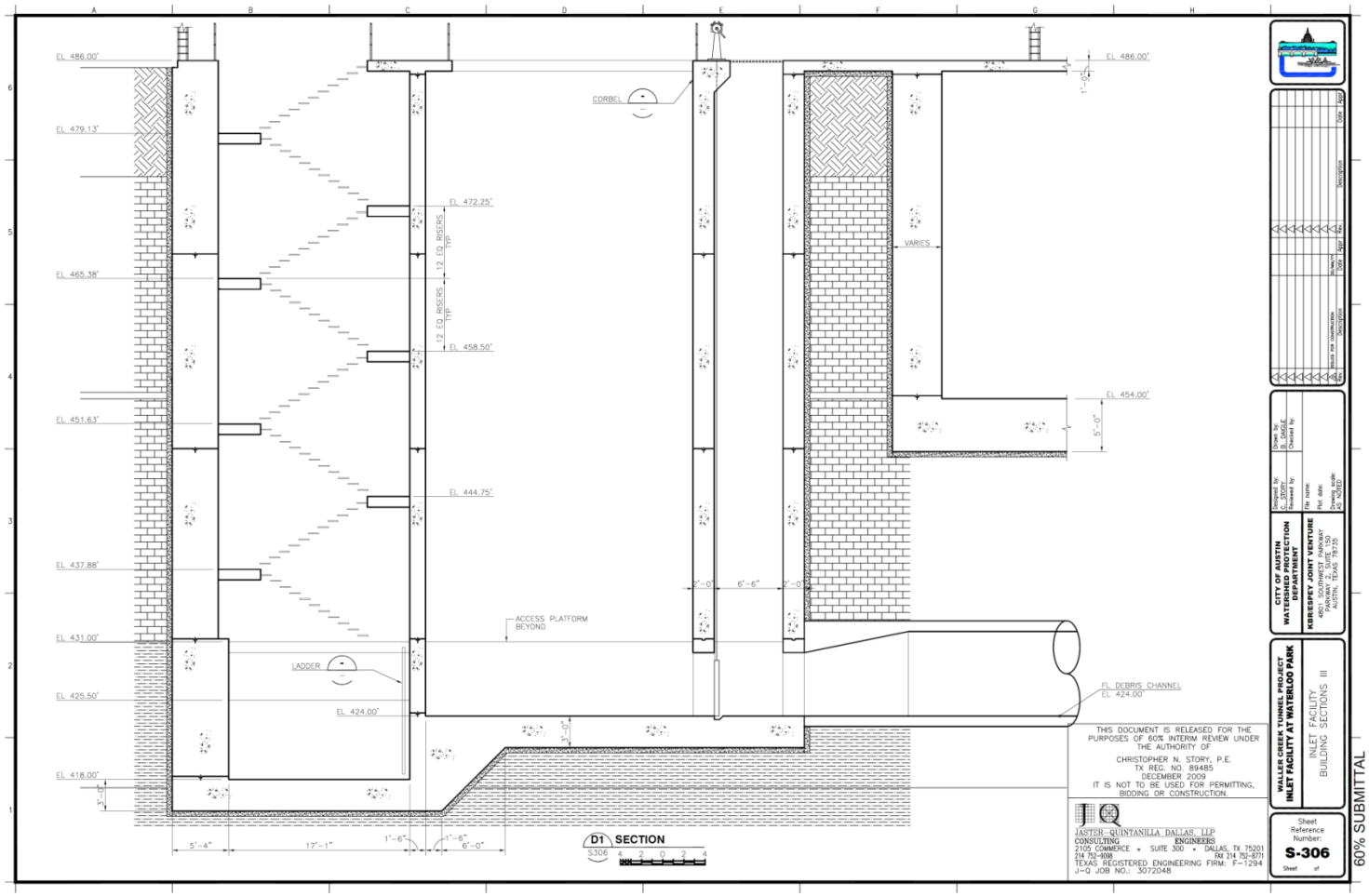

Figure 10: Waller Creek Tunnel Project; Morning Glory Spillway – Section

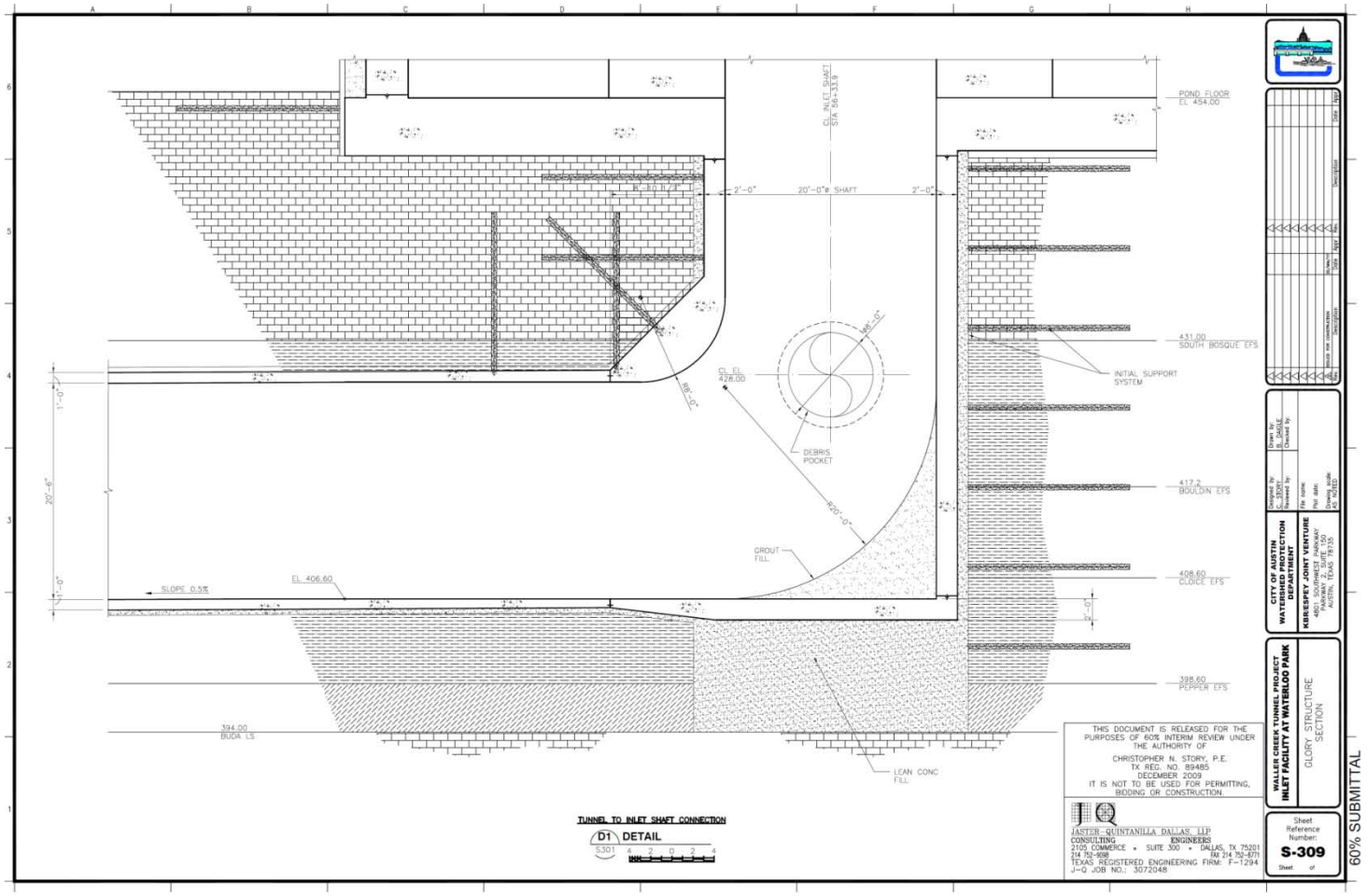

Figure 11: Waller Creek Tunnel Project; Morning Glory Spillway – Section

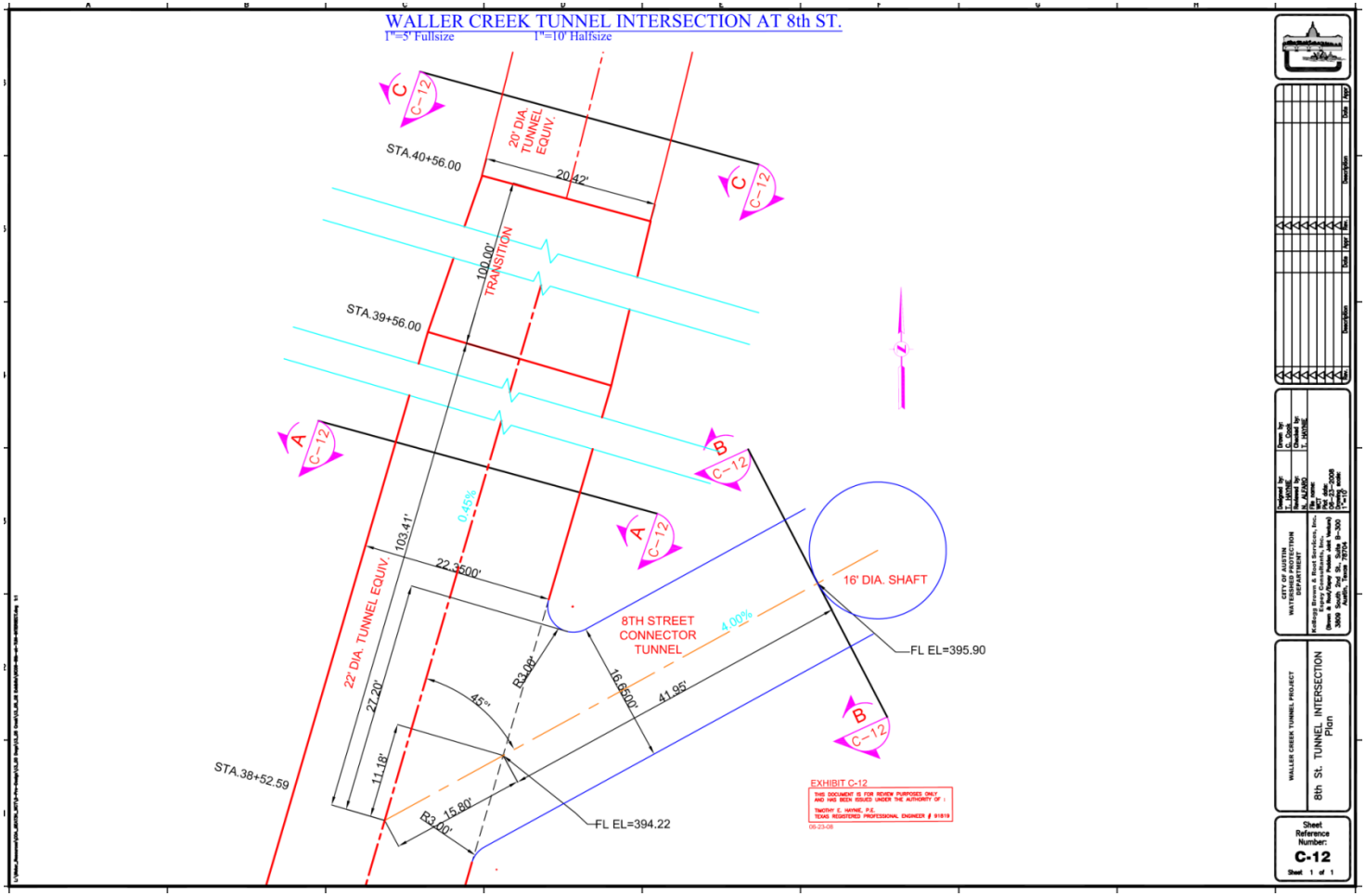

Figure 12: Waller Creek Tunnel Project; Tunnel Intersection at 8th Street-Plan

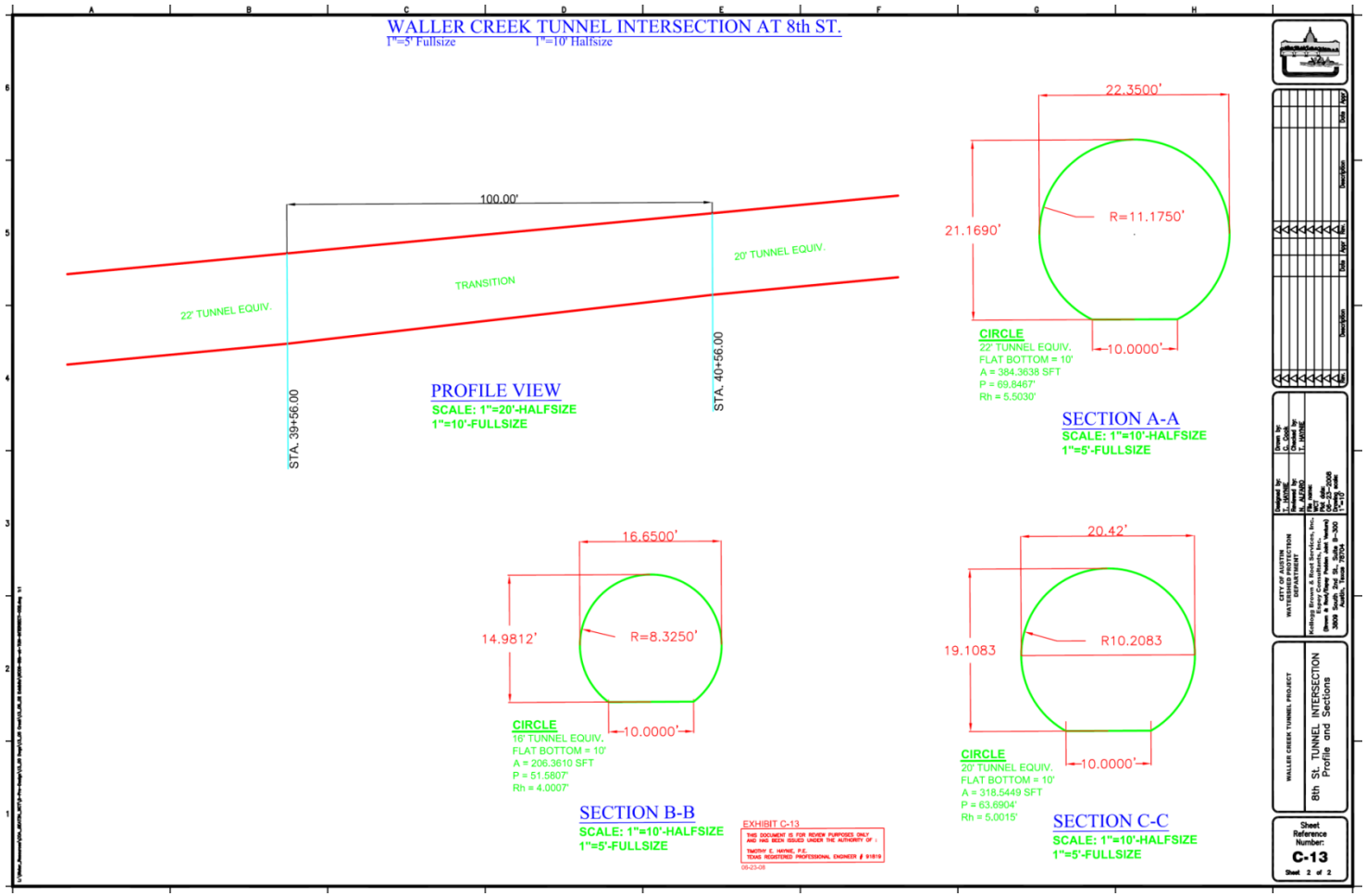

Figure 13: Waller Creek Tunnel Project; Tunnel Intersection at 8th Street–Profile and Sections

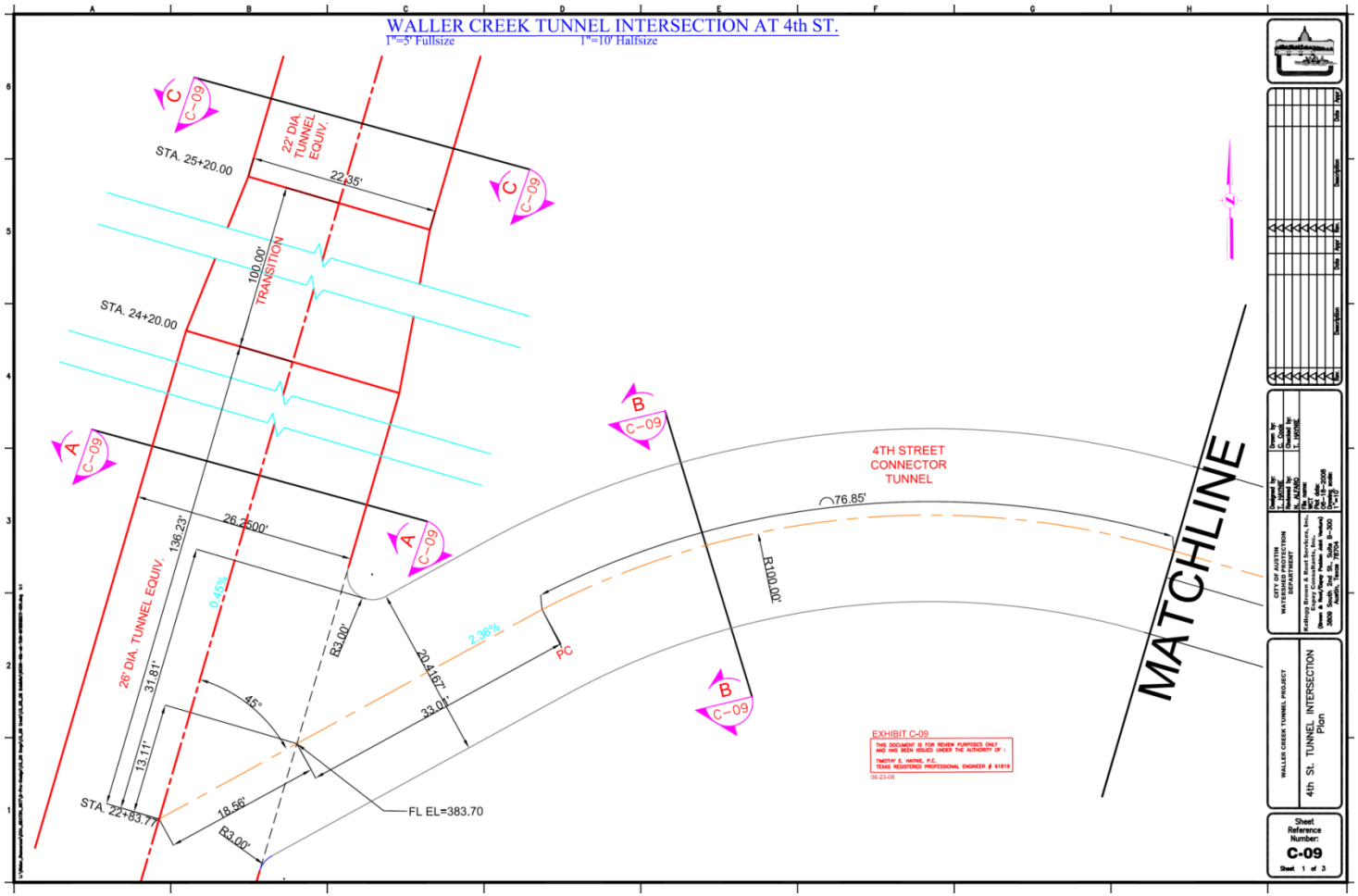

Figure 14: Waller Creek Tunnel Project; Tunnel Intersection at 4th Street-Plan

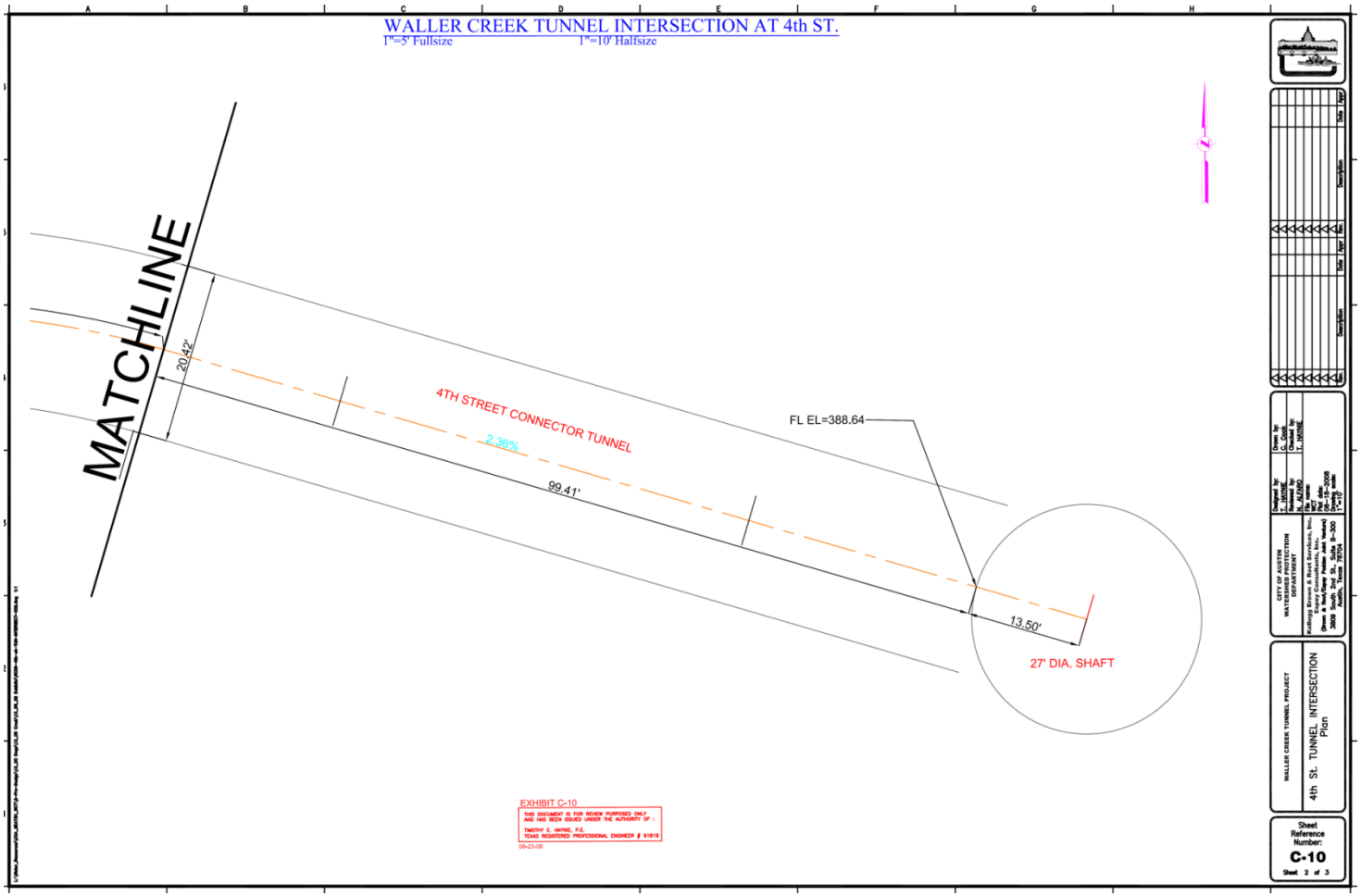

Figure 15: Waller Creek Tunnel Project; Tunnel Intersection at 4th Street-Plan

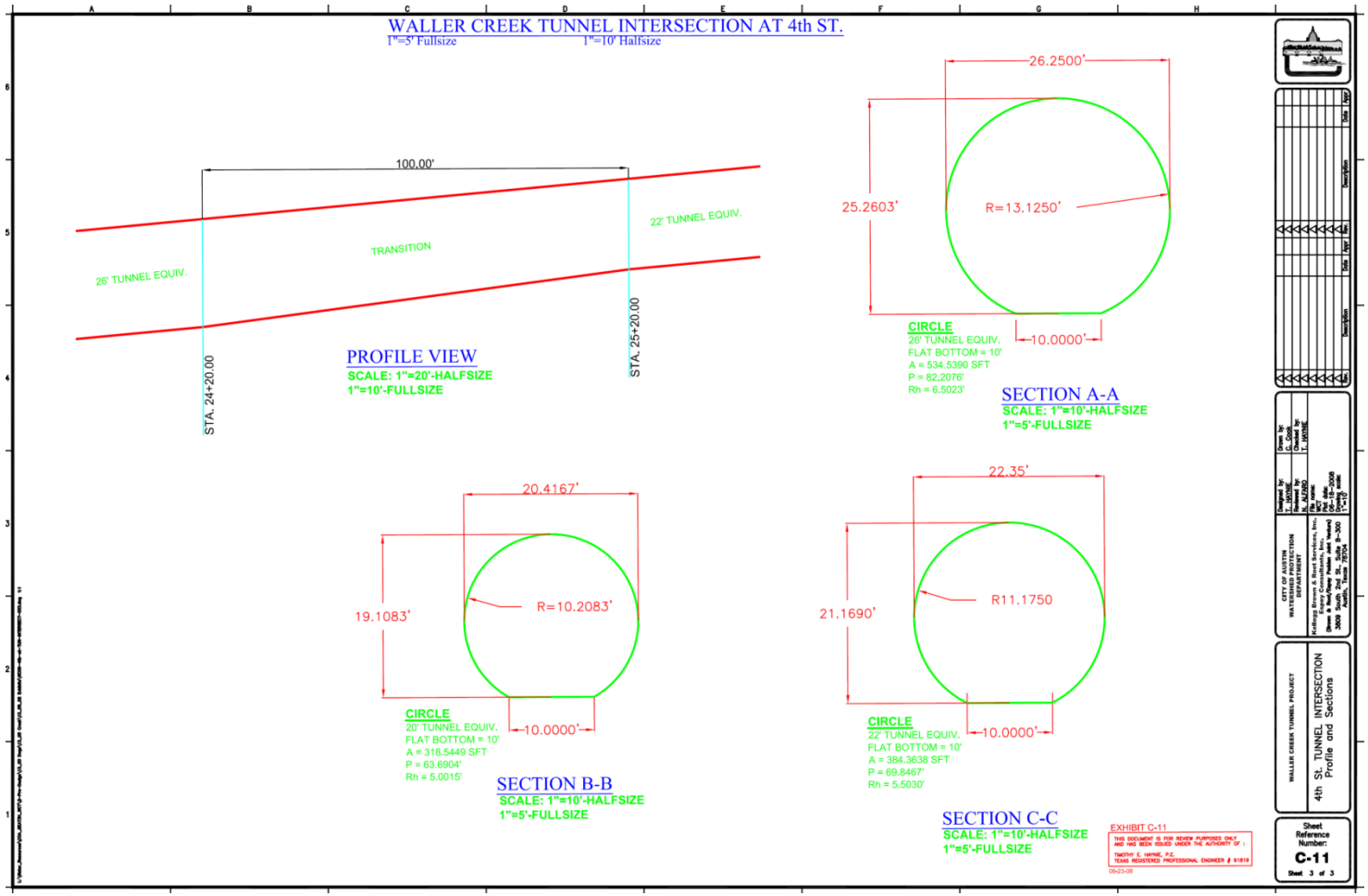

Figure 16: Waller Creek Tunnel Project; Tunnel Intersection at 4th Street–Profile and Sections

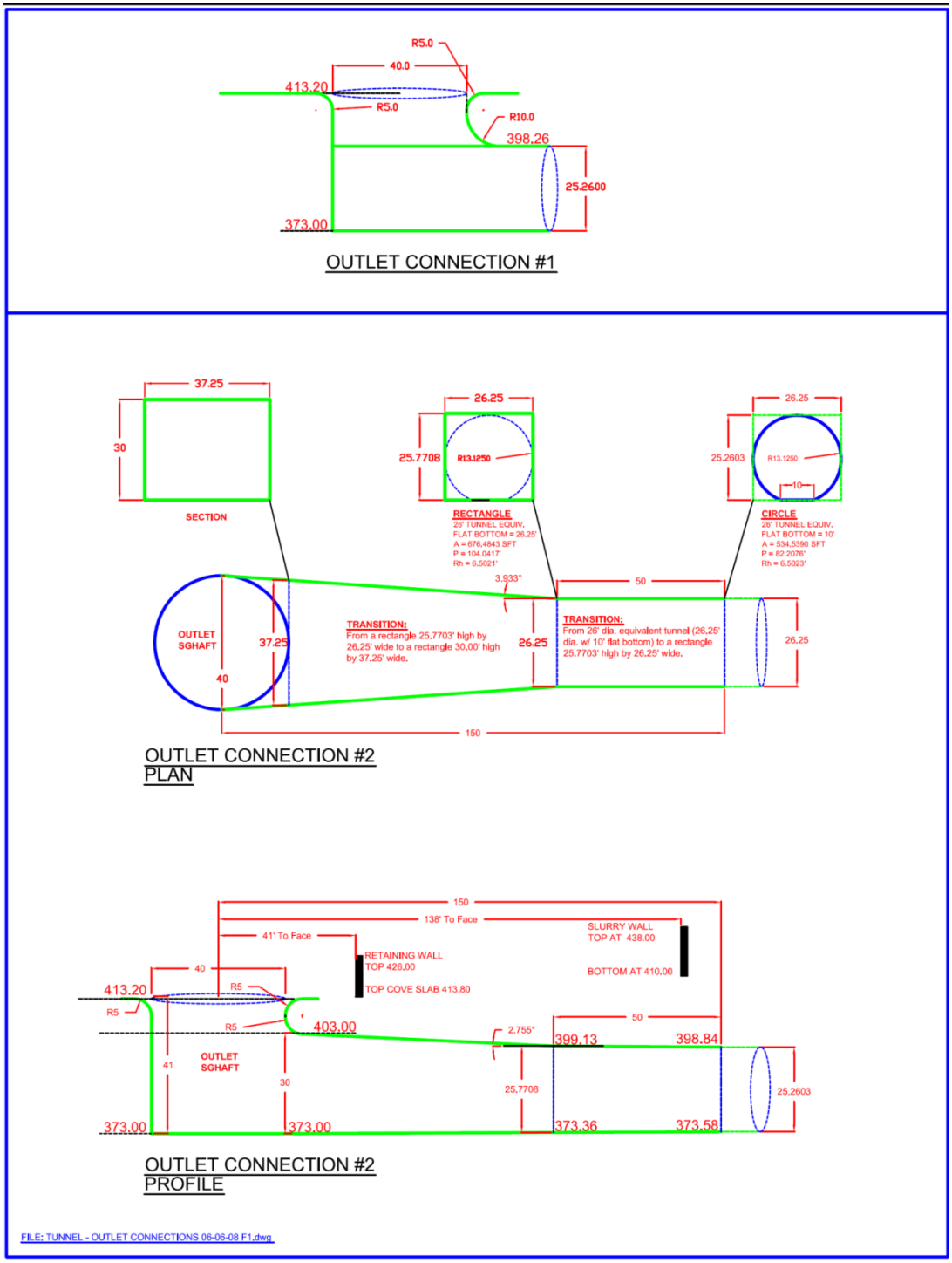

Figure 17: Waller Creek Tunnel Project; Outlet Connection Alternatives

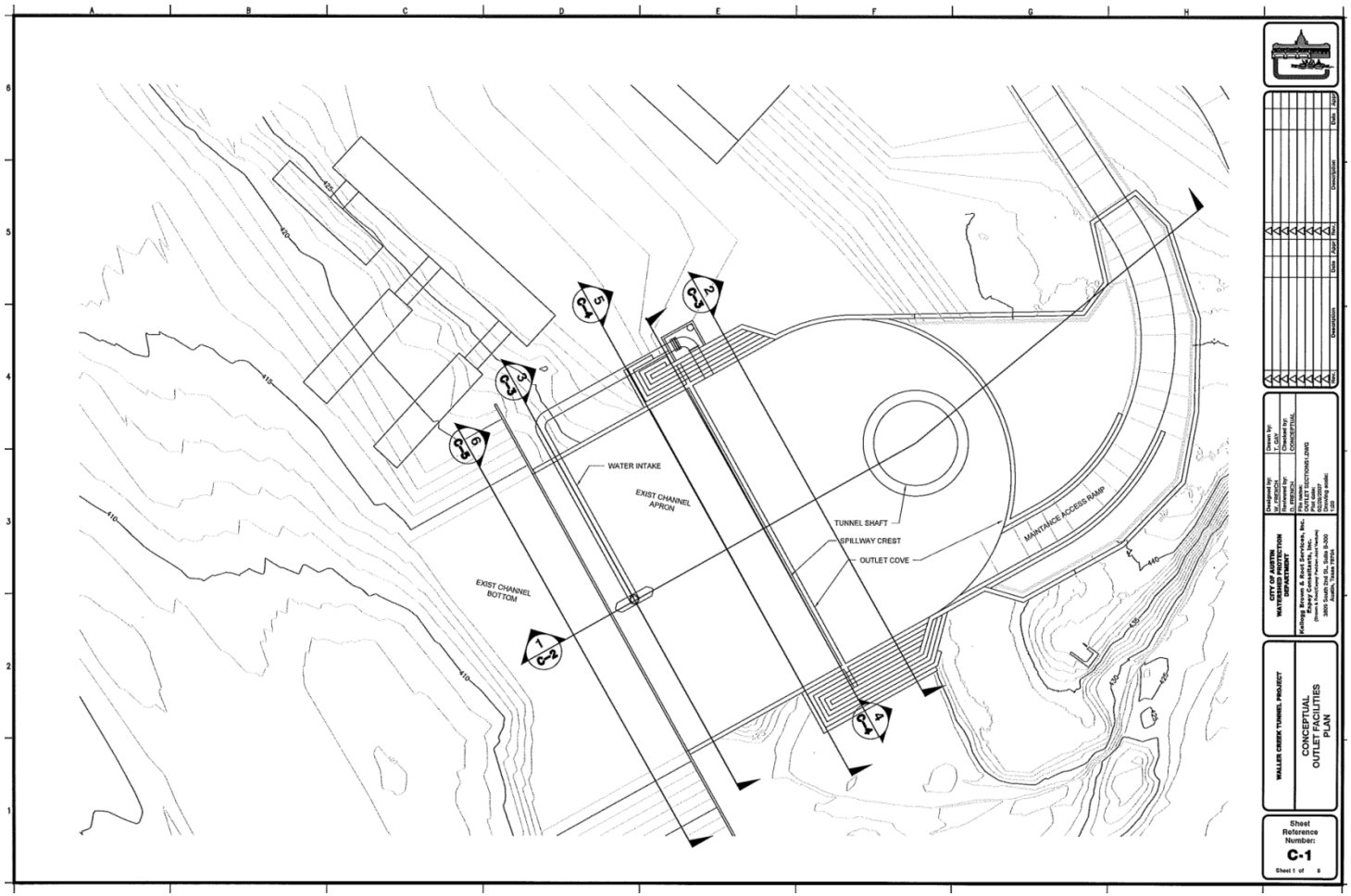

Figure 18: Waller Creek Tunnel Project; Outlet-Plan

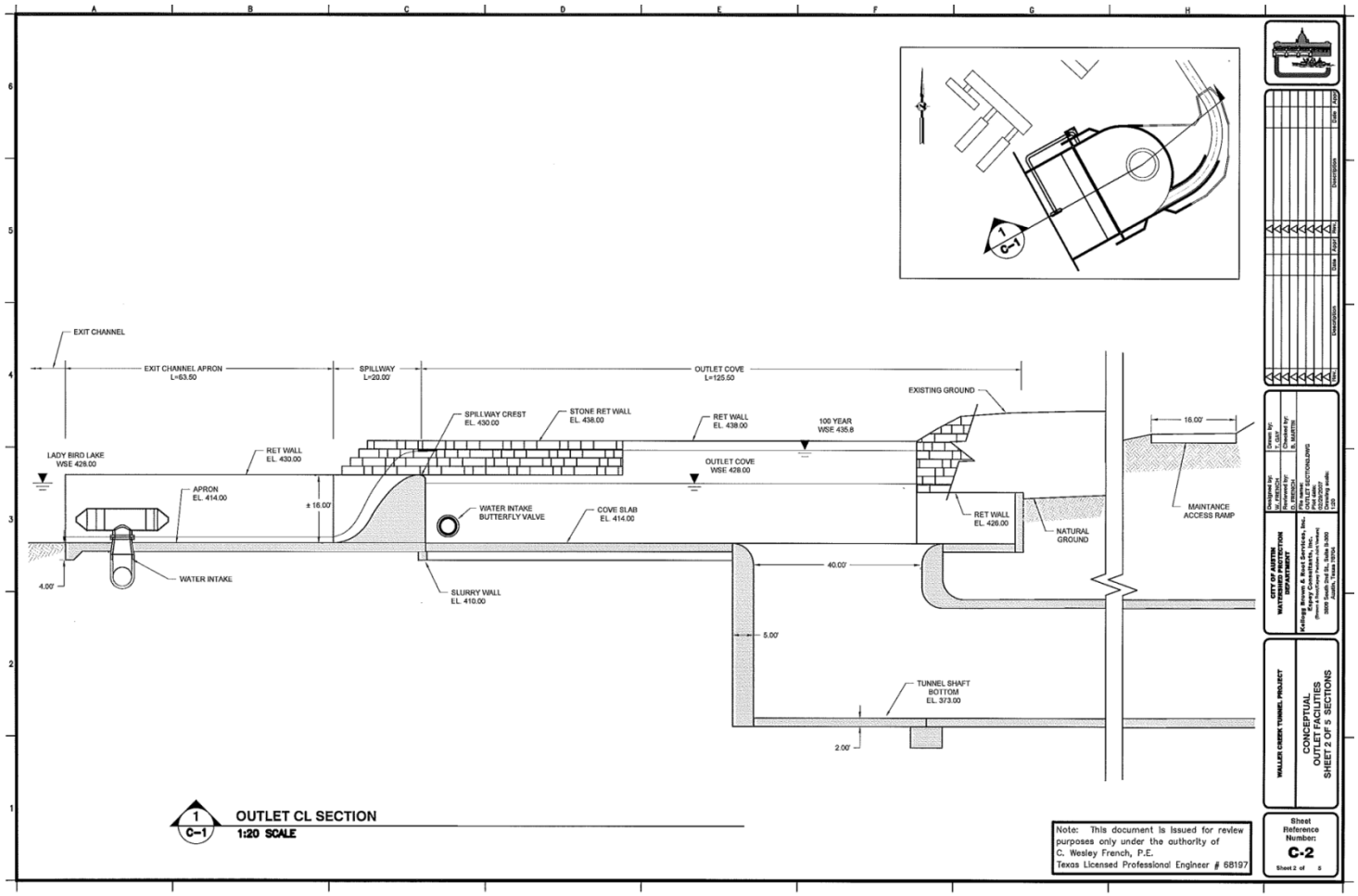

Figure 19: Waller Creek Tunnel Project; Outlet-Section

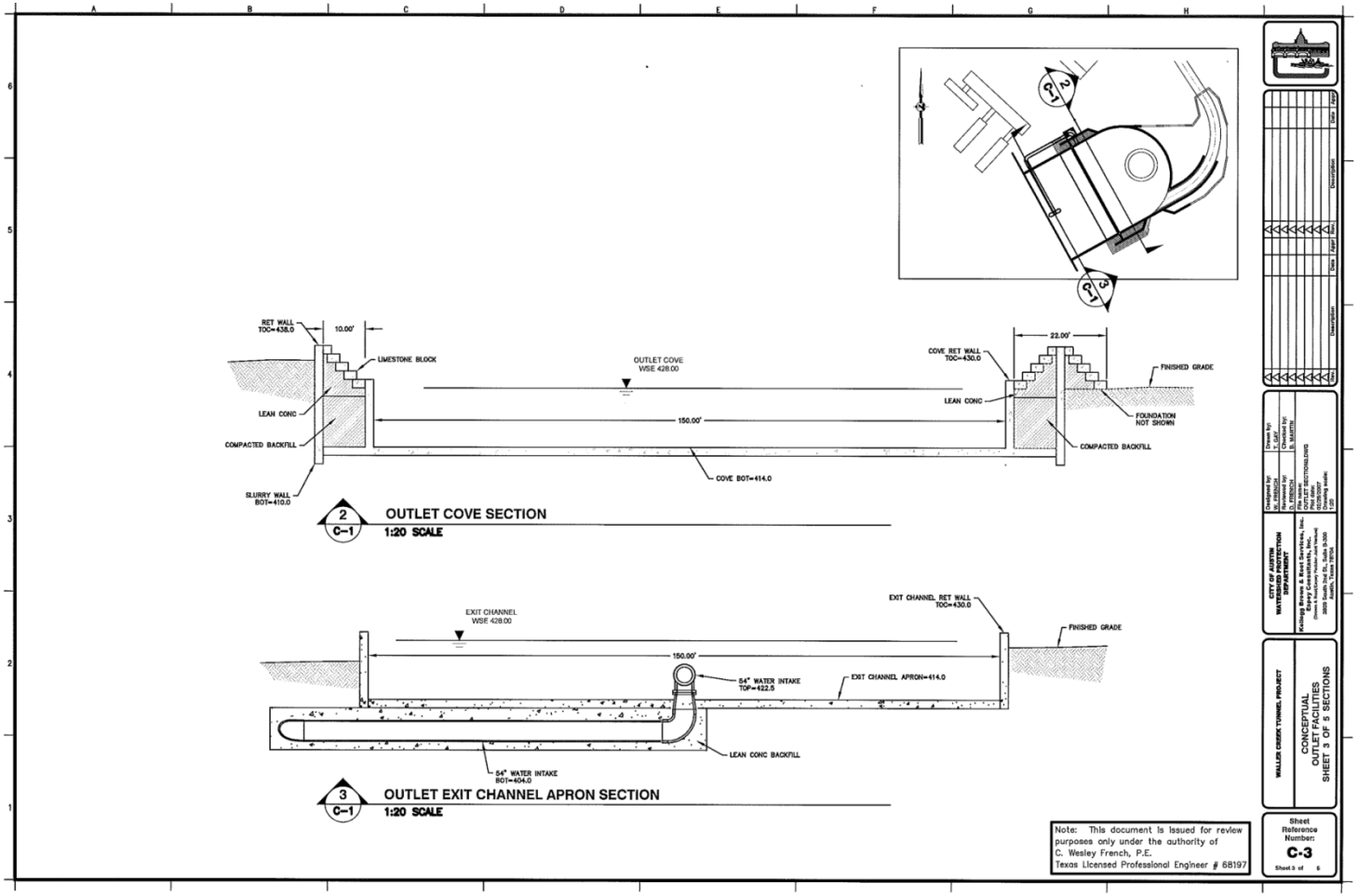

Figure 20: Waller Creek Tunnel Project; Outlet-Section

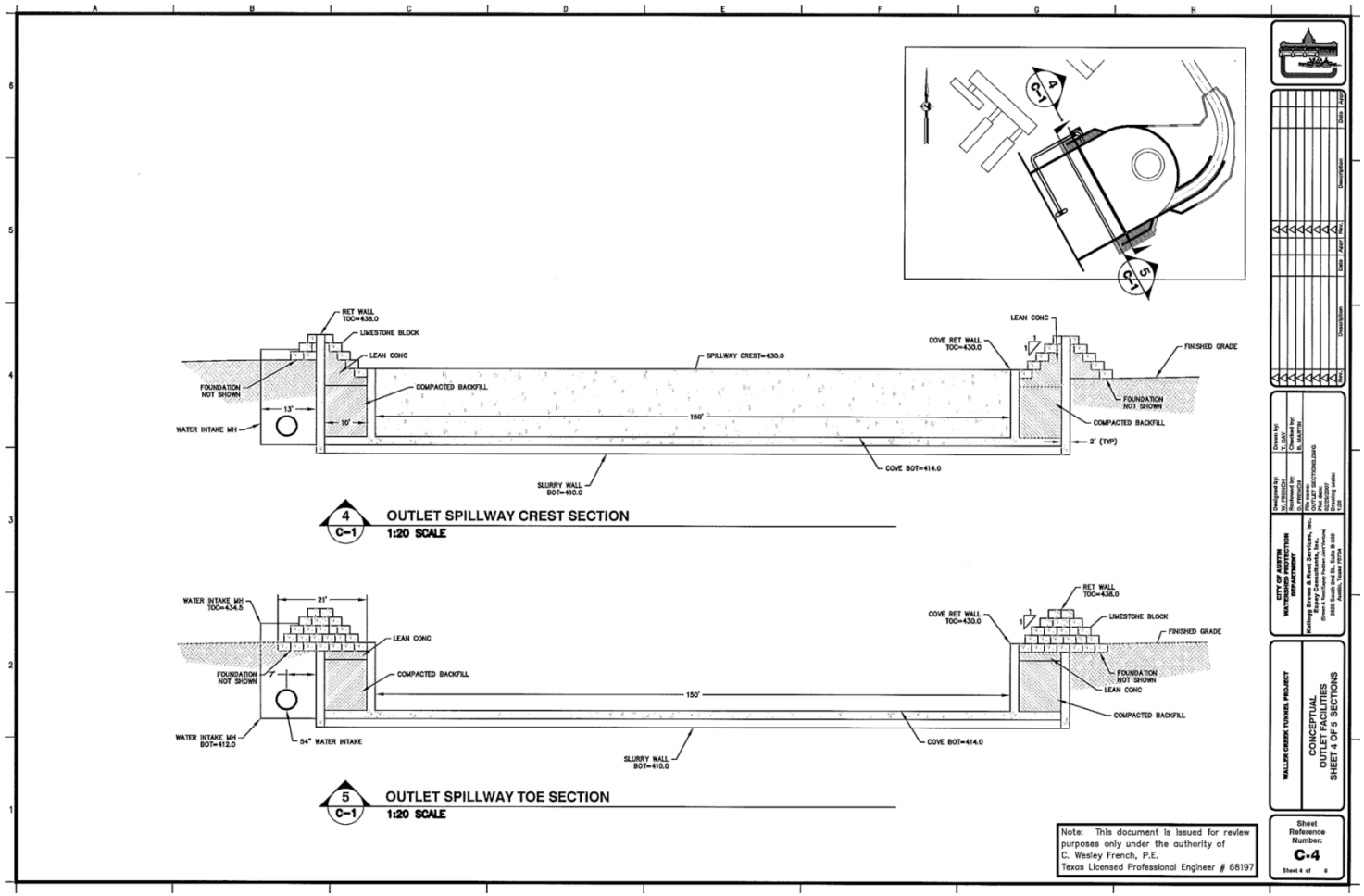

Figure 21: Waller Creek Tunnel Project; Outlet-Section

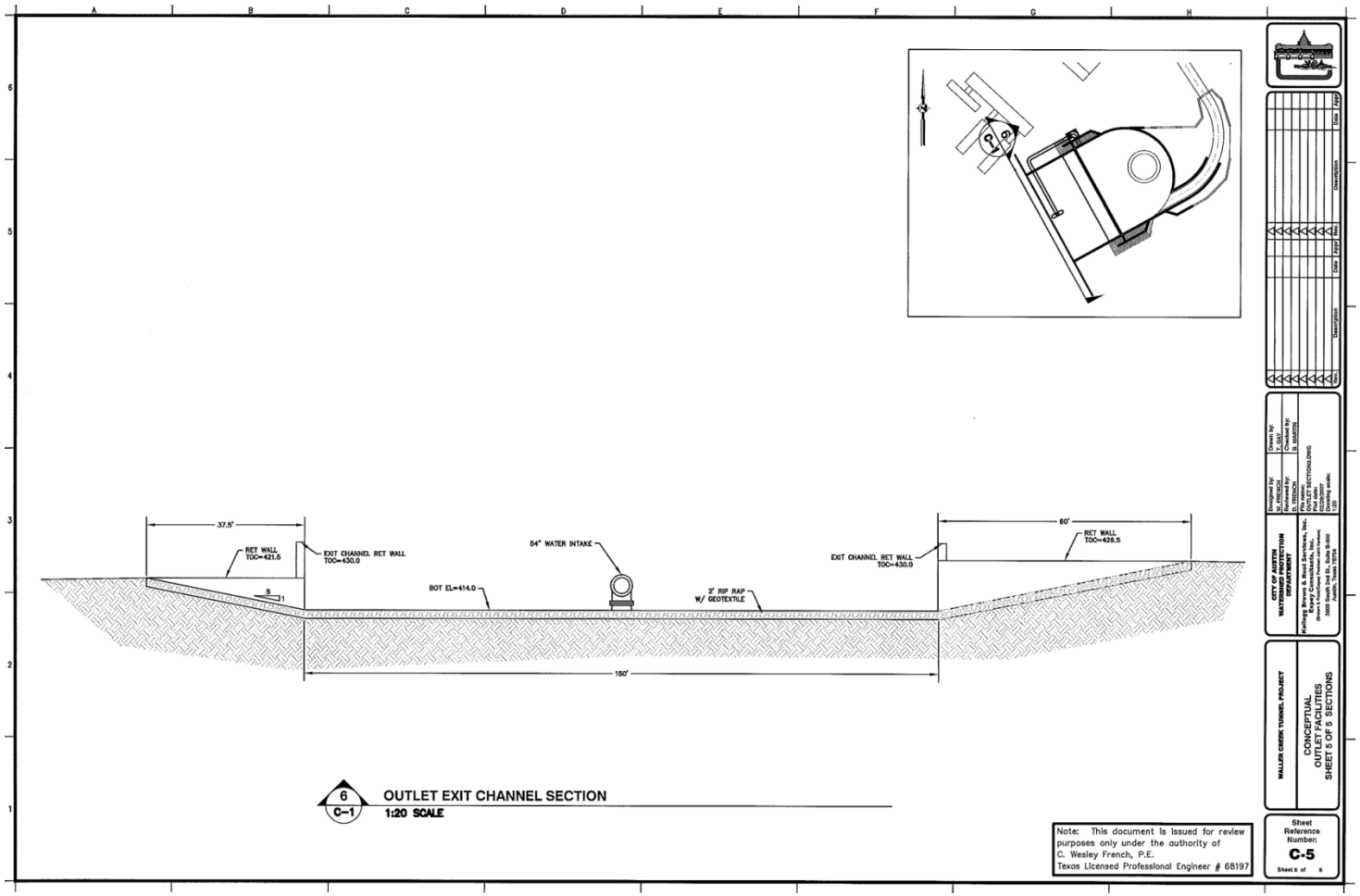

Figure 22: Waller Creek Tunnel Project; Outlet-Section

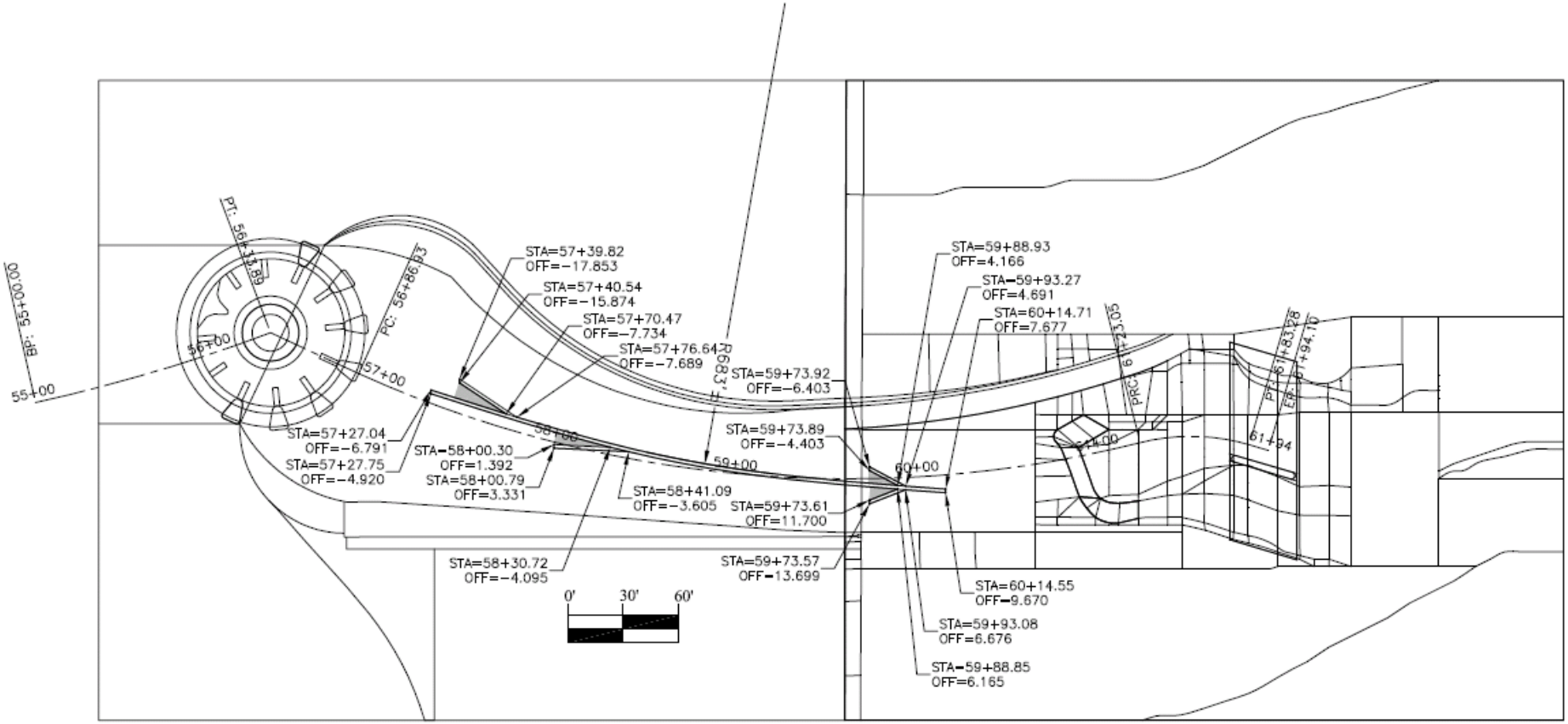

Figure 23: Inlet Channel Training Wall Configuration without Fill

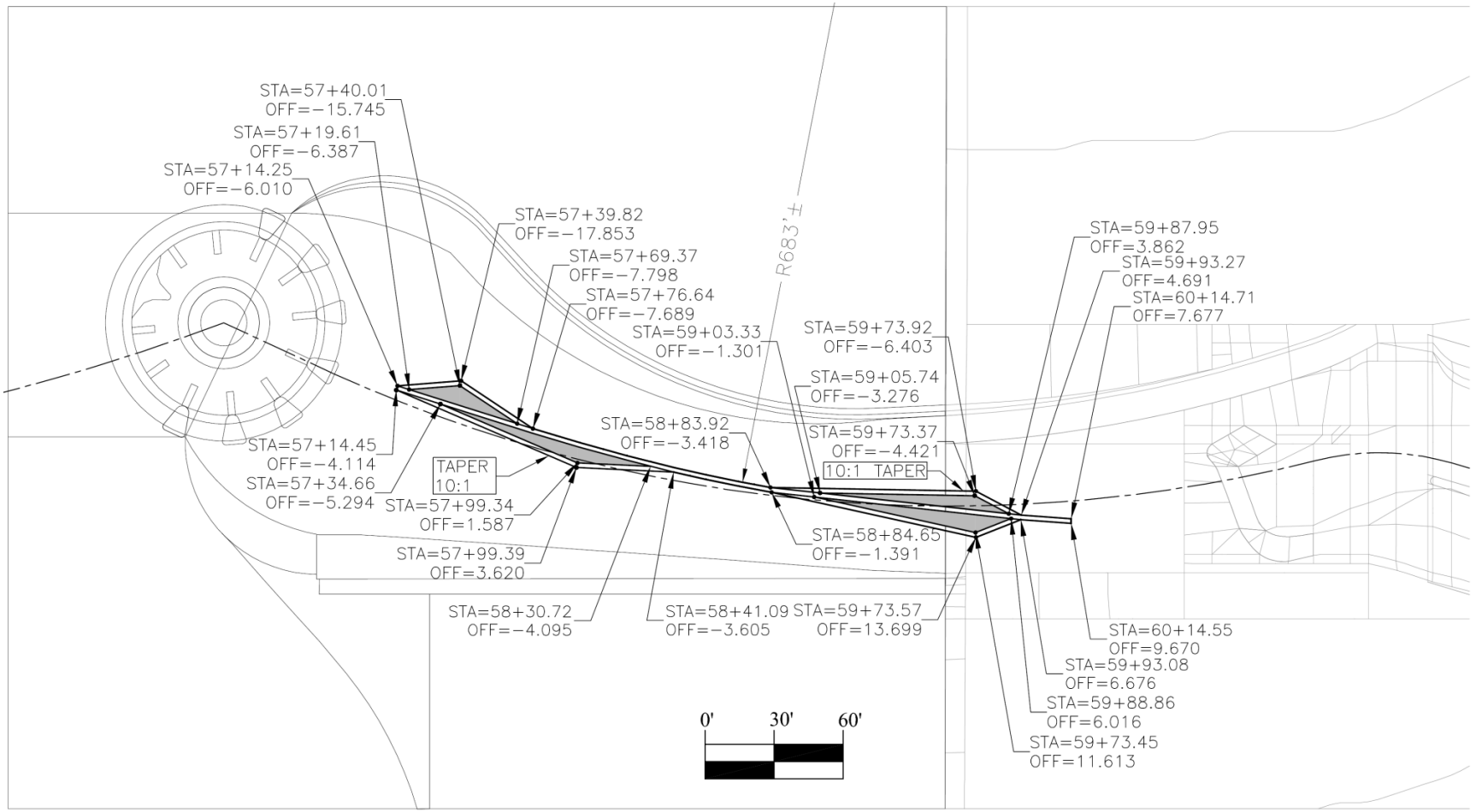

Figure 24: Final Inlet Channel Training Wall Configuration with Fill

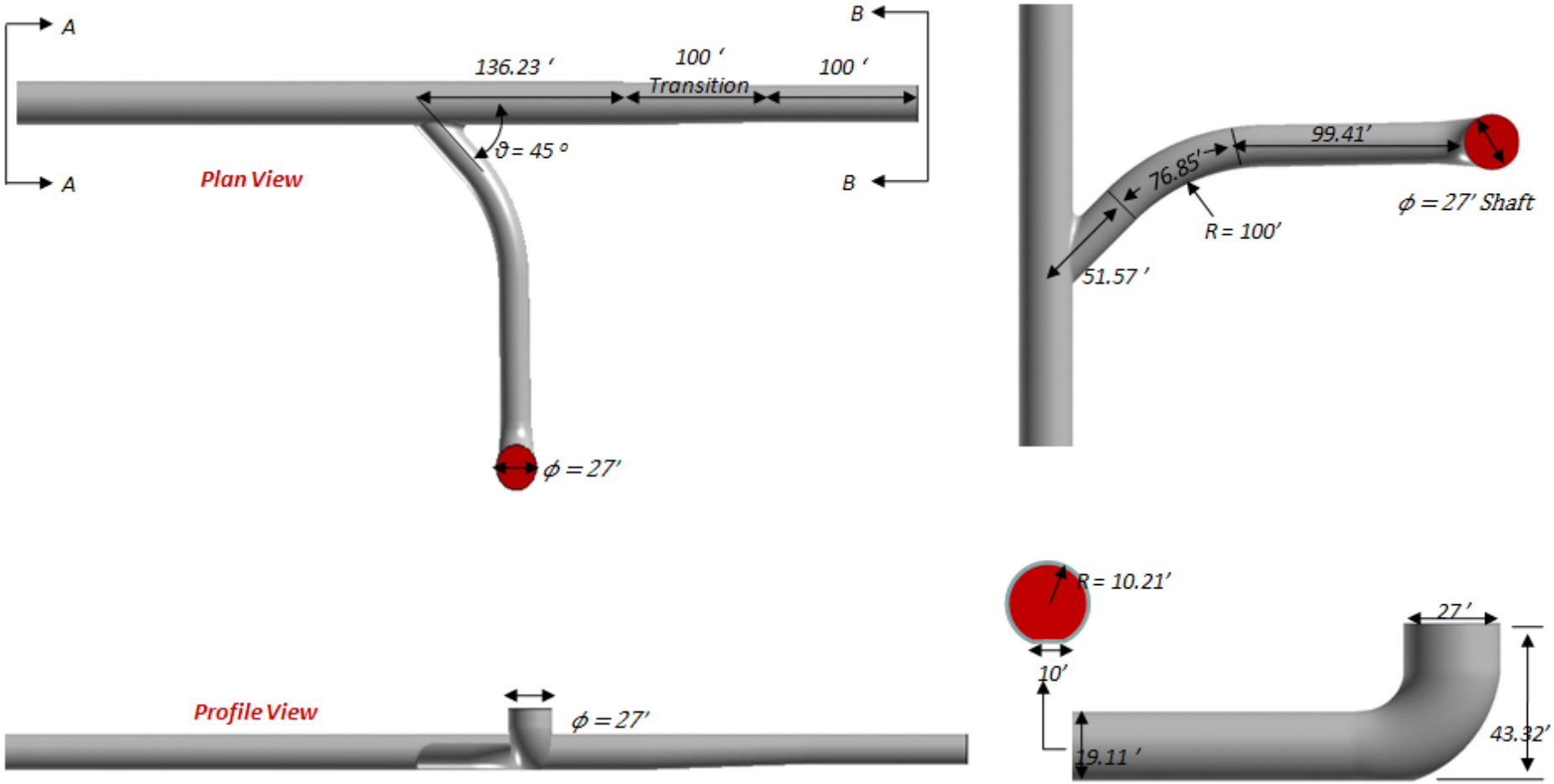

Figure 25: 4th Street Tunnel-Lateral Junction CFD Model Geometry

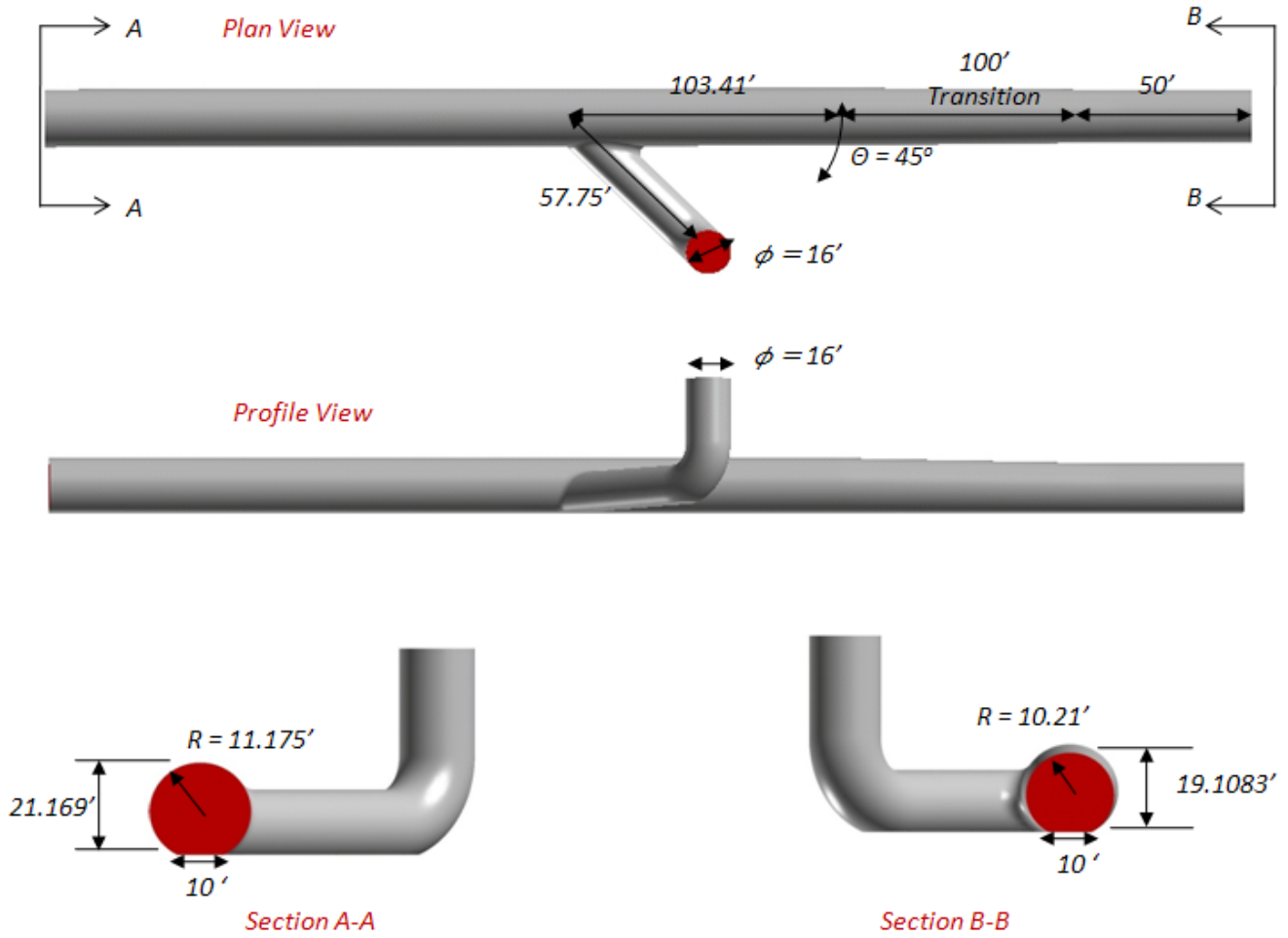

Figure 26: 8th Street Tunnel-Lateral Junction CFD Model Geometry

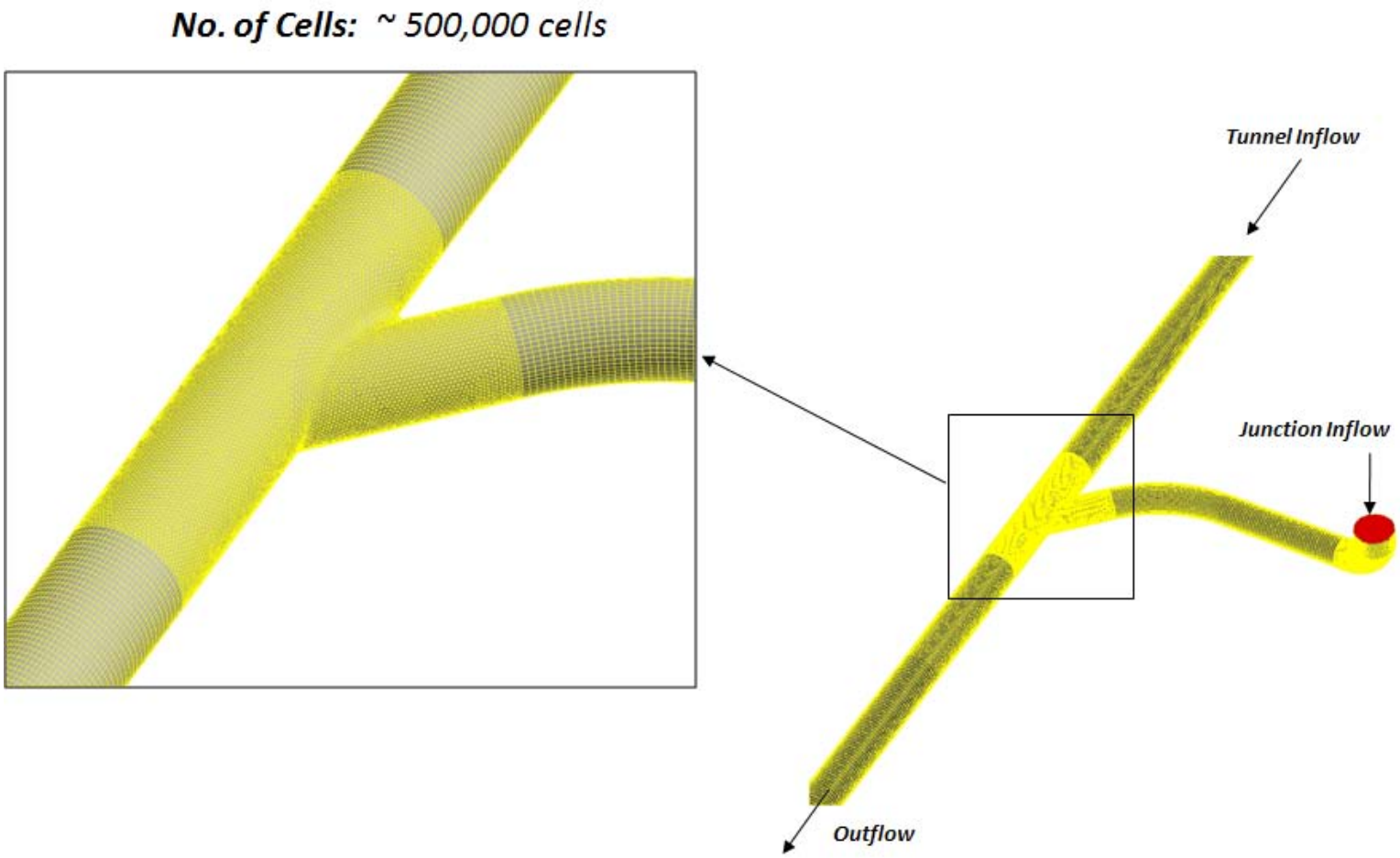

Figure 27: 4th Street Tunnel-Lateral Junction Computational Mesh

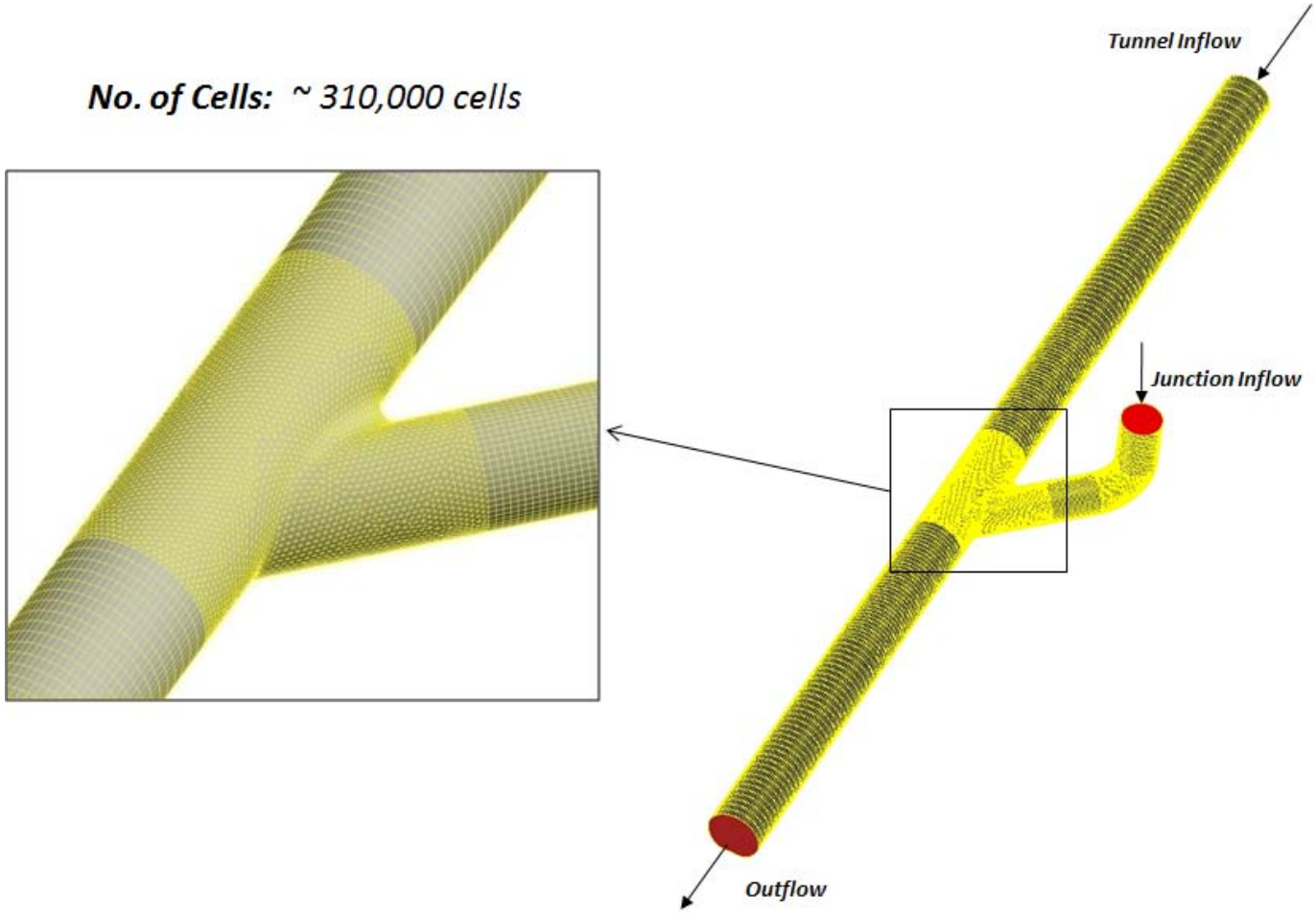

Figure 28: 8th Street Tunnel-Lateral Junction Computational Mesh

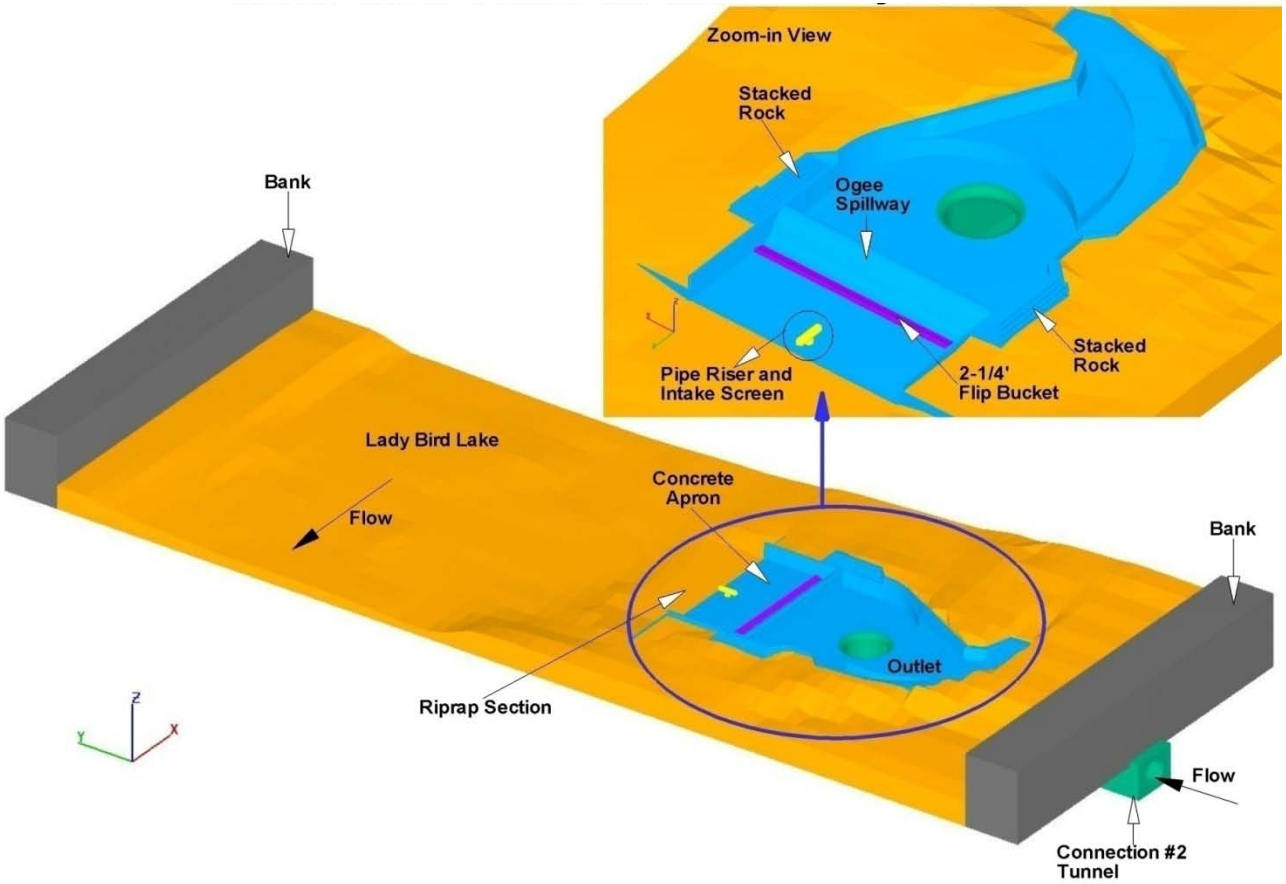

Figure 29: Waller Creek Tunnel Project; Outlet CFD Model

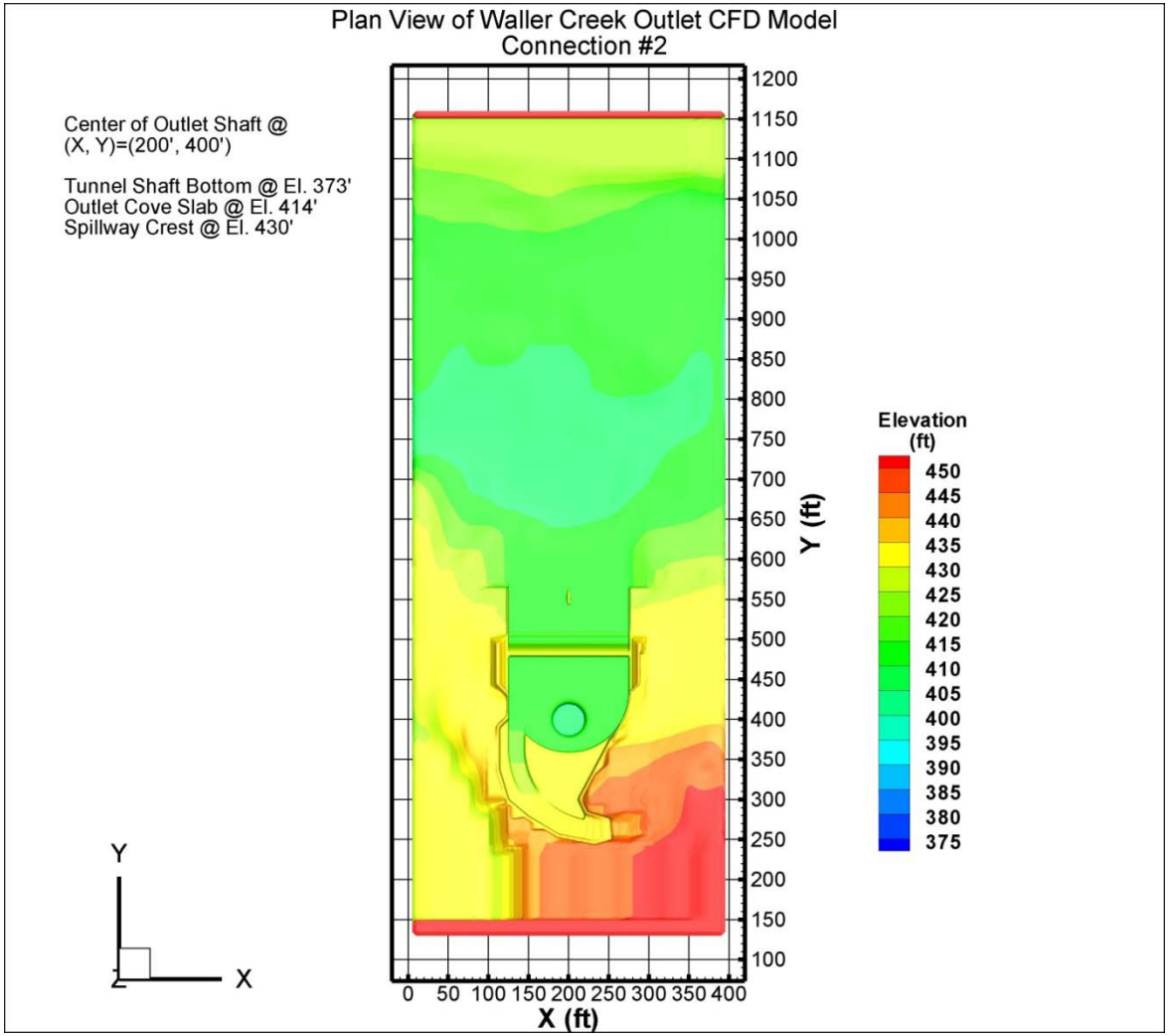

Figure 30: Plan View of Outlet CFD Model, Connection #2

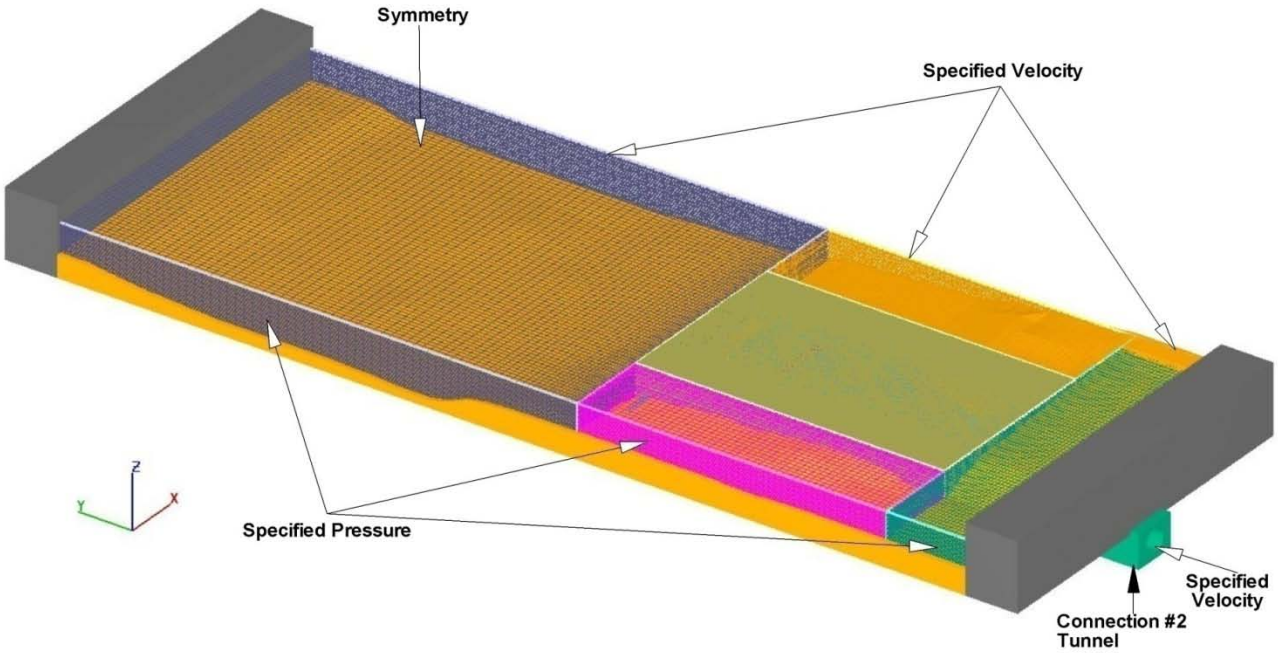

Figure 31: View of Mesh and Specifications of Boundary Conditions

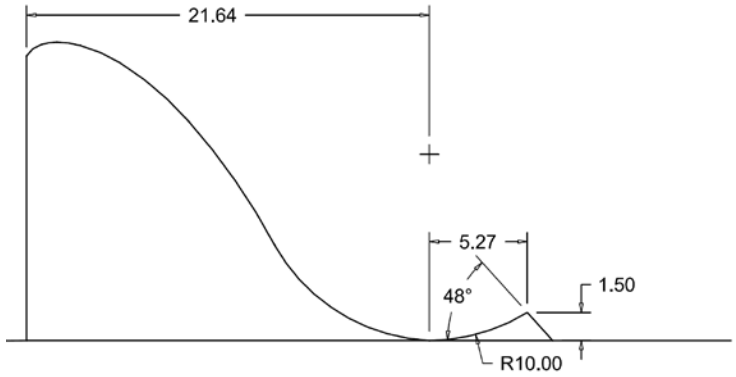

Flip Bucket 1.5ft

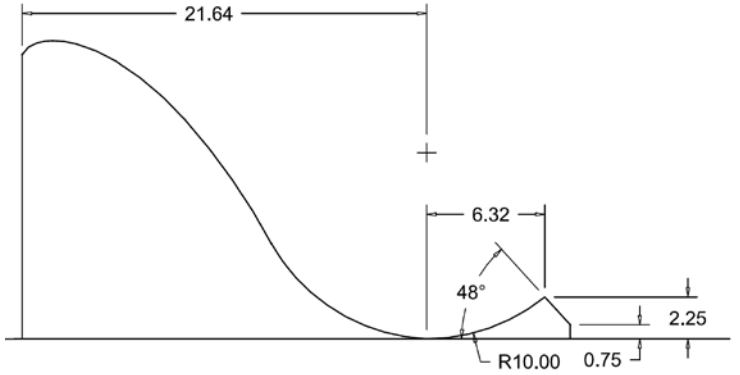

Flip Bucket 2.25ft

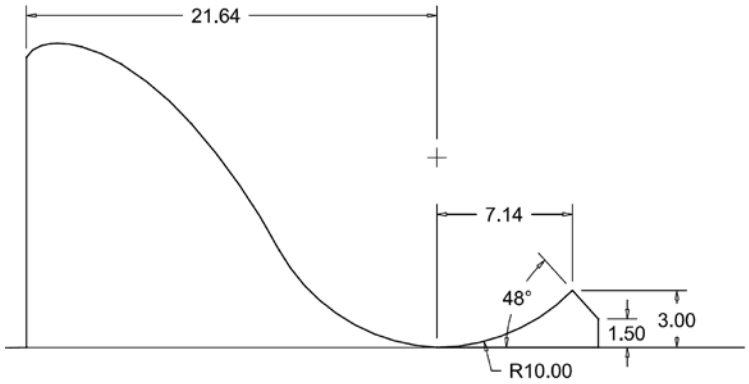

Flip Bucket 3ft

Figure 32: Outlet Spillway Flip Bucket Details

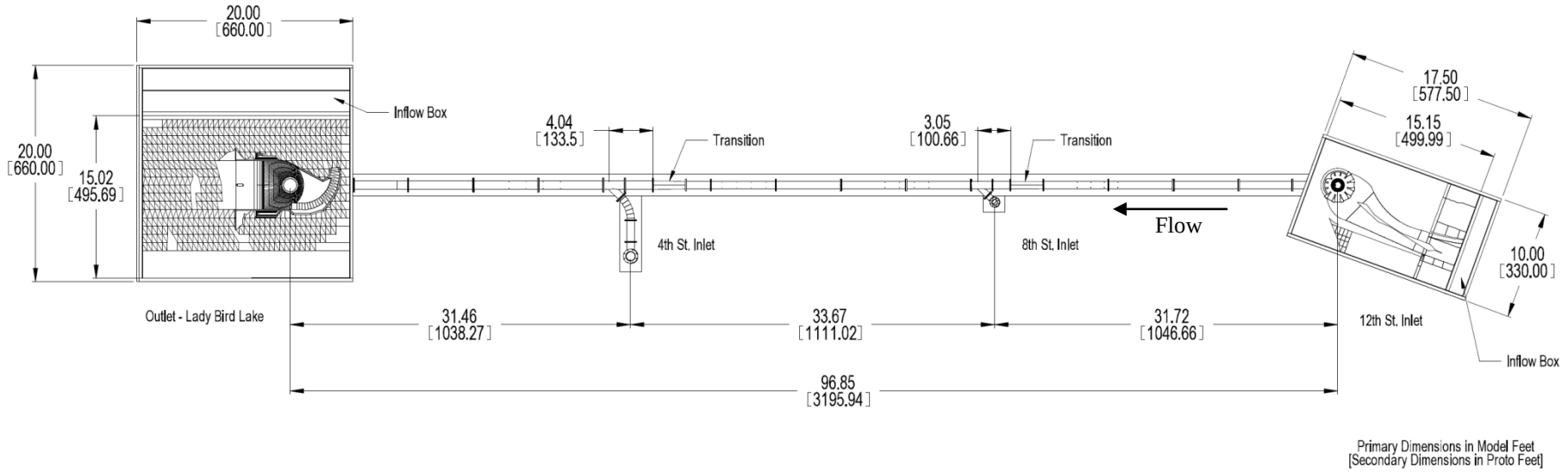

Figure 33: Waller Creek Tunnel Project Model Boundaries

Figure 34: Waller Creek Tunnel Project; 1:33 Scale Model-Inlet Channelization

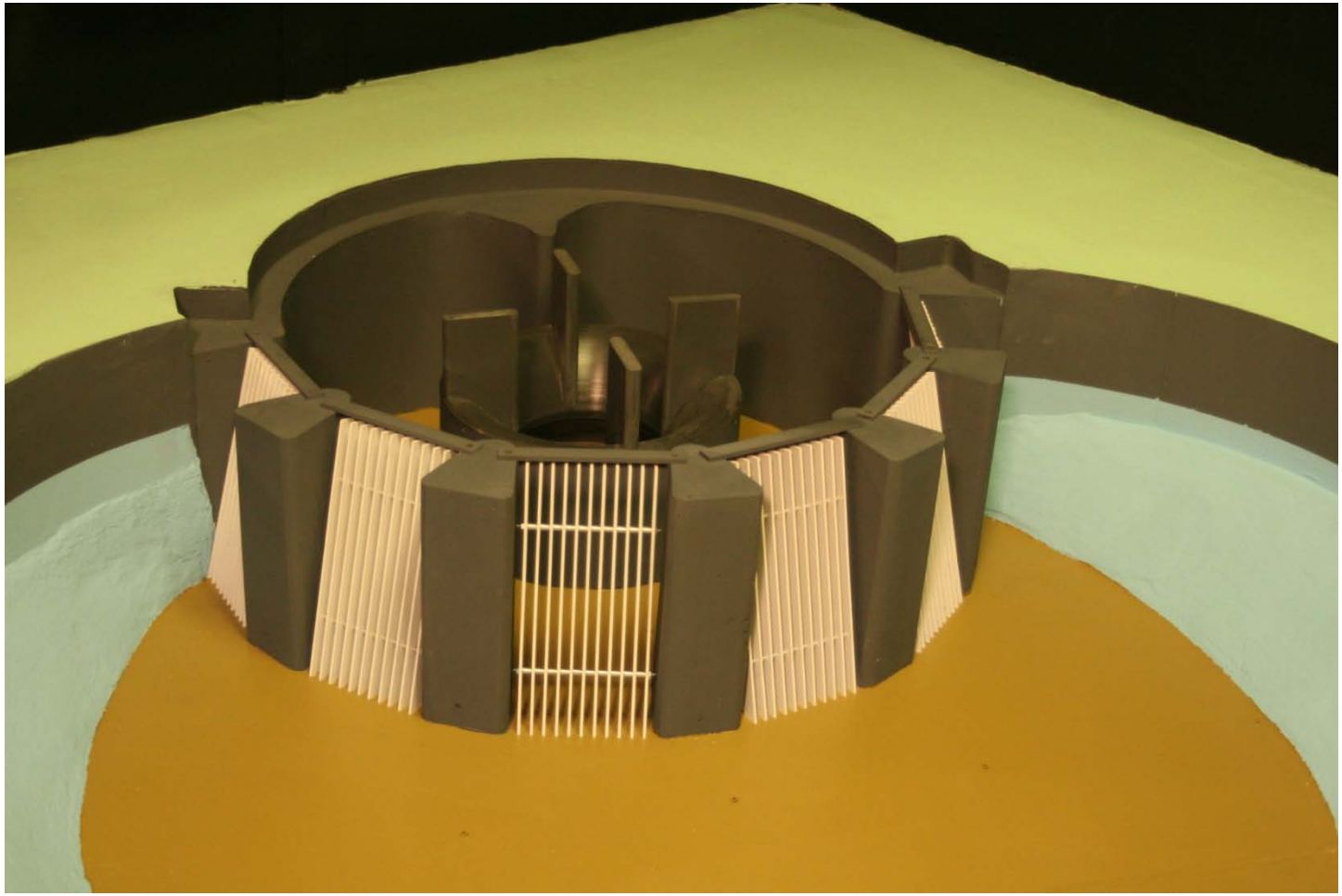

Figure 35: Waller Creek Tunnel Project; 1:33 Scale Model-Bar Screens and Morning Glory Spillway

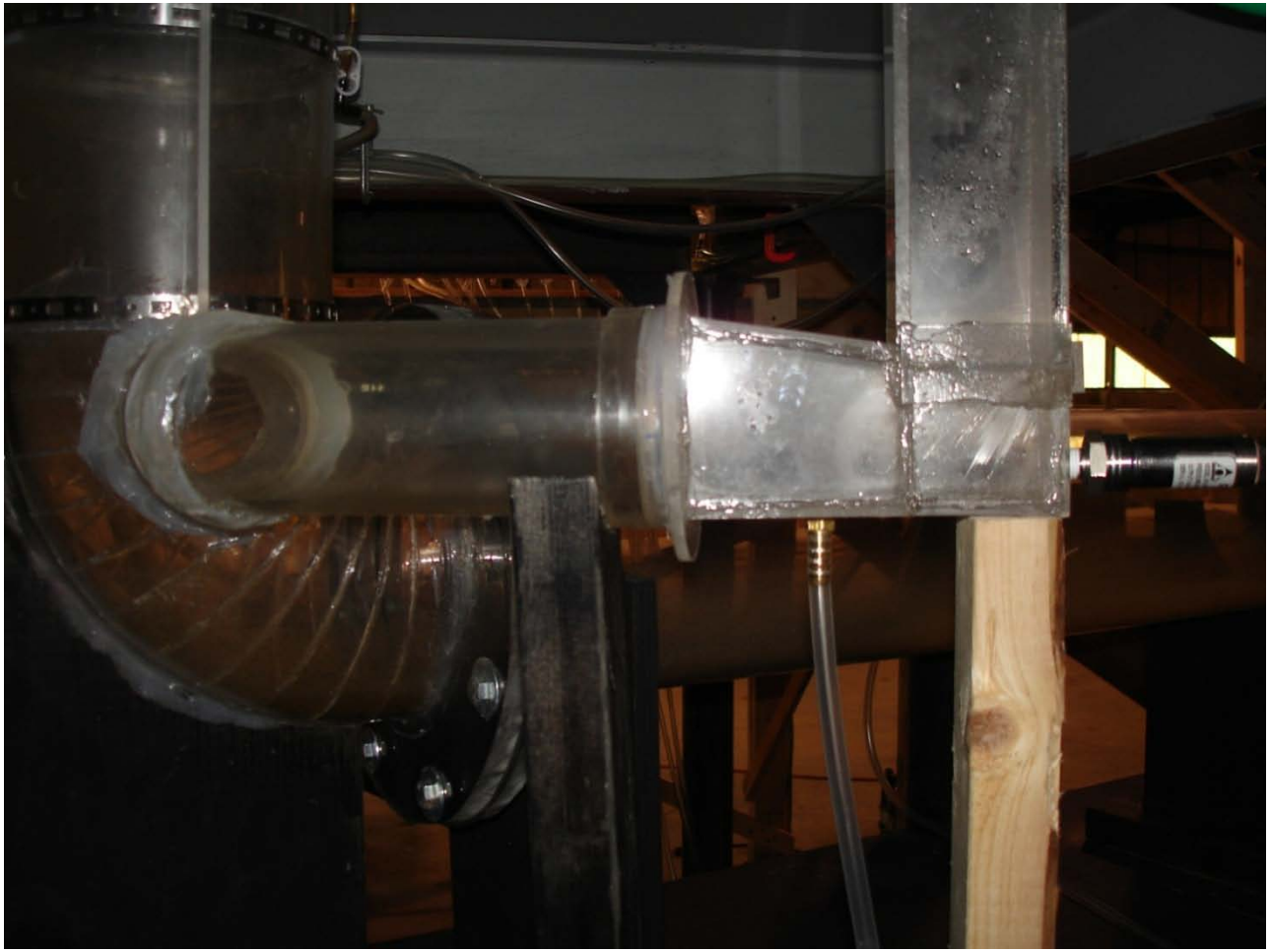

Figure 36: Waller Creek Tunnel Project; 1:33 Scale Model-Inlet Drop Shaft, Elbow and Portal Connection

Figure 37: Waller Creek Tunnel Project; 1:33 Scale Model- 8th Street Lateral Junction Elbow

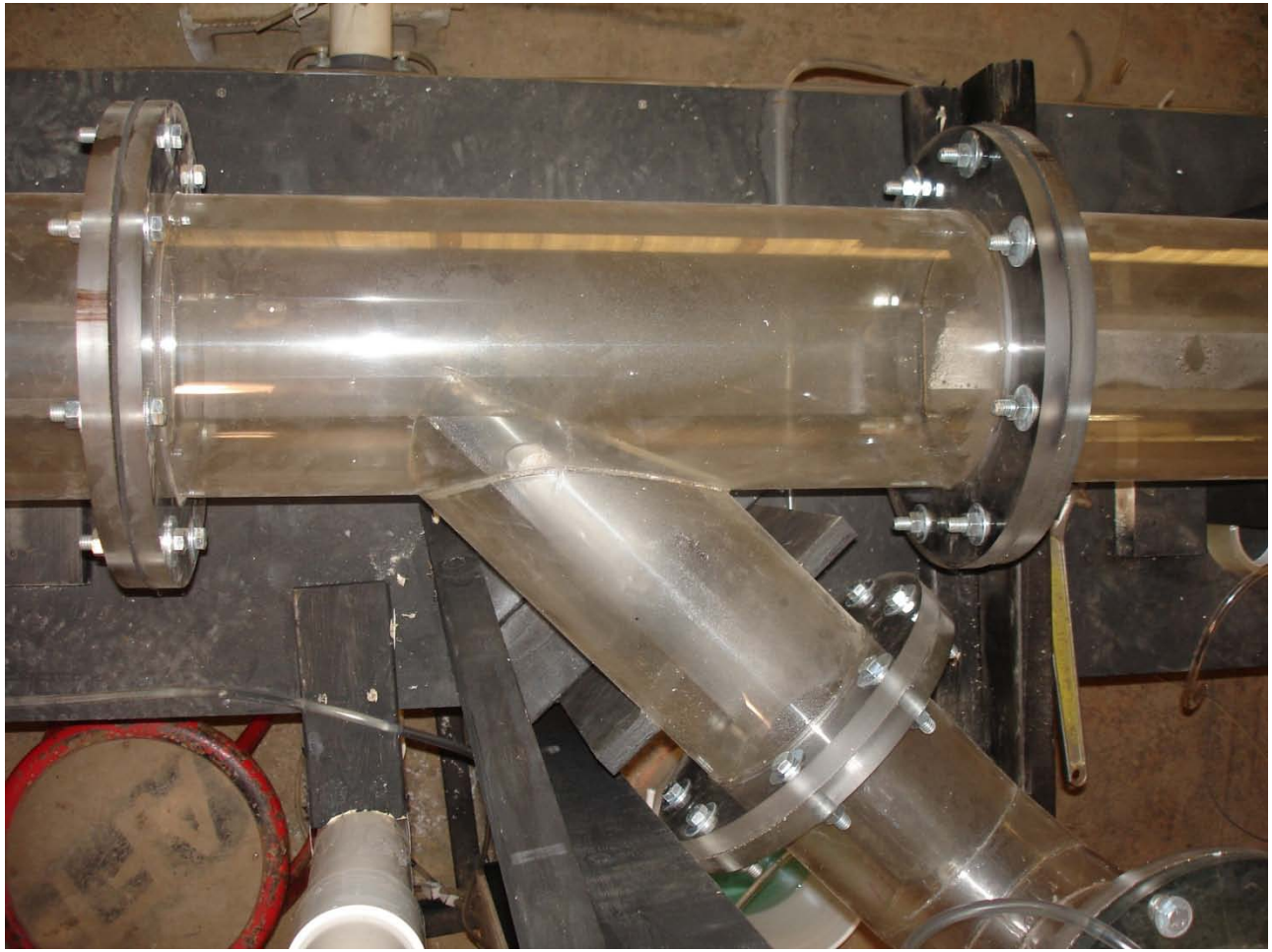

Figure 38: Waller Creek Tunnel Project; 1:33 Scale Model-8th Street Lateral Junction

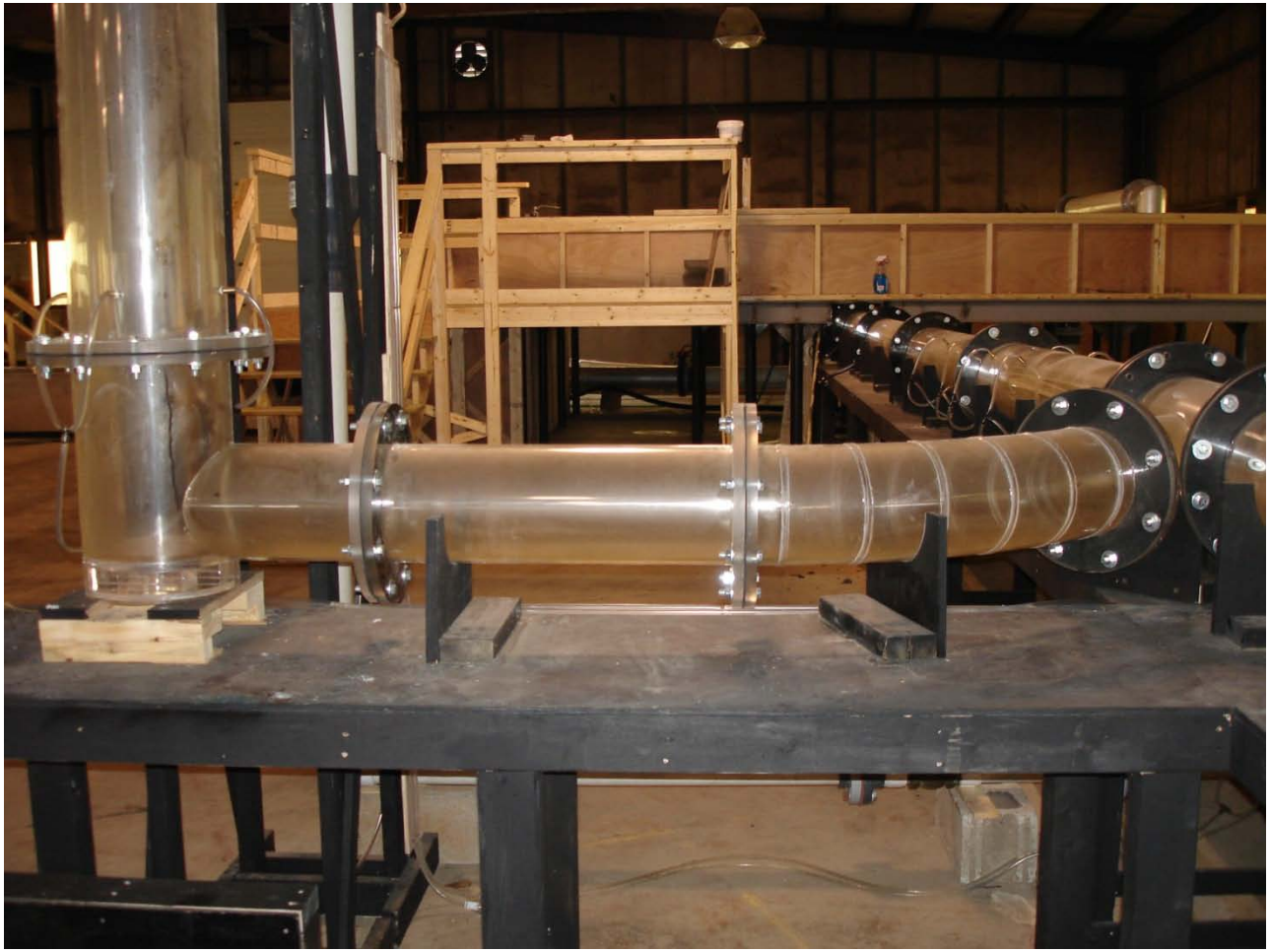

Figure 39: Waller Creek Tunnel Project; 1:33 Scale Model-4th Street Lateral Junction Drop Shaft Connection

Figure 40: Waller Creek Tunnel Project; 1:33 Scale Model-4th Street Lateral Junction

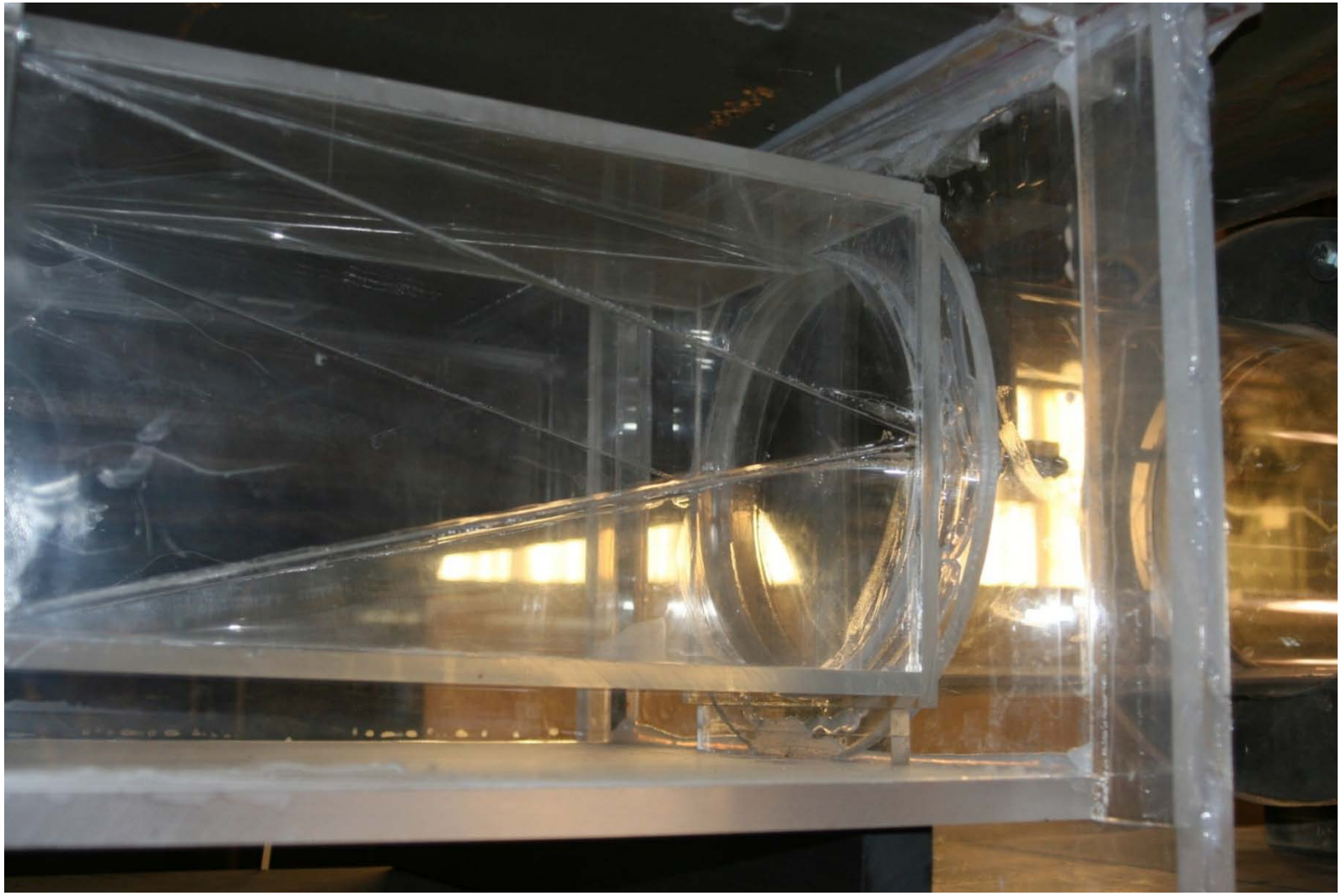

Figure 41: Waller Creek Tunnel Project; 1:33 Scale Model-Outlet Connection

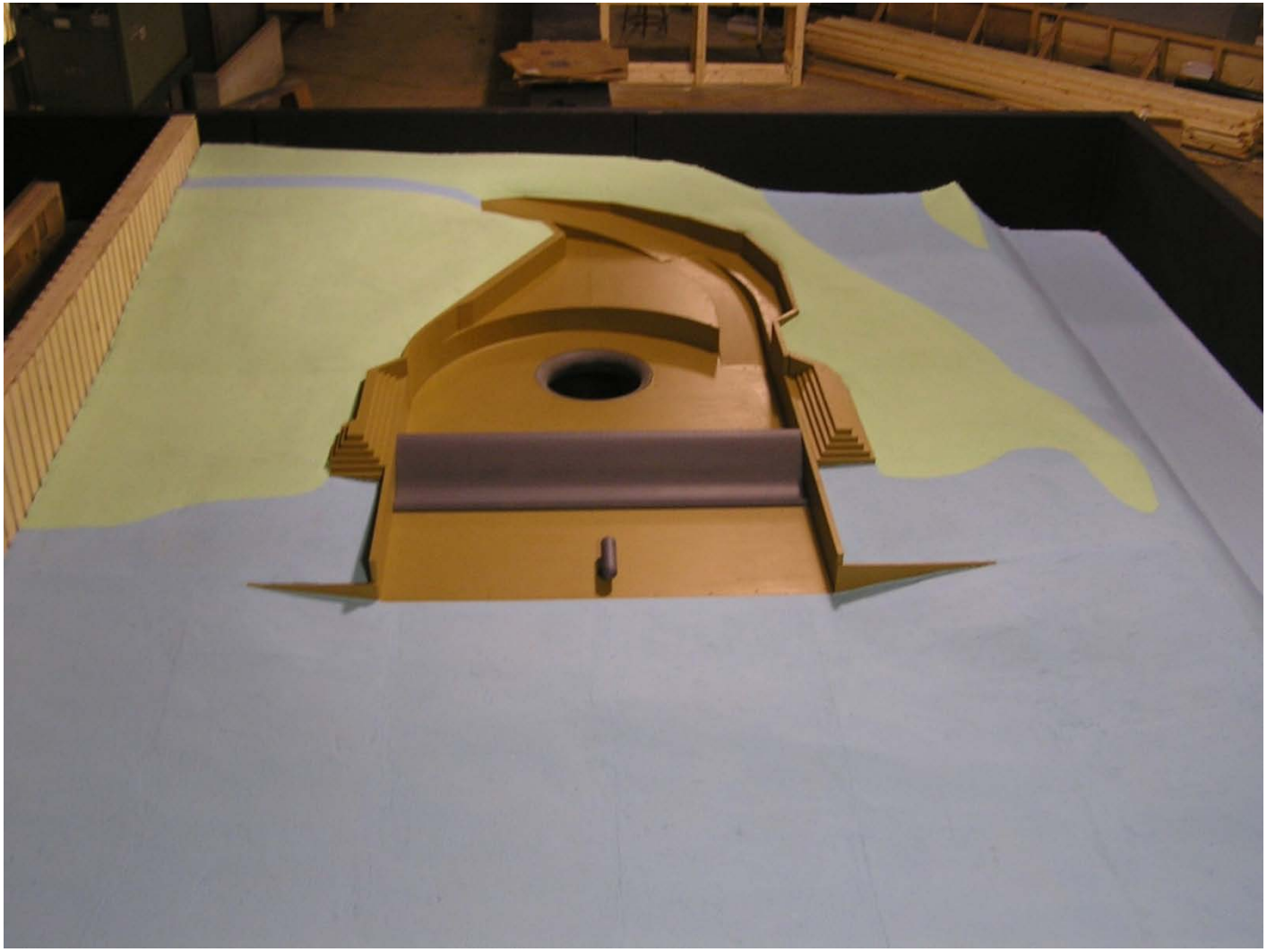

Figure 42: Waller Creek Tunnel Project; 1:33 Scale Model-Outlet

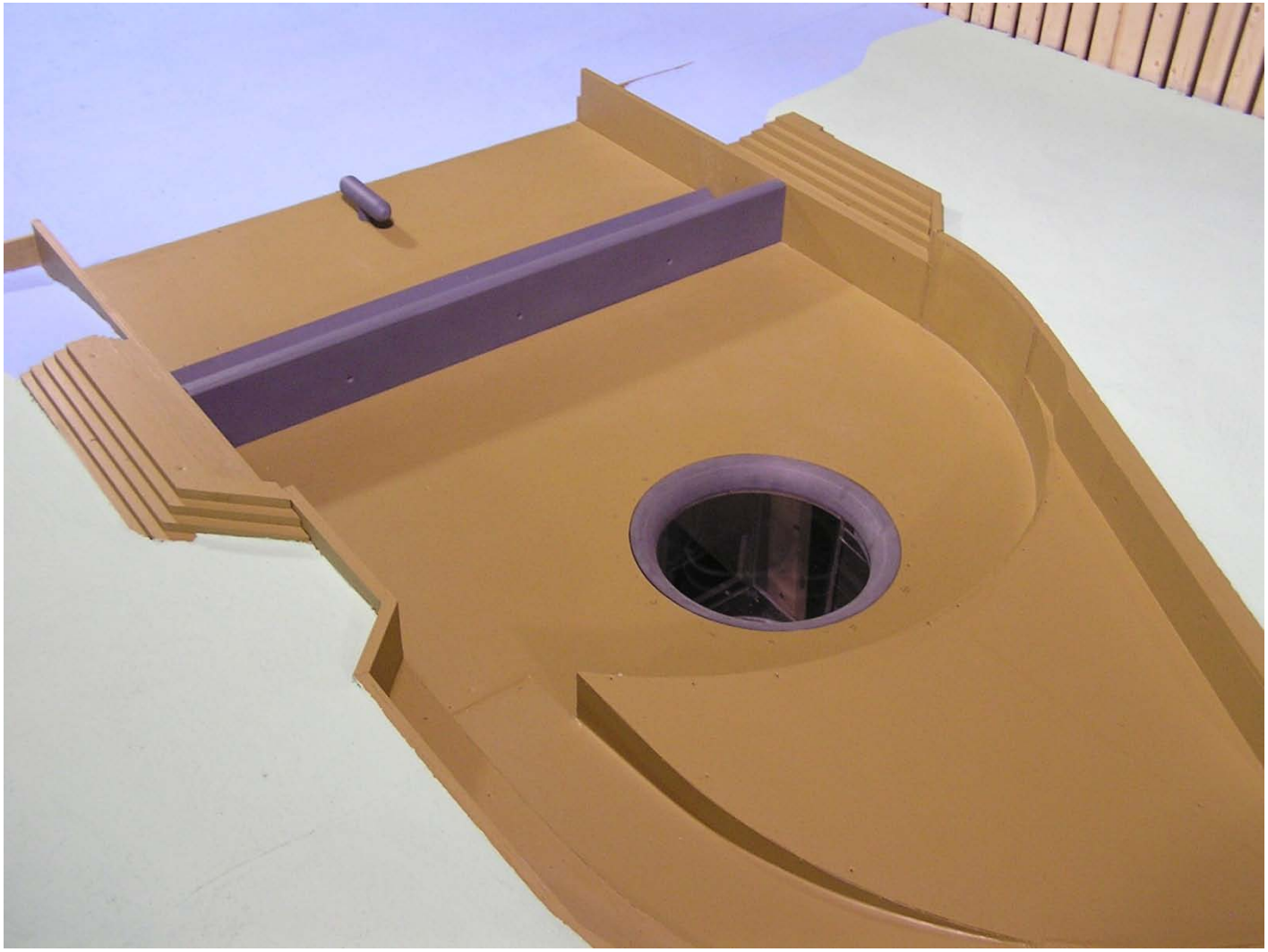

Figure 43: Waller Creek Tunnel Project; 1:33 Scale Model-Outlet Cove

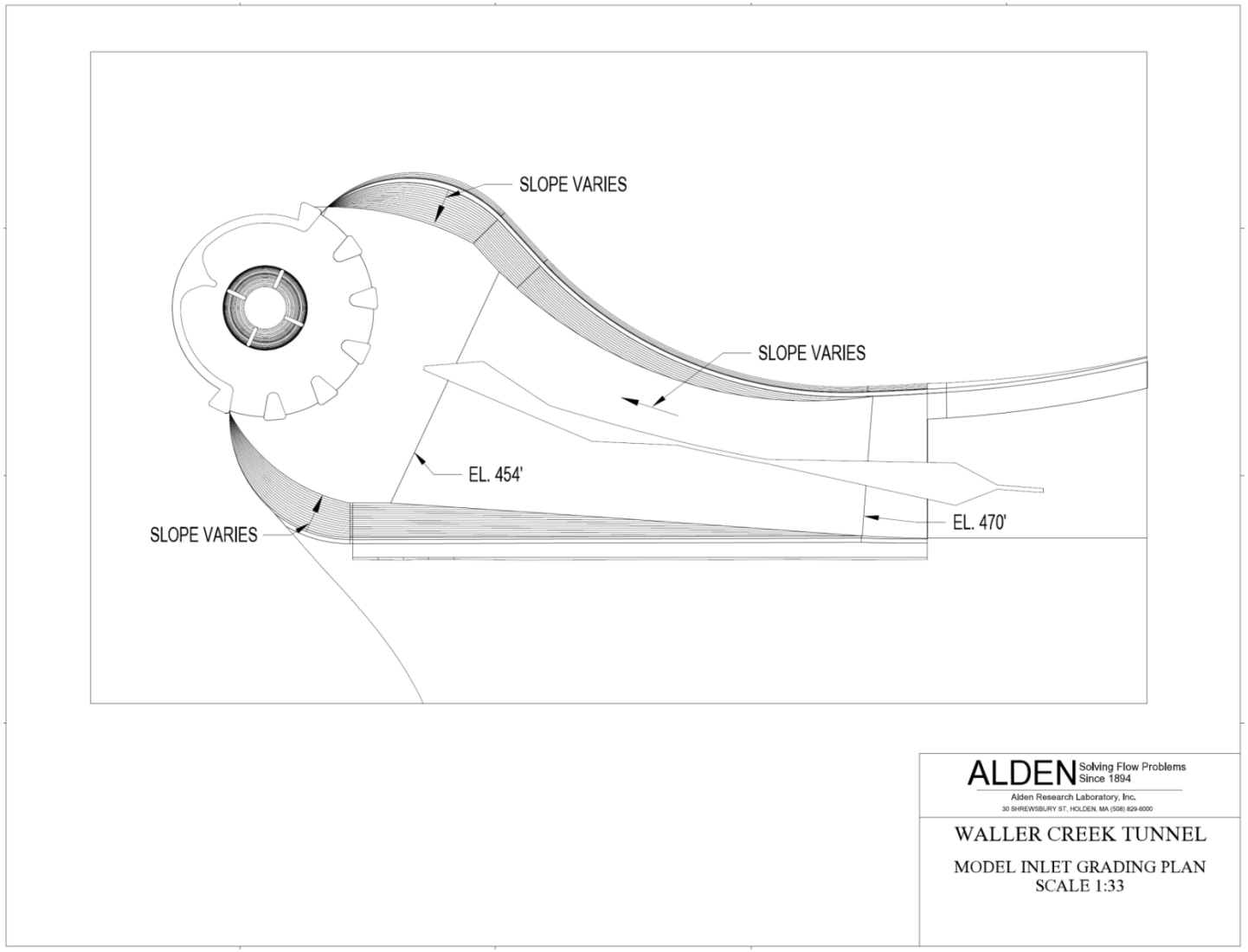

Figure 44: Waller Creek Tunnel Project; 1:33 Scale Model – Inlet Pool Grading Plan

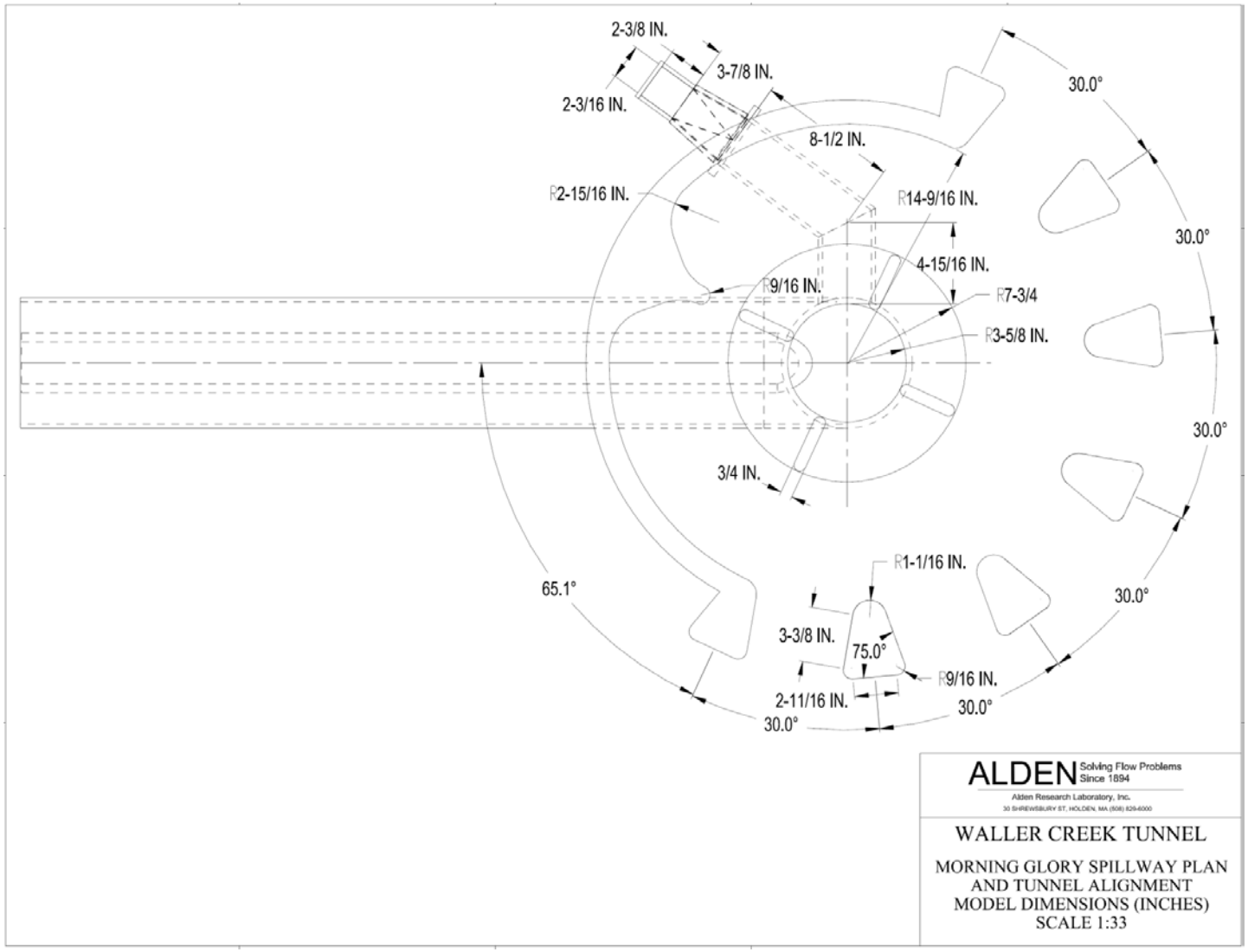

Figure 45: Waller Creek Tunnel Project; 1:33 Scale Model Morning Glory Spillway Dimensions –Plan

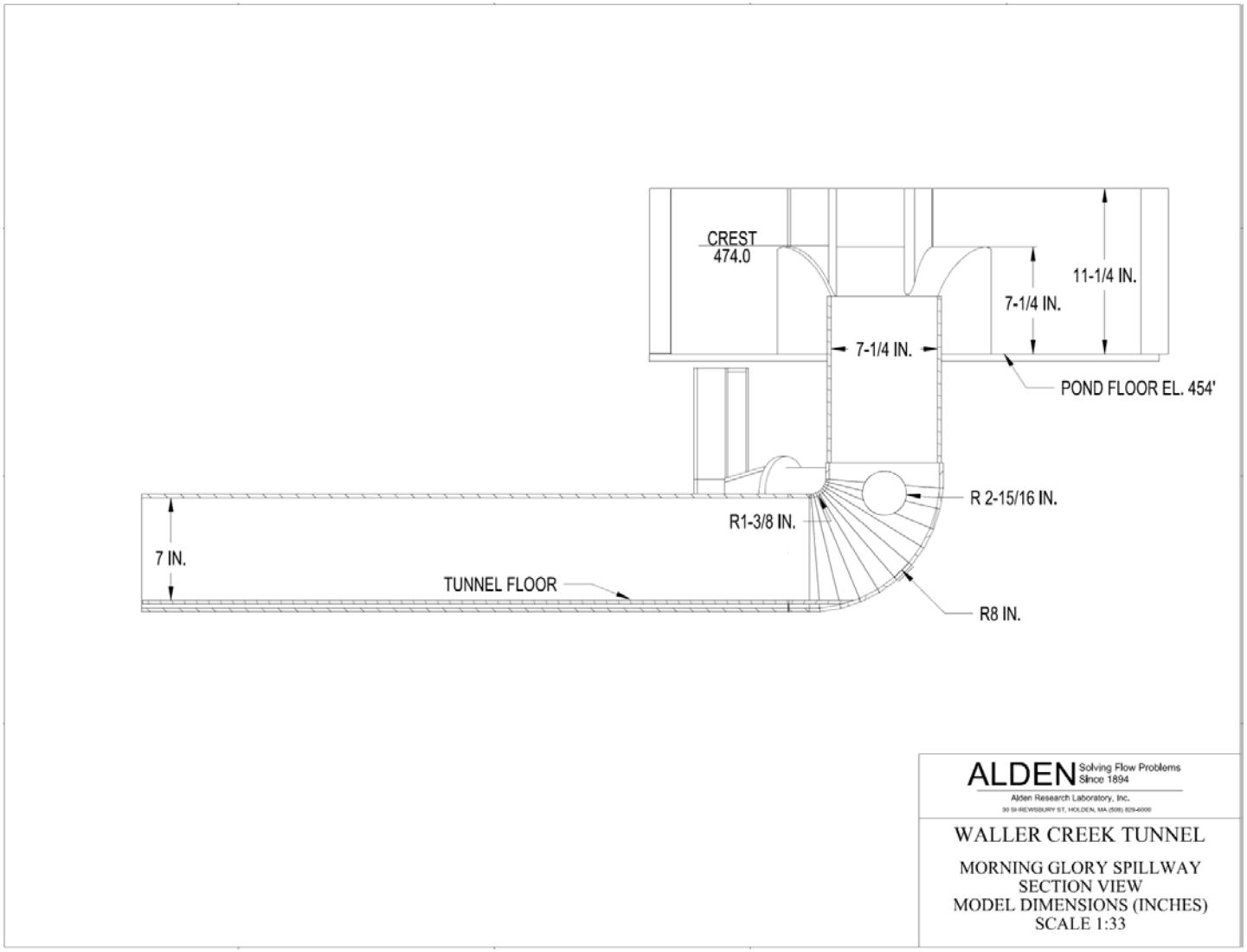

Figure 46: Waller Creek Tunnel Project; 1:33 Scale Model Morning Glory Spillway Dimensions – Section

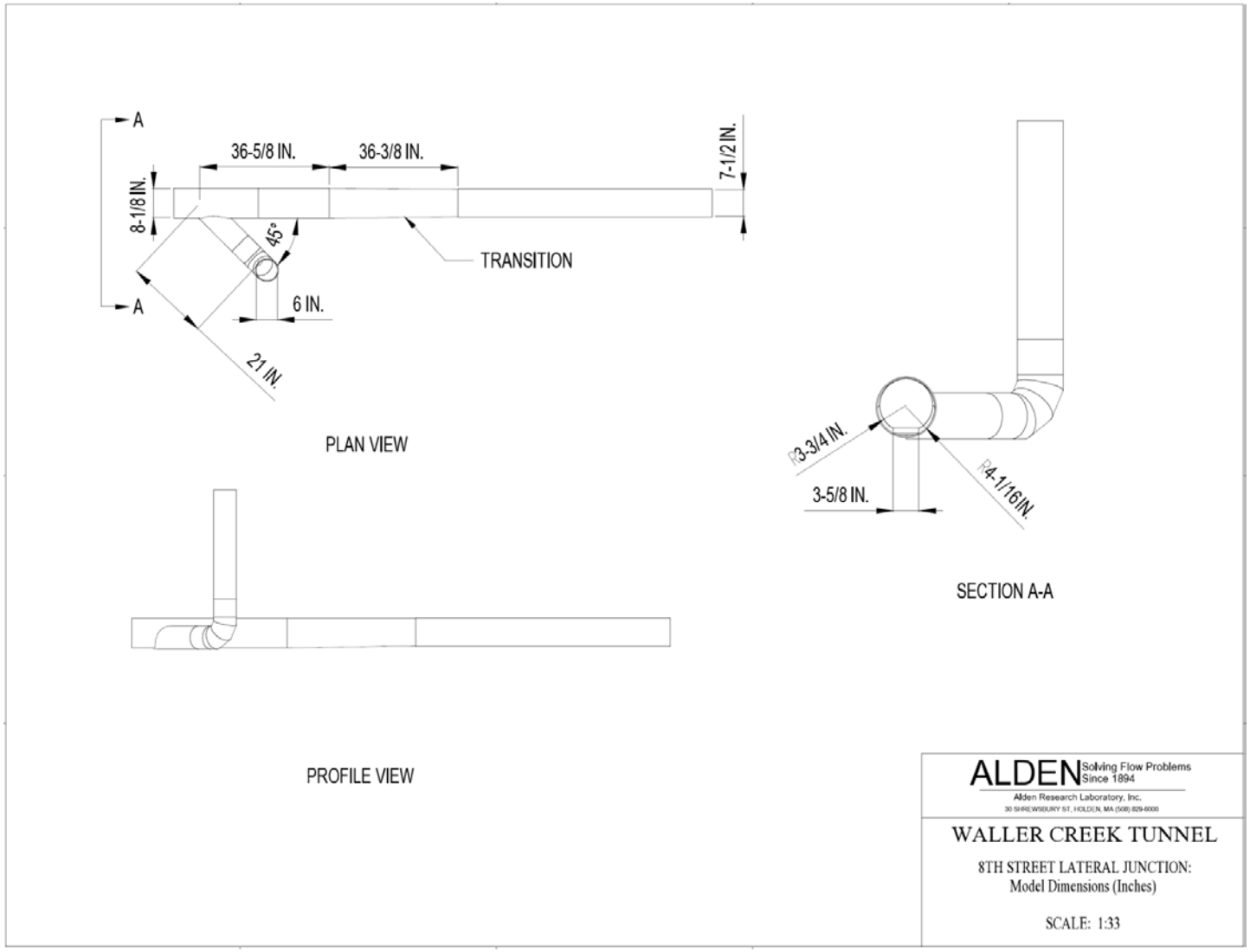

Figure 47: Waller Creek Tunnel Project; 1:33 Scale Model 8th Street Lateral Dimensions

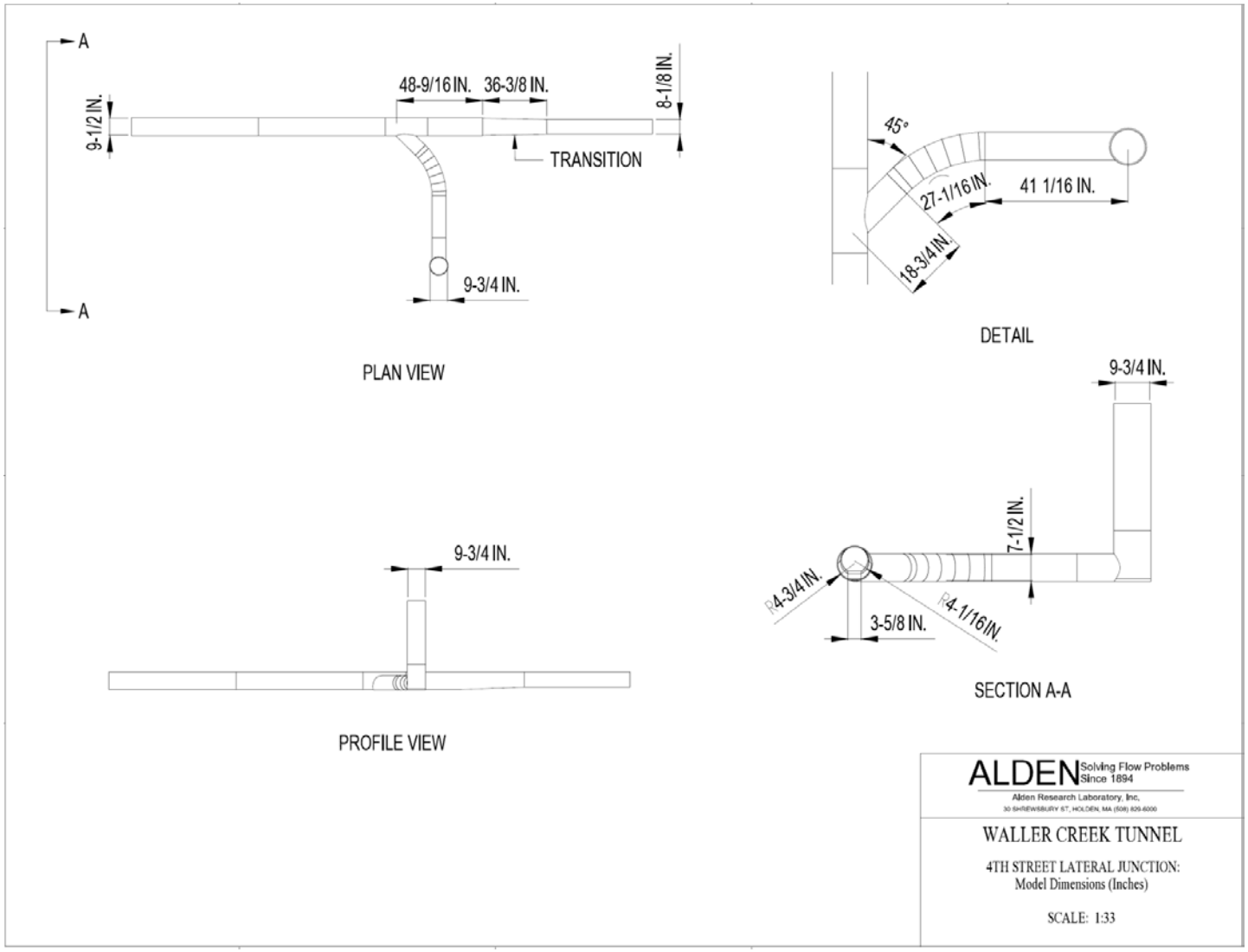

Figure 48: Waller Creek Tunnel Project; 1:33 Scale Model 4th Street Lateral Dimensions

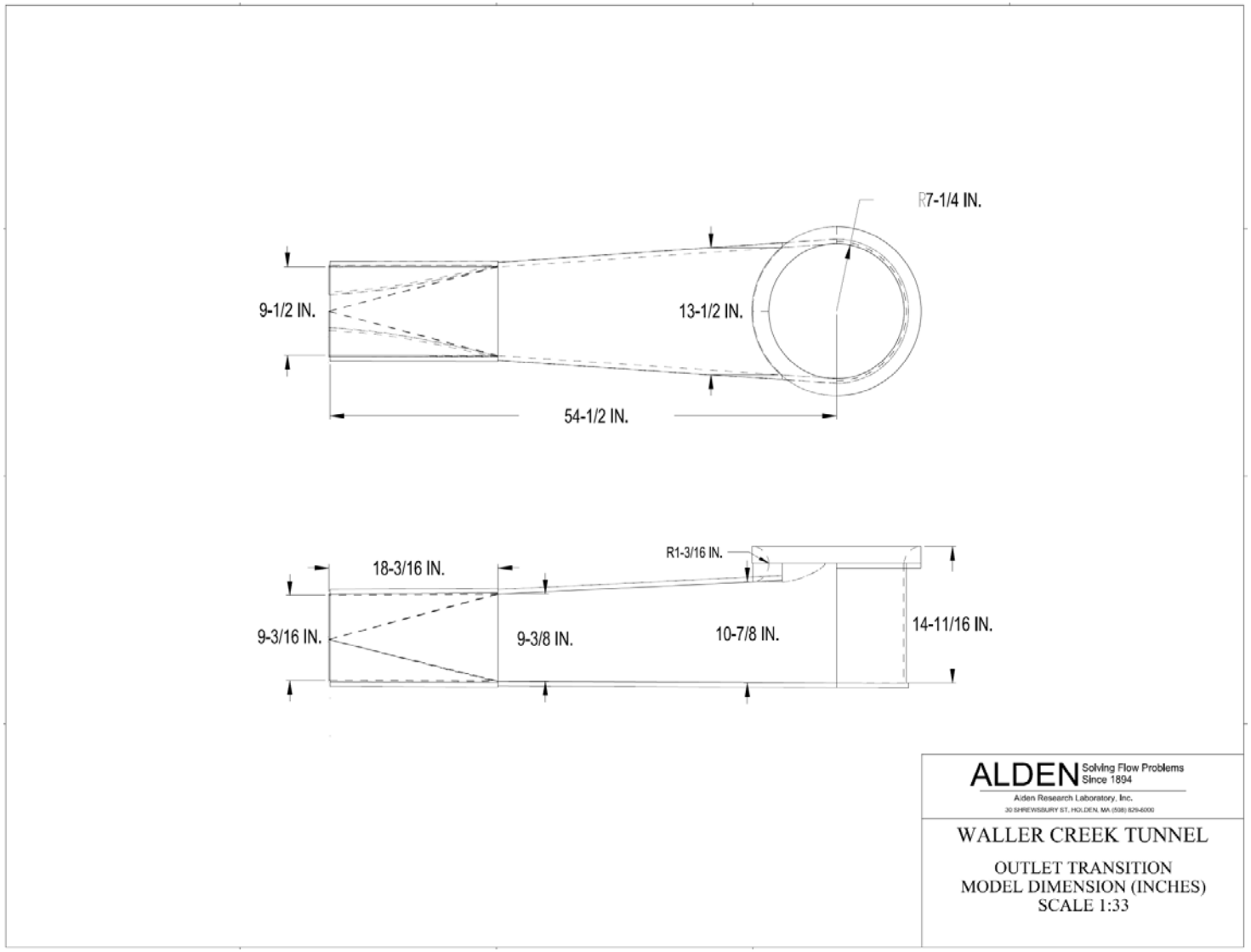

Figure 49: Waller Creek Tunnel Project; 1:33 Scale Model Outlet Transition Dimensions

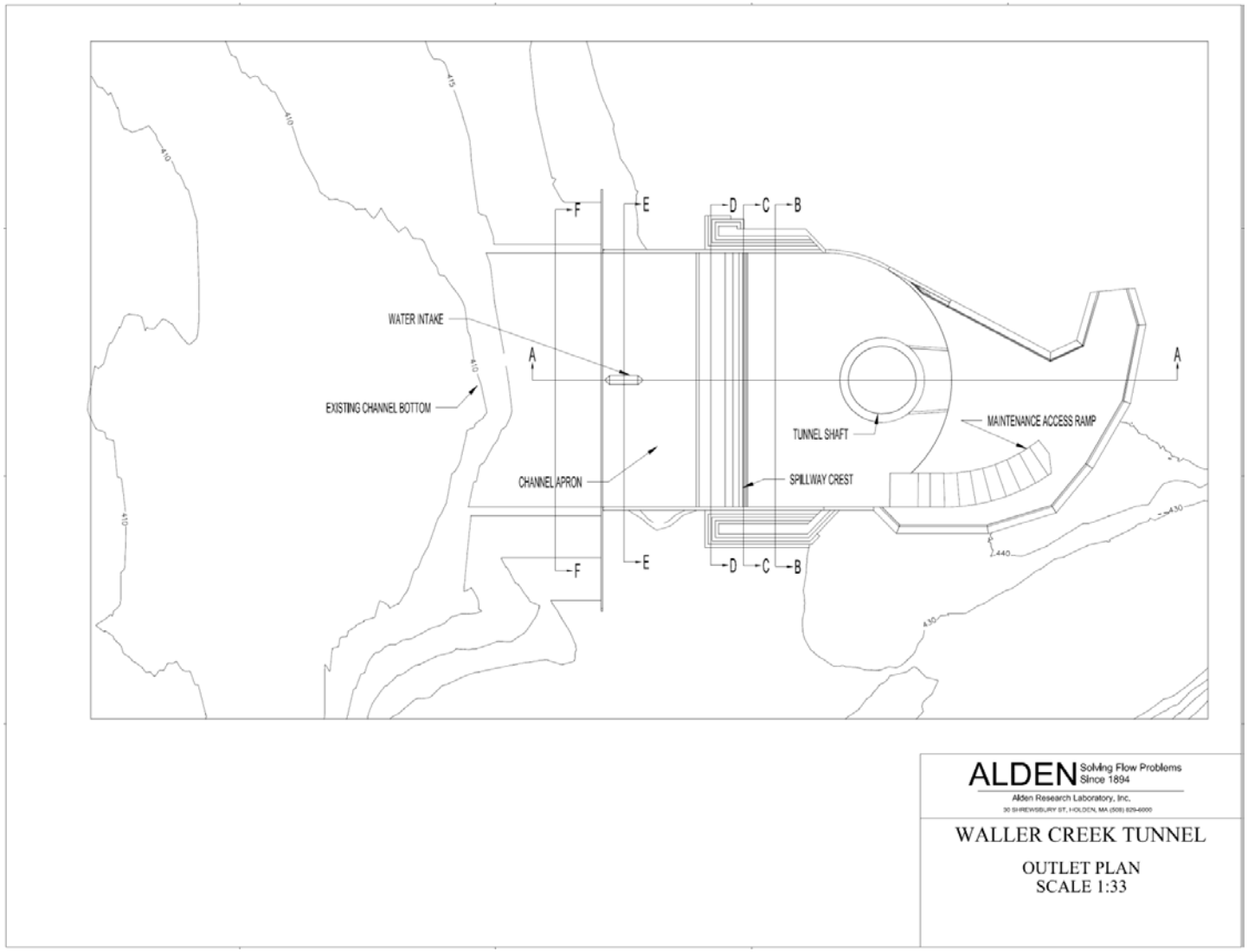

Figure 50: Waller Creek Tunnel Project; 1:33 Scale Model Outlet Plan

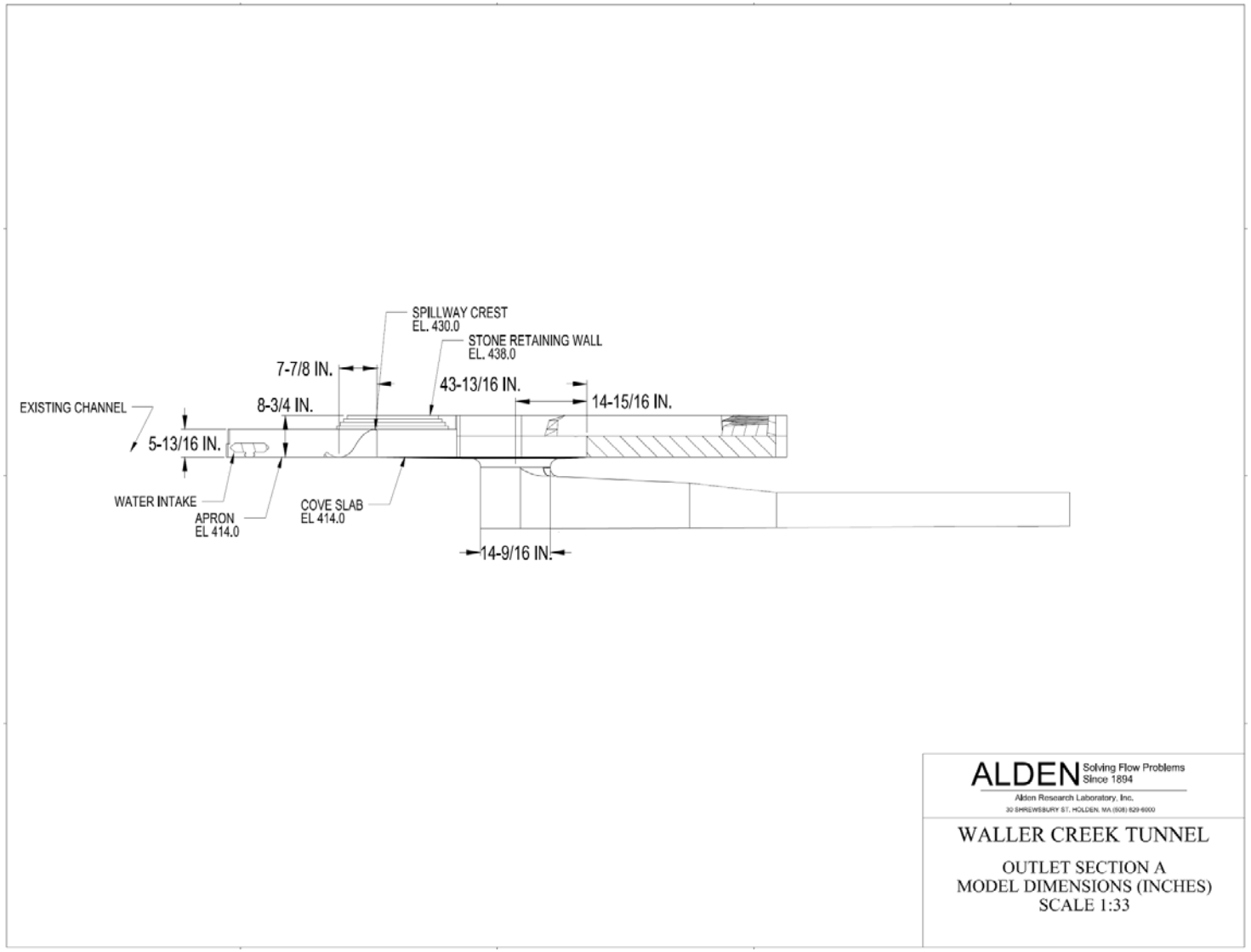

Figure 51: Waller Creek Tunnel Project; 1:33 Scale Model Outlet Dimensions –Section A

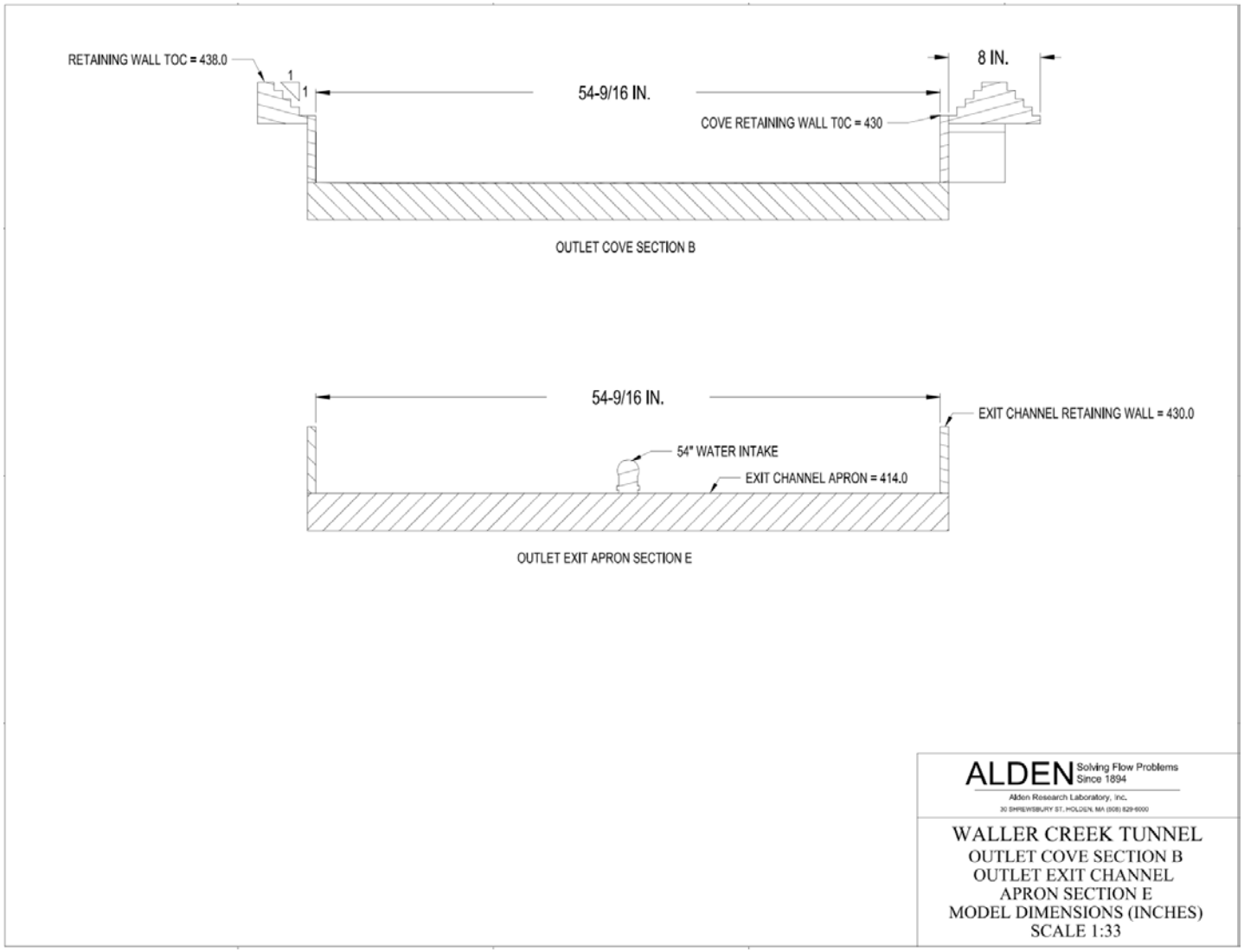

Figure 52: Waller Creek Tunnel Project; 1:33 Scale Model Outlet Dimensions –Sections B and E

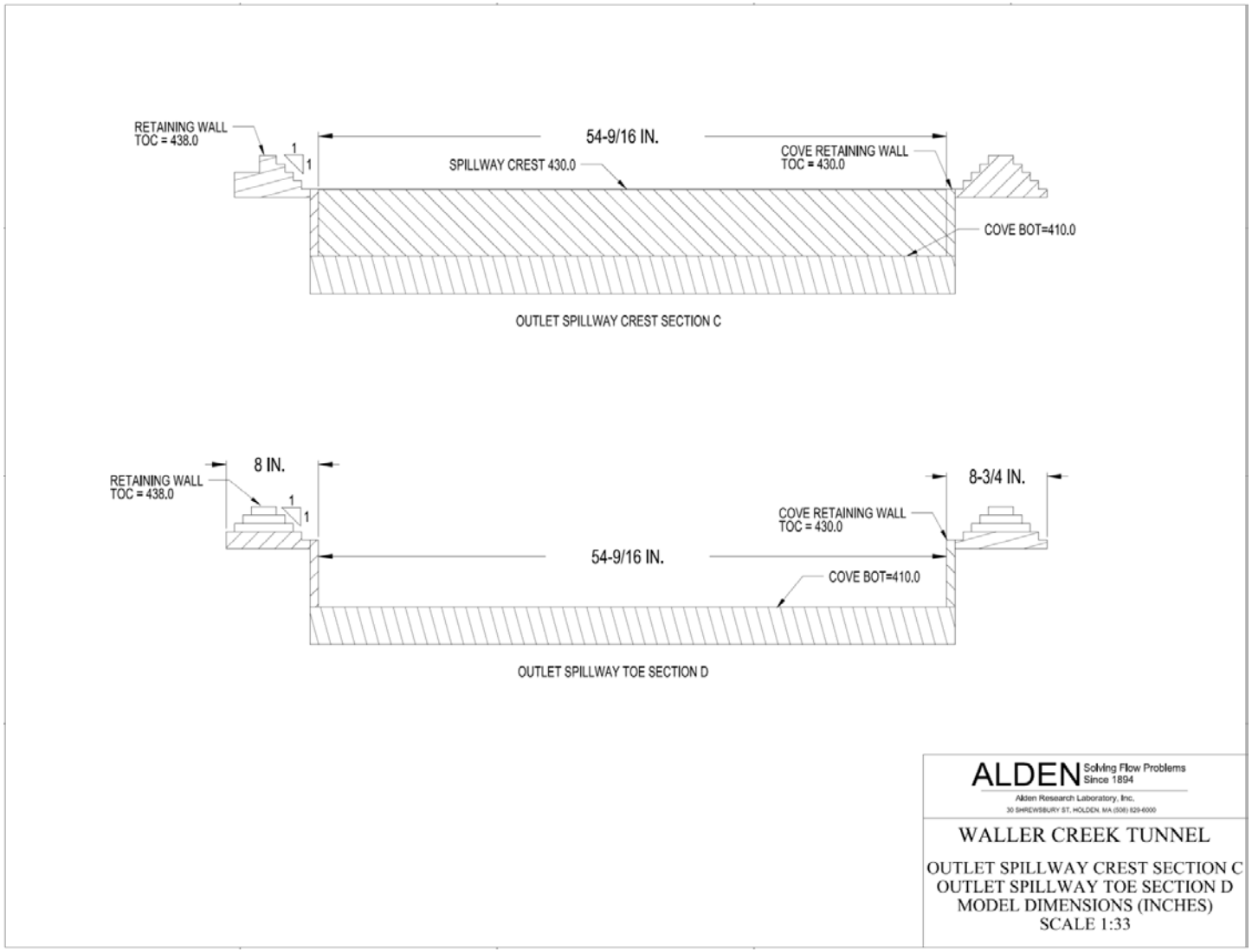

Figure 53: Waller Creek Tunnel Project; 1:33 Scale Model Outlet Dimensions –Sections C and D

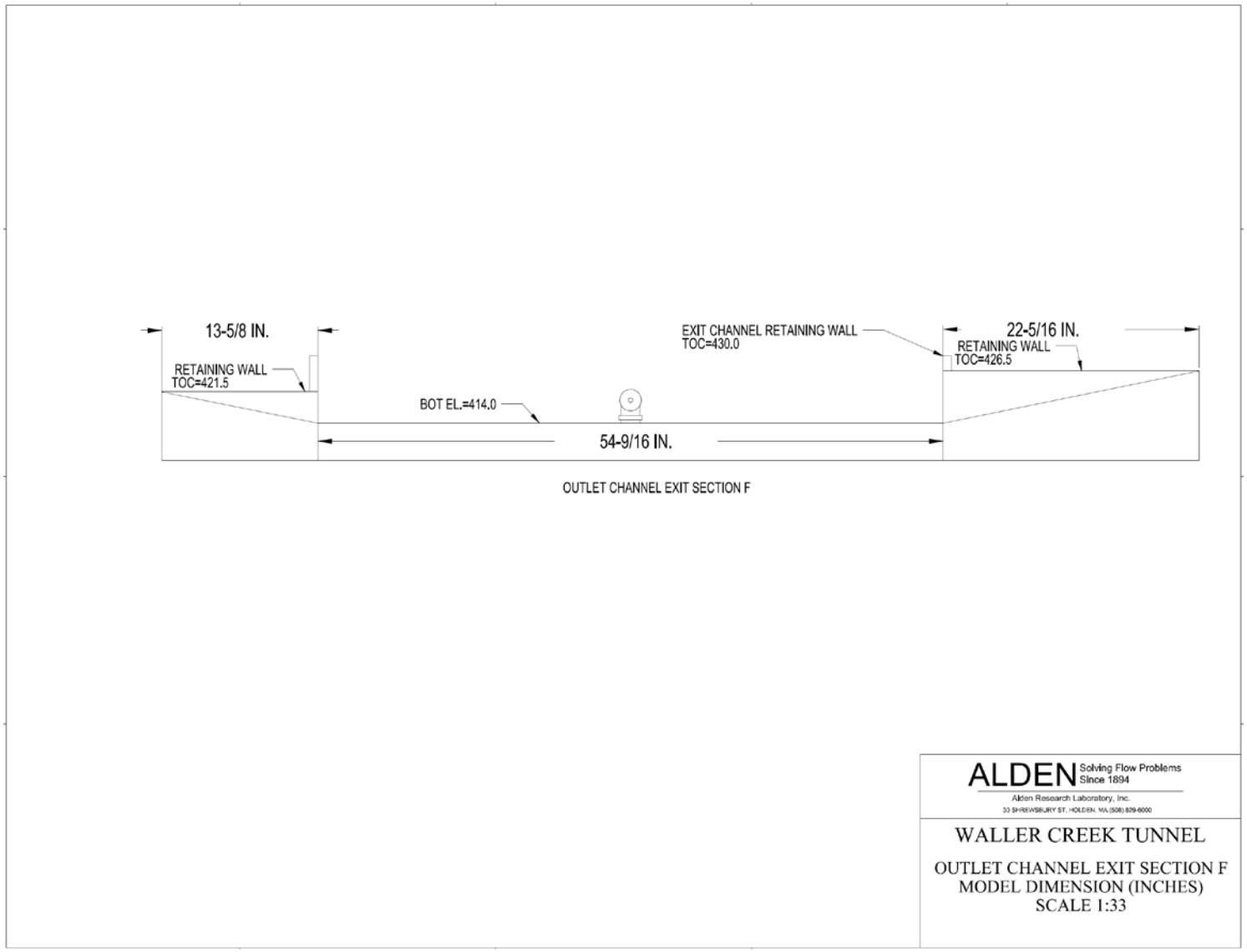

Figure 54: Waller Creek Tunnel Project; 1:33 Scale Model Outlet Dimensions –Section F

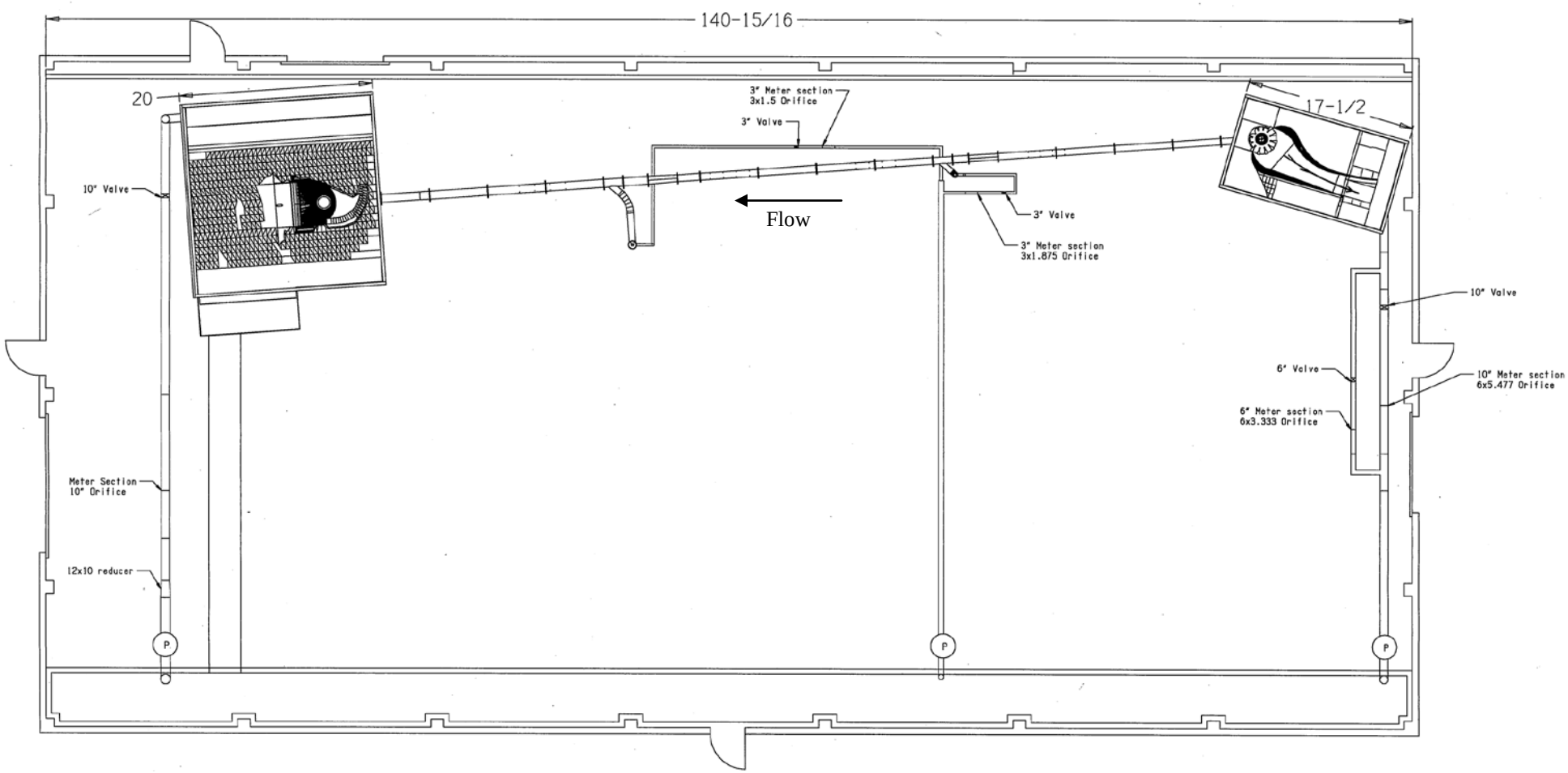

Figure 55: Waller Creek Tunnel Project; 1:33 Scale Model-Flow Loop

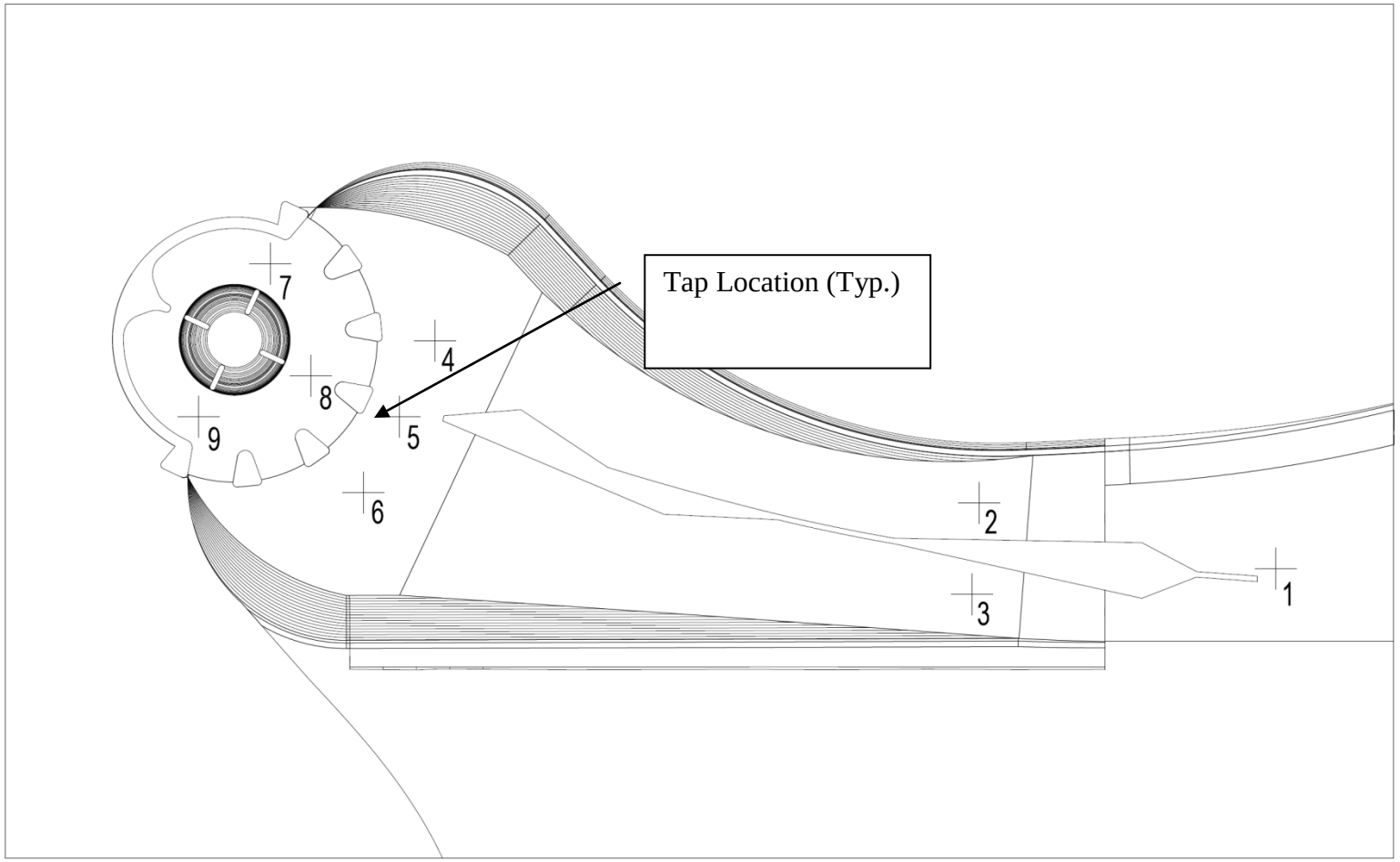

Figure 56: Waller Creek Tunnel Project; 1:33 Scale Model-Inlet Tap Locations

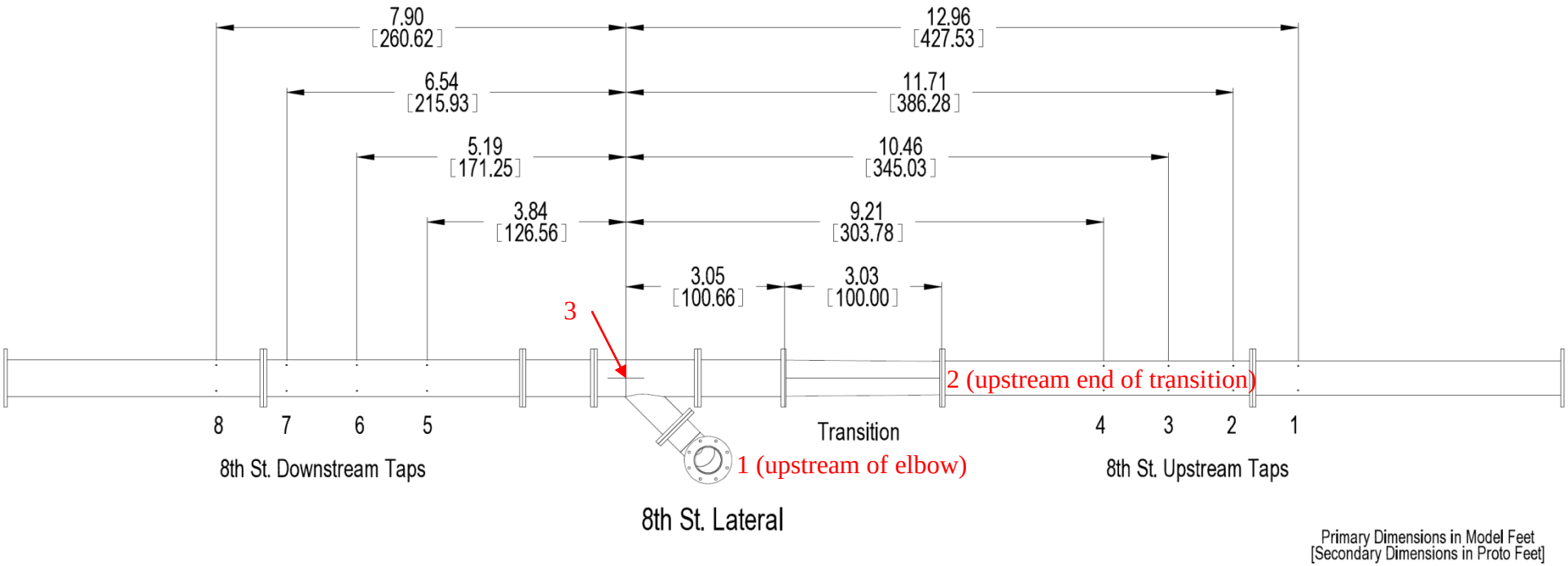

Figure 57: Waller Creek Tunnel Project; 1:33 Scale Model- 8th Street Lateral Tap Locations

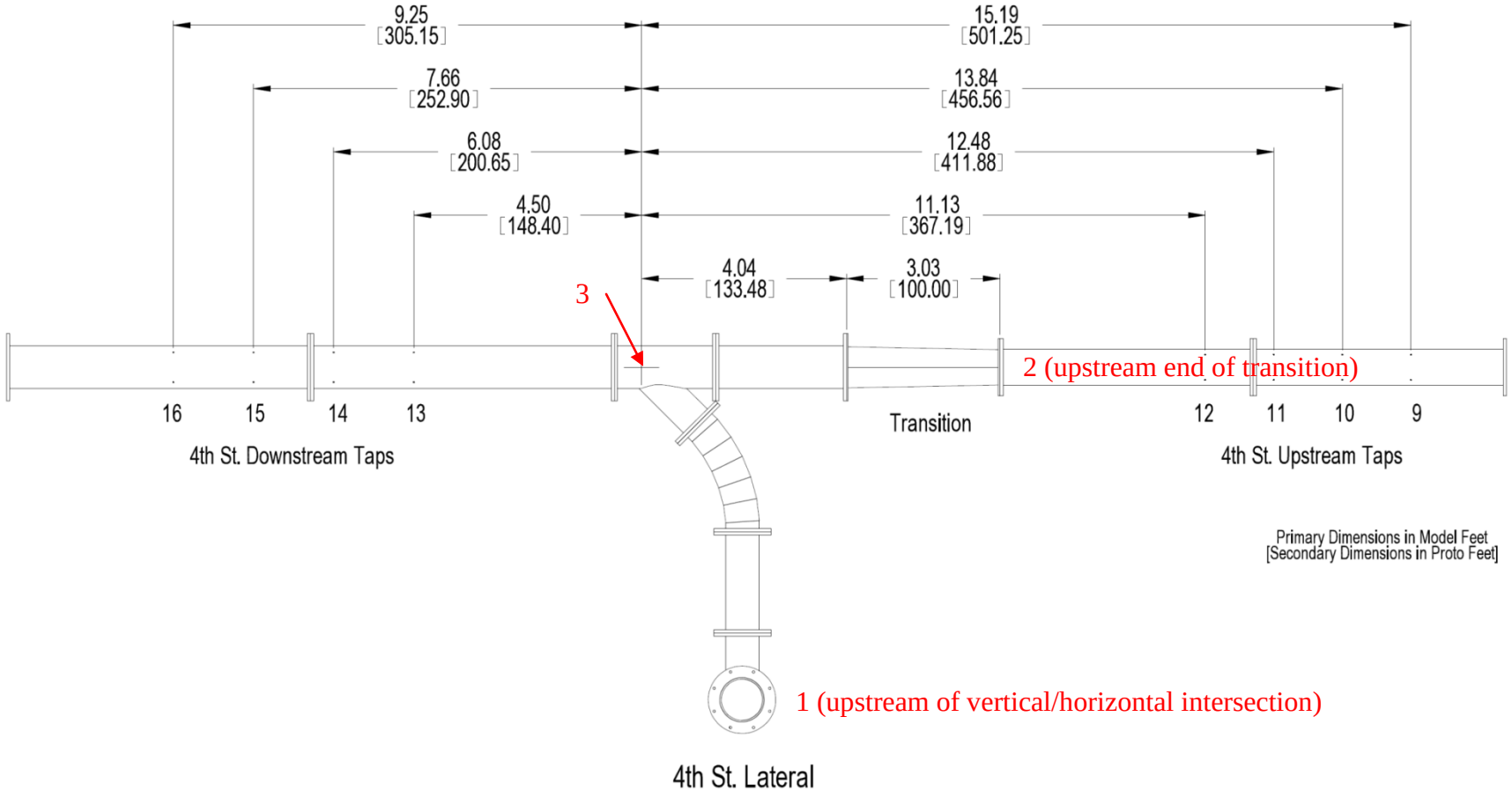

Figure 58: Waller Creek Tunnel Project; 1:33 Scale Model-4th Street Lateral Tap Locations

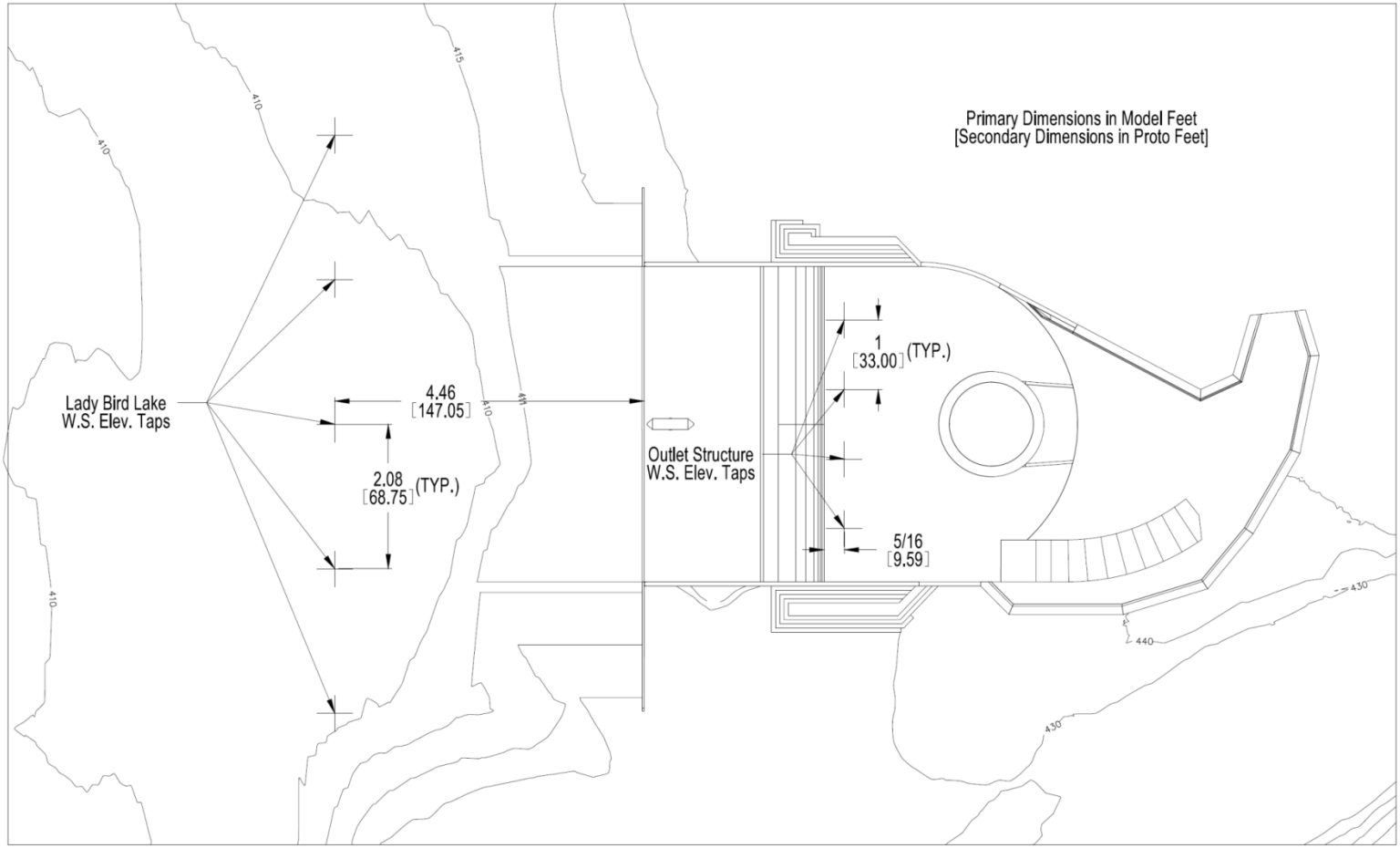

Figure 59: Waller Creek Tunnel Project; 1:33 Scale Model-Outlet Tap Locations

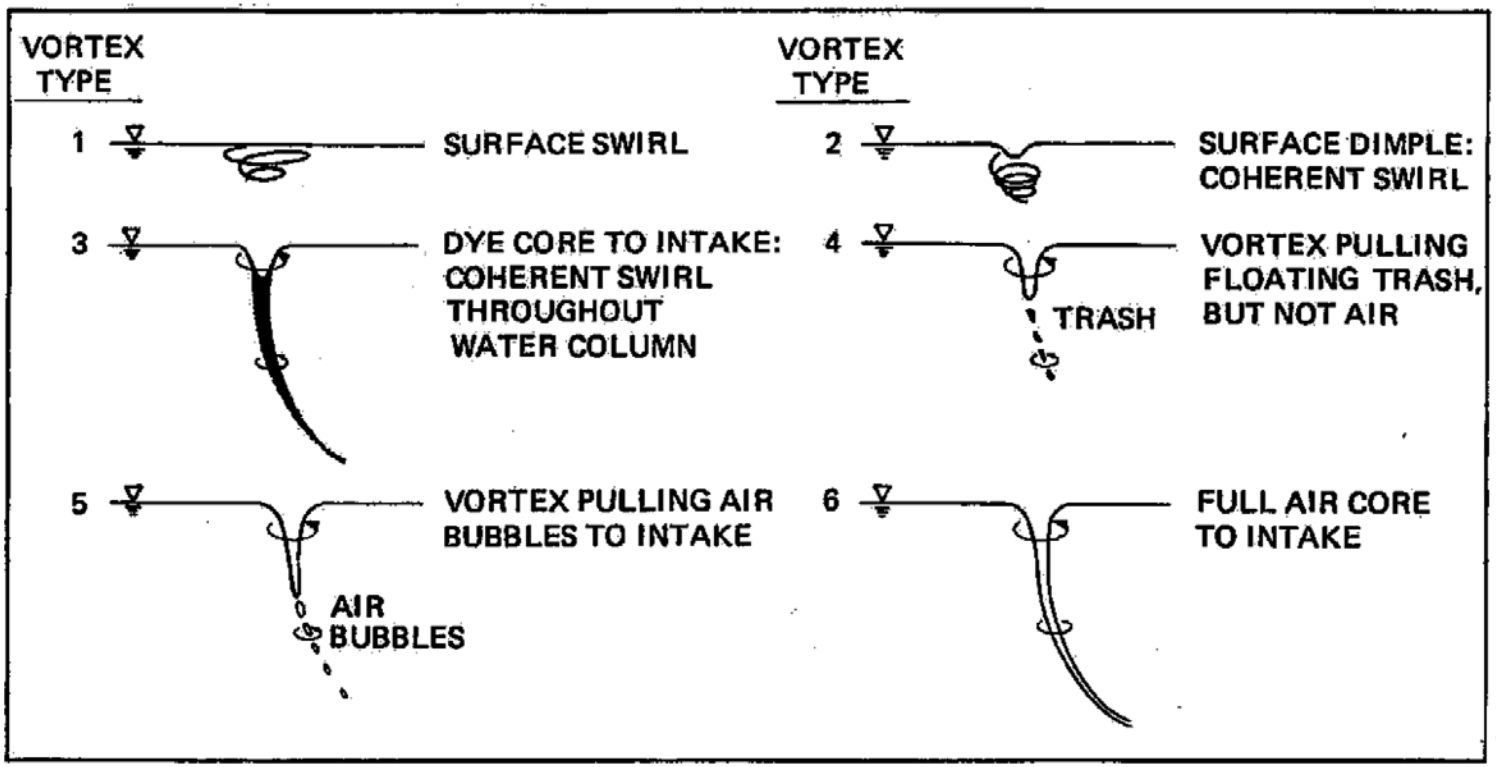

Figure 60: Vortex Classification

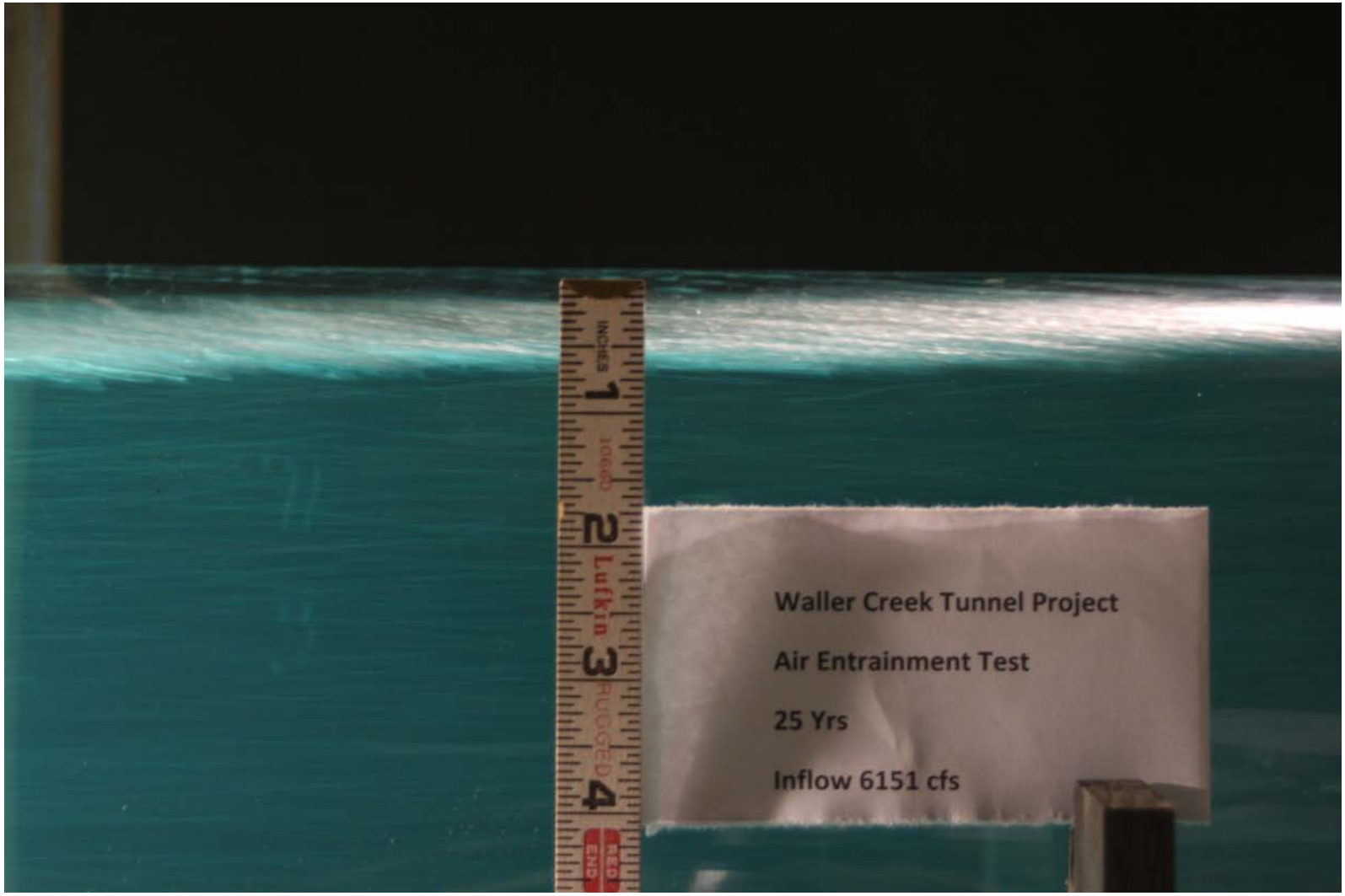

Figure 61: Waller Creek Tunnel Project; 1:33 Scale Model- Photograph of Volume Fraction of Air; 25 Year Flood Flow

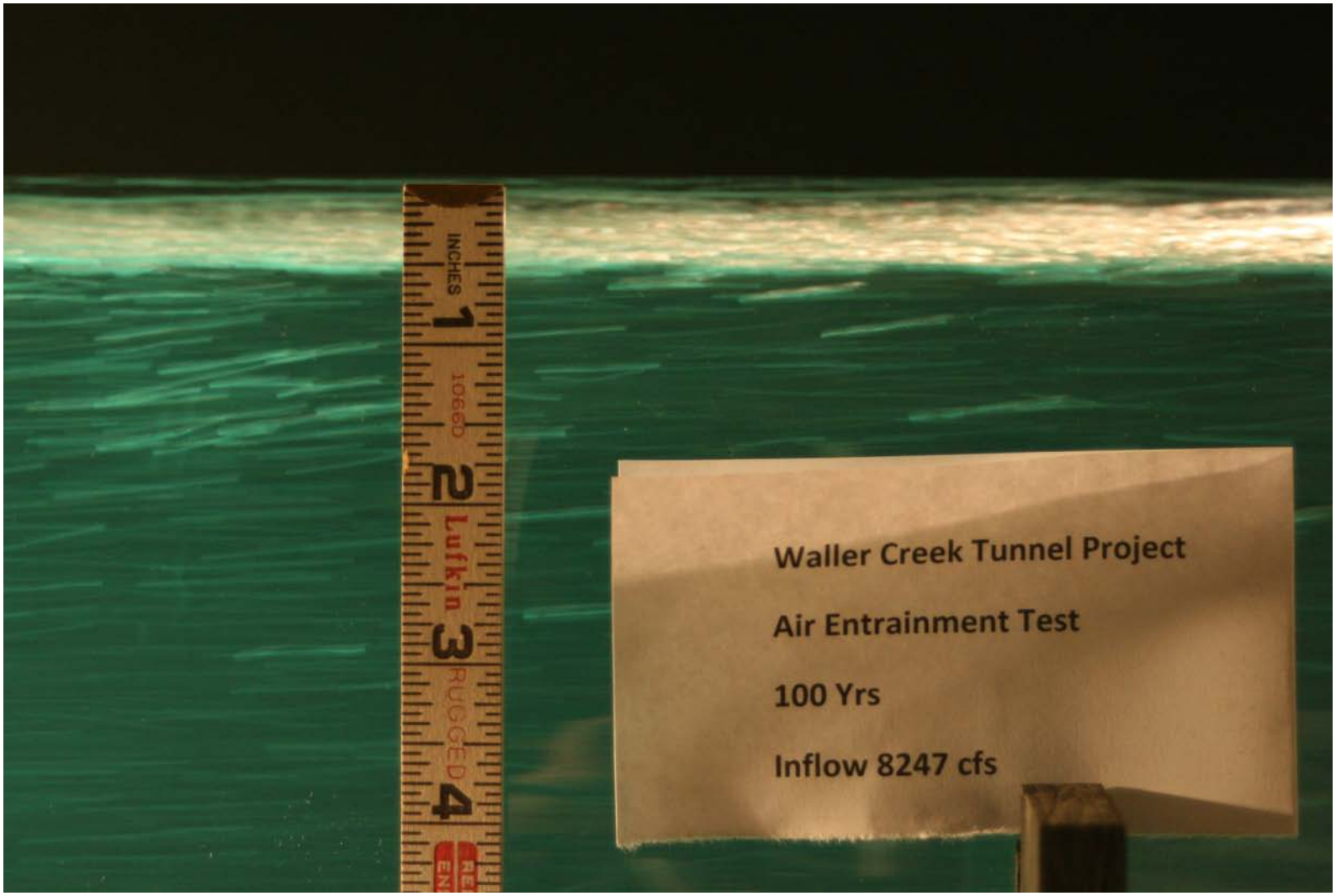

Figure 62: Waller Creek Tunnel Project; 1:33 Scale Model- Photograph of Volume Fraction of Air; 100 Year Flood Flow

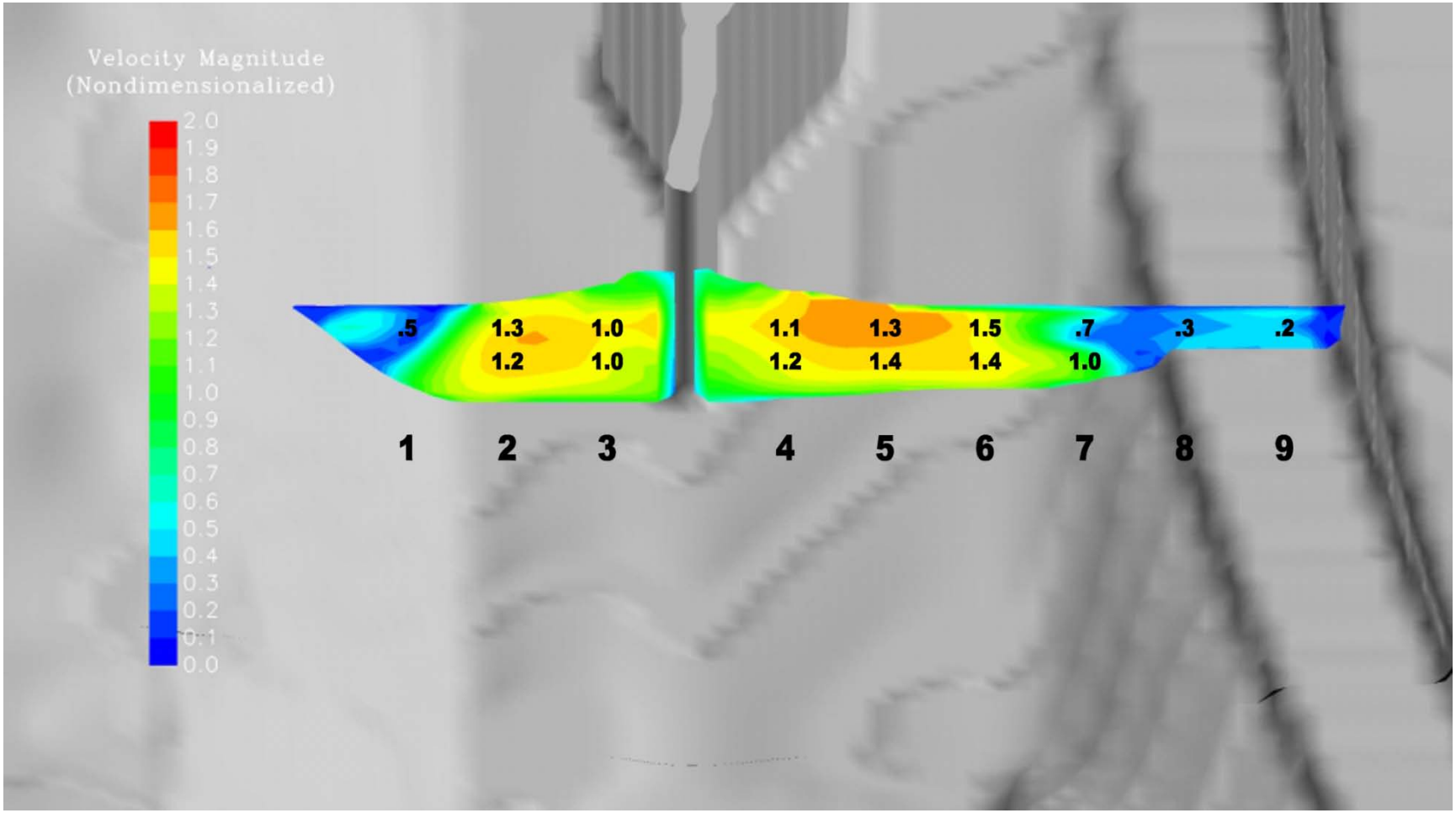

Figure 63: Waller Creek Tunnel Project; 1:33 Scale Model- Non-dimensionalized Velocity (Vpoint/Vaverage) Distribution at Model Inlet: 100 Year Peak Flow

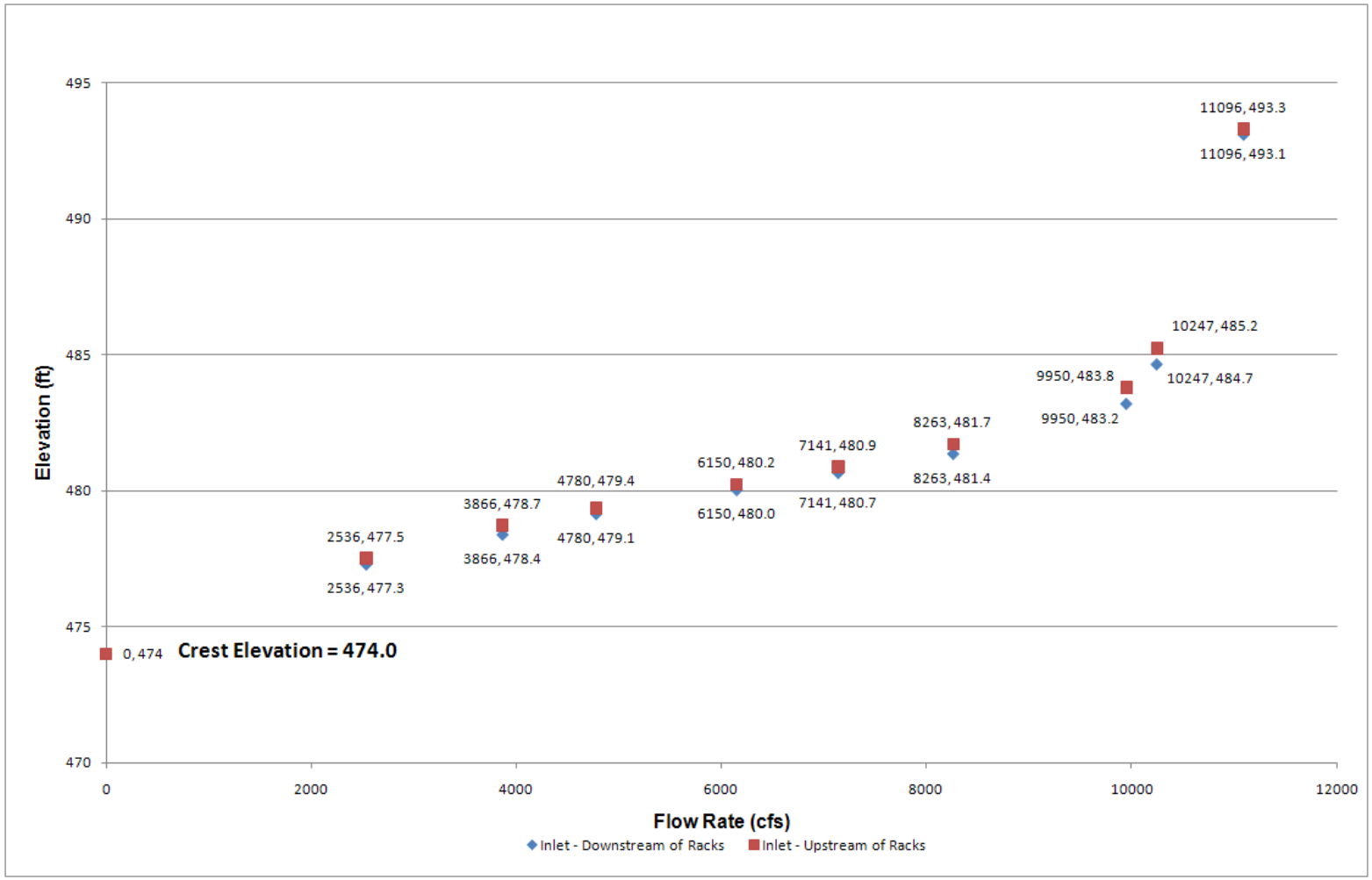

Figure 64: Waller Creek Tunnel Project; 1:33 Scale Model- Morning Glory Spillway Rating Curve

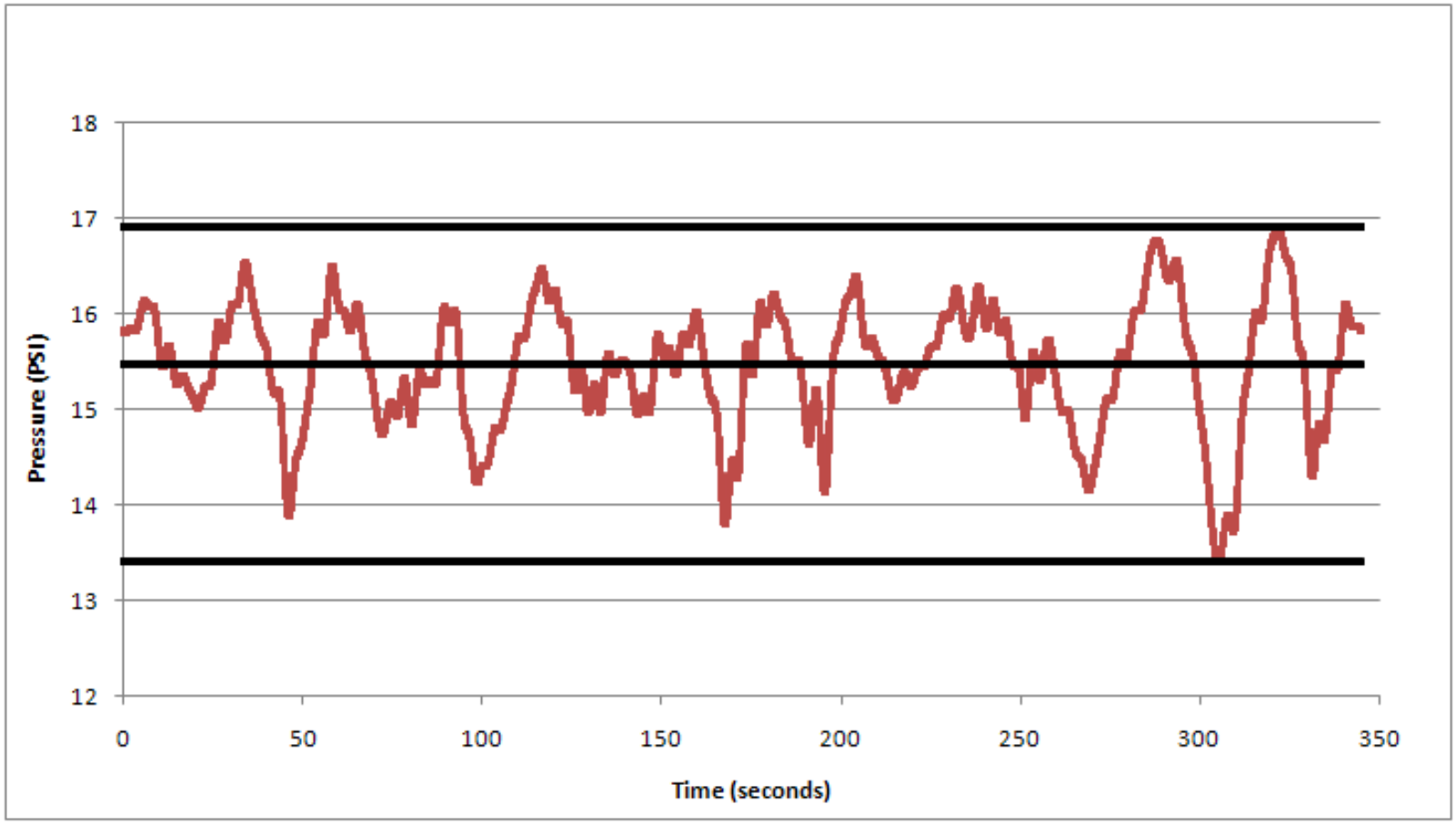

Figure 65: Waller Creek Tunnel Project; 1:33 Scale Model- Prototype Pressure Fluctuations at the Tunnel Portal to the Recirculation Pump Intake with Closed Valve at 100 year Peak Flow

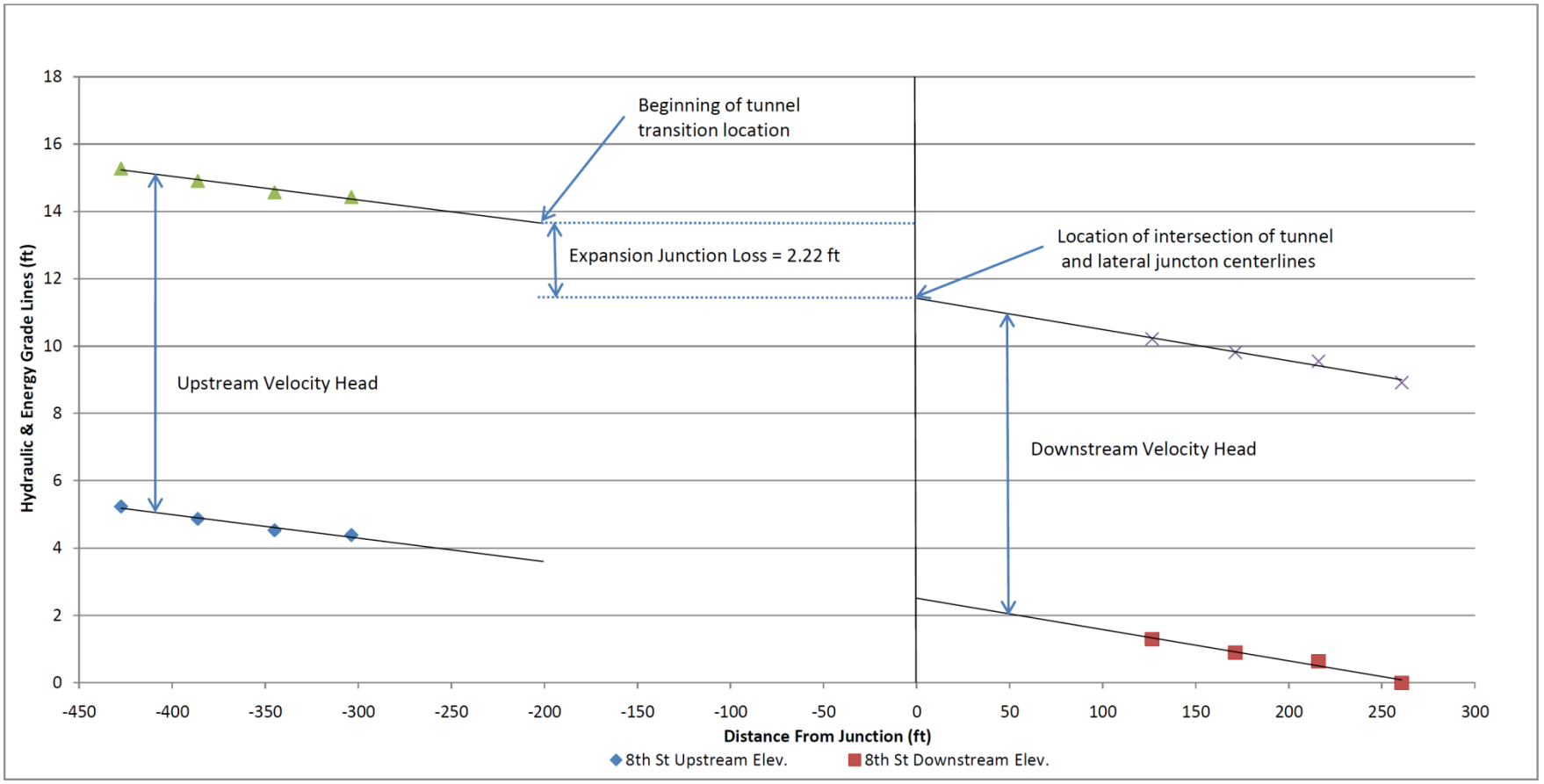

Figure 66: Waller Creek Tunnel Project; 1:33 Scale Model- 8th Street Lateral Junction Energy Gradient Line; 100 year Peak Tunnel/Peak Intervening

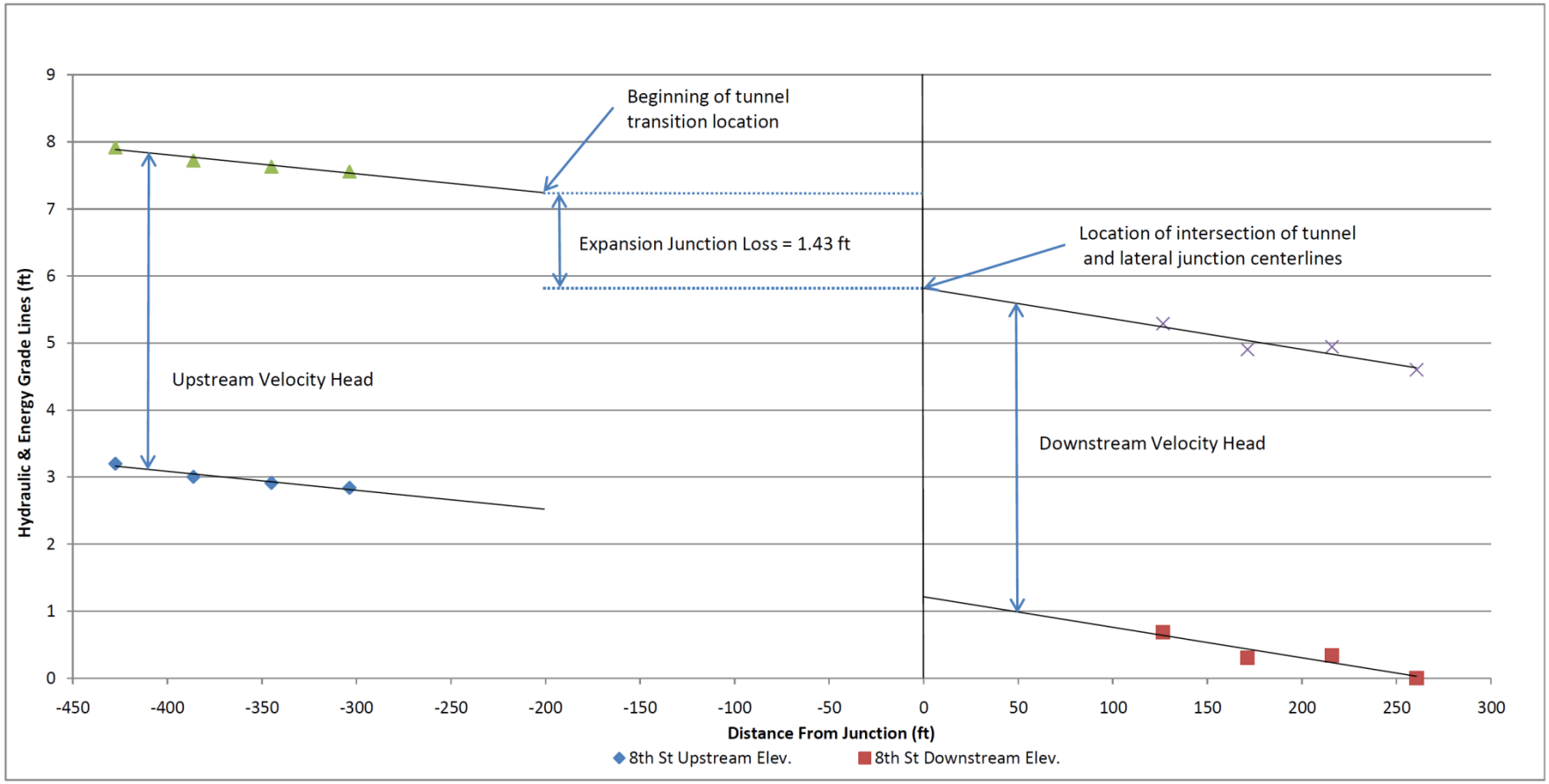

Figure 67: Waller Creek Tunnel Project; 1:33 Scale Model- 8th Street Lateral Junction Energy Gradient Line; 100 year Lagging Tunnel/Peak Intervening

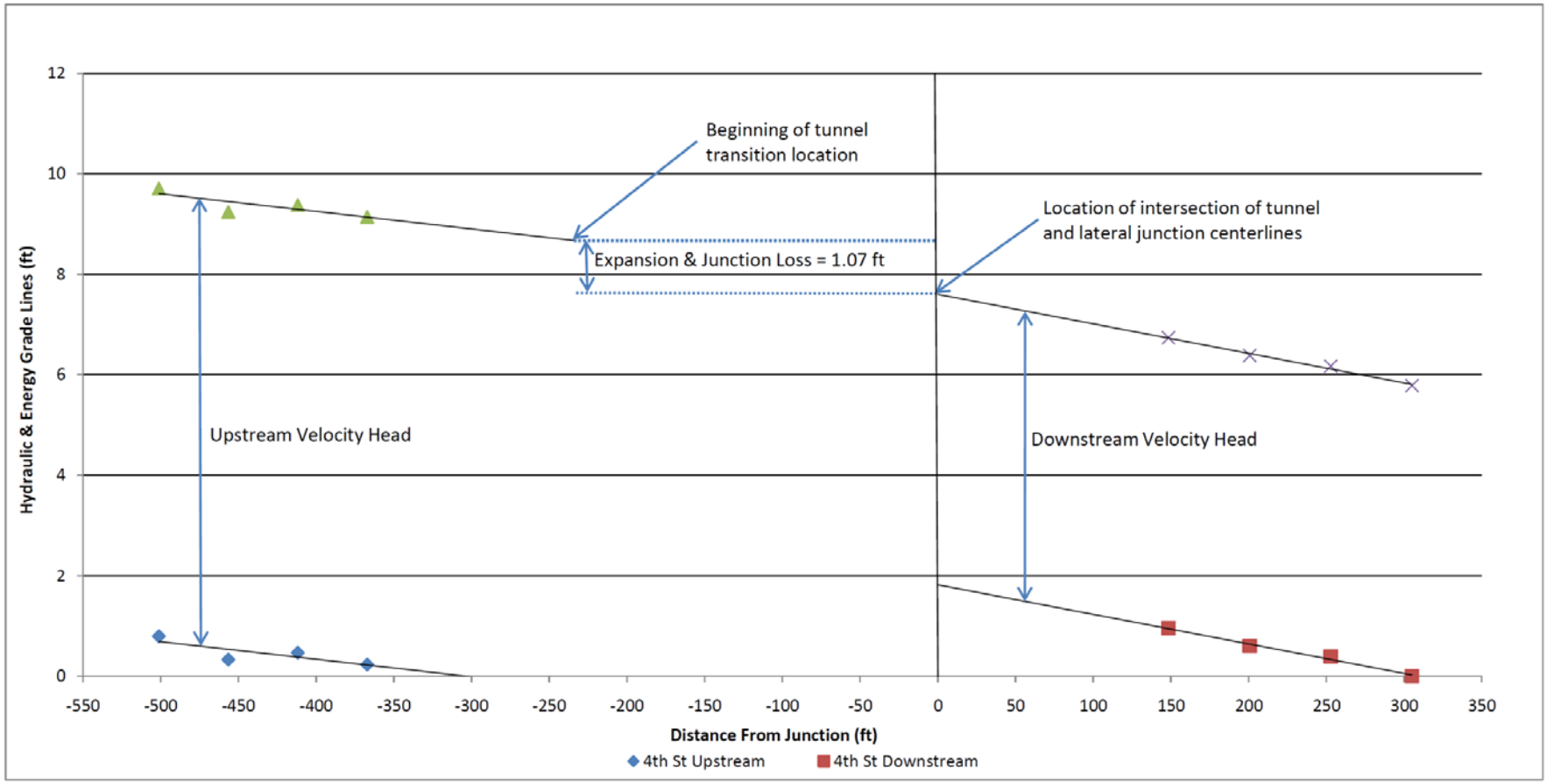

Figure 68: Waller Creek Tunnel Project; 1:33 Scale Model- 4th Street Lateral Junction Energy Gradient Line; 100 year Peak Tunnel/Peak Intervening

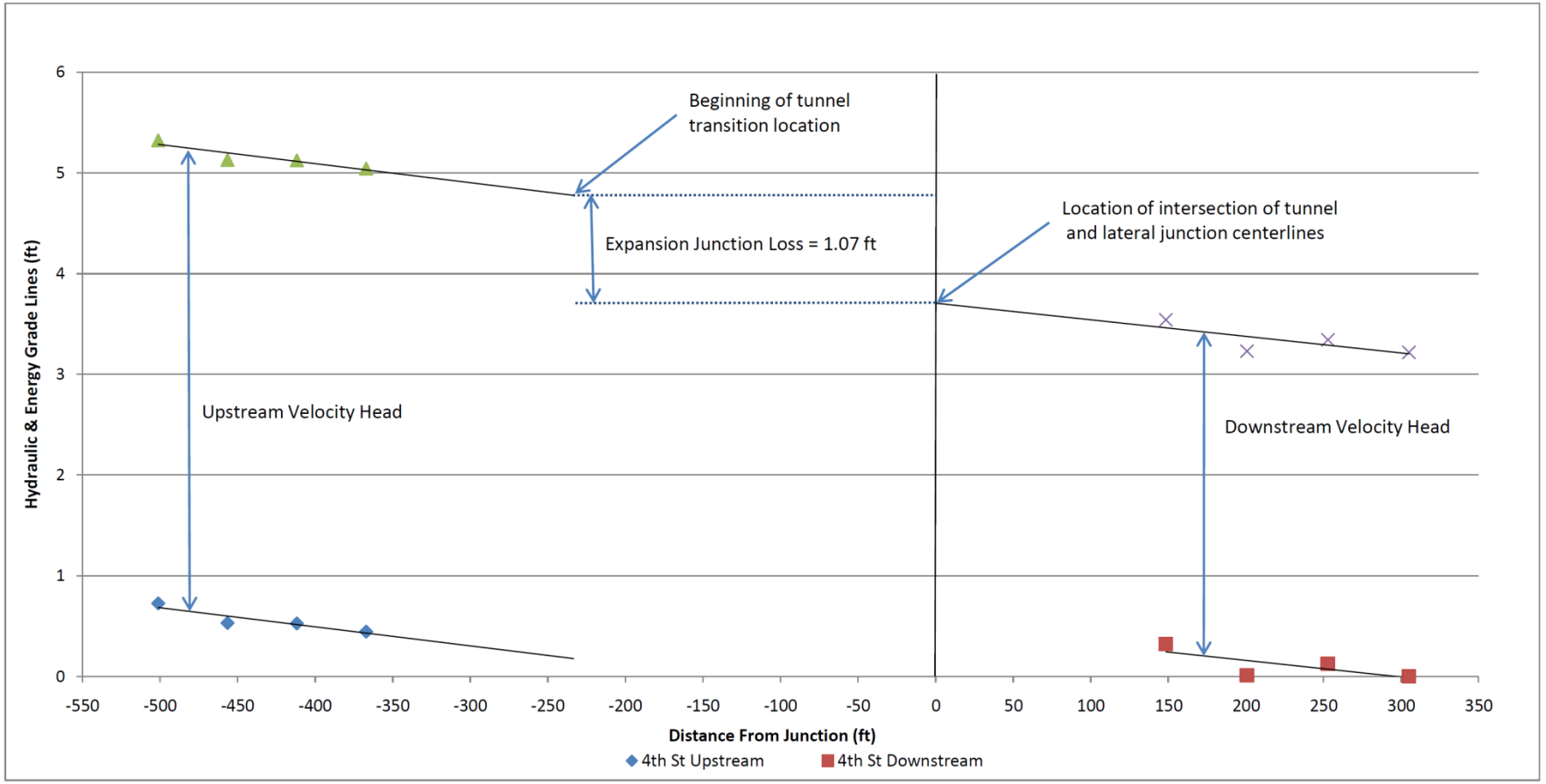

Figure 69: Waller Creek Tunnel Project; 1:33 Scale Model- 4th Street Lateral Junction Energy Gradient Line; 100 year Lagging Tunnel/Peak Intervening

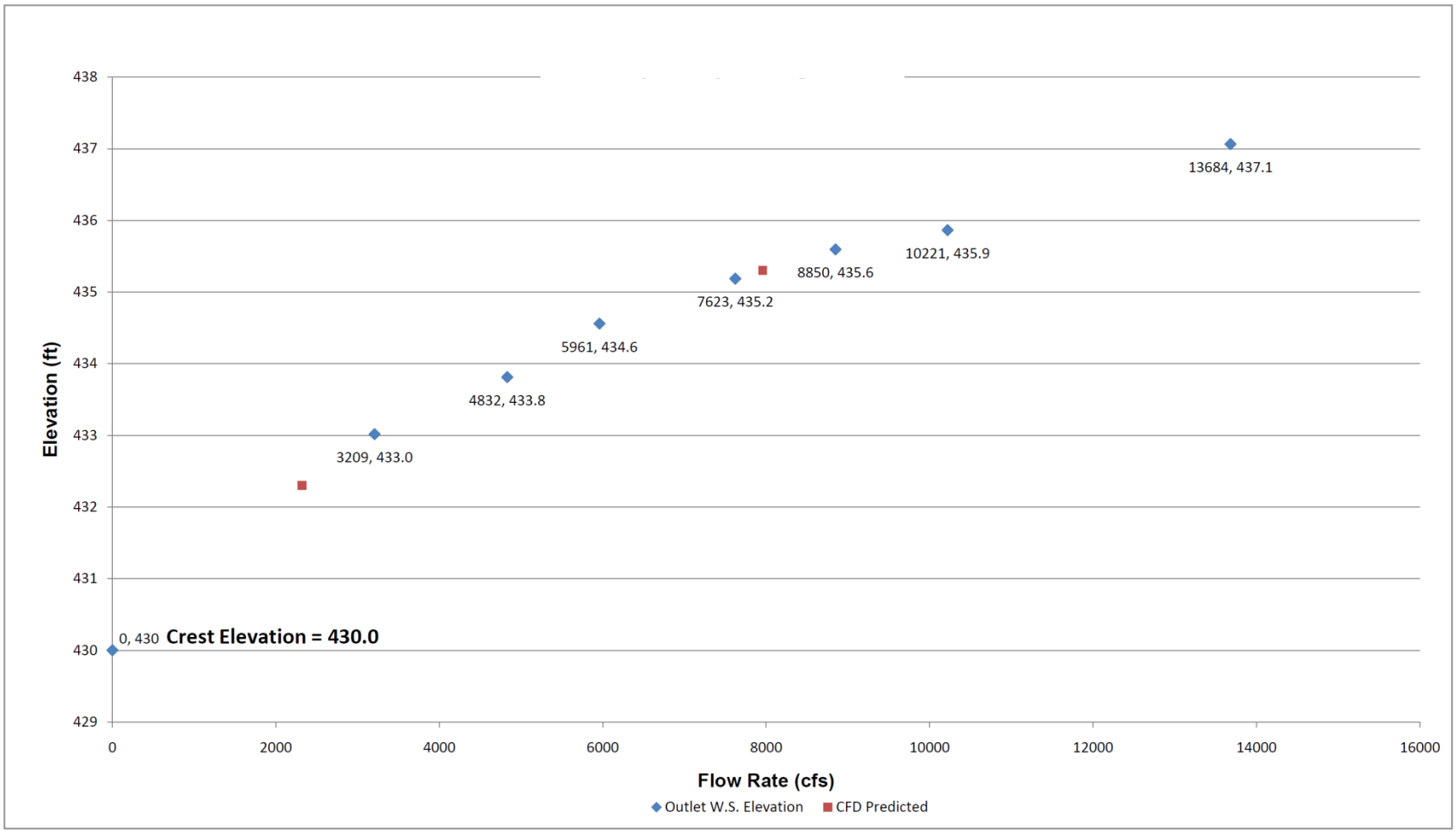

Figure 70: Waller Creek Tunnel Project; 1:33 Scale Model- Outlet Spillway Rating Curve